April 2014

Photocatalytic Degradation of a Series of Commercial Hair Dyes Using Immobilized TiO2

Elena V. Banegas Nunez
Worcester Polytechnic Institute

Johanna Leigh Hartmann
Worcester Polytechnic Institute

Photocatalytic Degradation of a Series of Commercial Hair Dyes Using Immobilized TiO_2

A Major Qualifying Project Submitted to Faculty of Worcester Polytechnic Institute in Partial Fulfillment of the Requirements for the Degree of Bachelor of Science

Submitted by:

Elena Banegas

Johanna Hartmann

Submitted to:

Project Advisor:

Professor Terri Camesano

Professor Stephen Kmiotek

Site Advisor:

Dr. Marie Noëlle Pons

May 1, 2014

Acknowledgements

We would like to express our gratitude to Professor's Terri Camesano and Stephen Kmiotek for providing us the opportunity to travel to France for this experience. Also, our deepest regards to Doctor Marie-Noëlle Pons for allowing us to perform research in her lab and her support and guidance along the way. We would also like Dr. Pons's PhD candidates, Aziz Assaad, Amine Bouarab, and Yuhai Zhang, for their help in the experiments.

Abstract

The TiO_2-mediated photocatalytic degradation of both synthetic and natural dyes in DI and tap water were studied to compare their discoloration, kinetics, mineralization, and toxicity. The systems evaluated, however, were complex due to the unknown concentrations of the several ingredients present in the commercial products. The Langmuir-Hinshelwood approach was applied to evaluate the degradation rate constants of the solutions and the *Lactuca sativa* L. test was used as a method to determine the relative toxicities. Results show that DI favors the kinetics and mineralization of the solutions due to the lack of competing species such as organics, inorganics, and metallic ions present in tap water.

Table of Contents

List of Figures

List of Tables

List of Equations

Introduction

Dyes are among the synthetic compounds of possible environmental concern because of their extensive and widespread use (Fibbri, et al. 2010). Their presence in wastewater is considered because dyes are employed in many fields such as photochemical, textile, photographic, and foodstuffs. Physical wastewater techniques such as adsorption or enzymatic decomposition may be efficient in removing dye-pollutants from wastewater. However, they are non-destructive methods as the dyes still maintain their chemical and physical integrity, leading to "secondary pollution" (Konstantinou and Albanis, 2003). Additionally, the presence of complex and stable aromatic structures in dyes makes conventional treatments ineffective for the discoloration and mineralization of the organic carbon of these dyes (Fibbri, et al. 2010).

In the last decade, advanced oxidation processes (AOPs) have been proven more effective in the degradation of dyes in aqueous systems (Konstantinou and Albanis, 2003). Glaze et al. defined AOPs as water treatment processes which involve the generation of very reactive species such as hydroxyl radicals •OH which "oxidize a broad range of pollutants quickly and non-selectively" (Glaze et al., 1987). Photocatalysis is among these techniques and has been demonstrated to be effective in discoloring and mineralizing dye effluent (Neppolian et. al, 2002).

In this work, the TiO_2-mediated photocatalysis of several synthetic and natural hair dyes in DI and tap water was explored. Both the discoloration and mineralization rates of the potentially harmful compounds present in these readily available commercial products were studies using techniques such as spectroscopy. The goal has been to compare the particular effectiveness of photocatalysis on different dyes and on both DI and tap water.

Background

Dyes in Wastewater

According to Bouzida, et al., dyes can be discharged into the environment from three major sources: (a) from dye manufacturers, (b) from industries that uses dyes (i.e. paper, plastic, textile, etc.), and (c) from household discharges carrying leached dyes from commercial products (Bouzaida et al., 2004). These discharged dyes can undergo oxidation, hydrolysis, or other chemical reactions that can produce dangerous byproducts (Konstantinou and Albanis, 2003). Due to the complexity and stability of the variety of dyes, a unique treatment that effectively eliminates all types of dyes has yet to be developed. Current technologies for the removal of synthetic dyes include adsorption, microbiological or enzyme decomposition, and photocatalysis (Forgacs, Cserháti et al. 2004).

Adsorption

Adsorption of synthetic dyes onto inorganic and organic supports have been studied and used to decolorize dye wastewater. Carbon-based inorganic supports have shown successful adsorption properties, however, the production of the carbon sorbent is energy consuming. Other inorganic supports have been investigated such as silica and alumina. Organic supports have also been examined since they are generated from waste or by-products of processes and renewable sources. Some organic supports include orange peel, pasteurized wastewater solids, waste banana pith and pulverized fungi (Forgacs, Cserháti et al. 2004). These adsorption methods using both inorganic and organic supports do have some disadvantages. The process only decolorizes dye wastewater and does not degrade the dye molecules, leaving harmful compounds in the wastewater. Moreover, this adsorption process is not selective and other chemicals in the effluent will compete with the synthetic dye for adsorption onto the supports. (Forgacs, Cserháti et al. 2004)

Microbiological and Enzymatic Decomposition

Microorganisms have been proven to decolorize and degrade synthetic dye compounds. The microorganisms tested include yeasts, fungi, algae, and different strains of bacteria. The efficiency of the discoloration and degradation of the dyes depends upon the dyes' structure. Different microorganisms work more efficiently for different dye colors. In particular, the white-rot fungus has proven to be successful in the biodegradation and discoloration of several dyes and has been studied extensively (Forgacs, Cserháti et al. 2004). It has been proposed that the success of the white-rot fungus is due to its high enzyme production. The use of enzymes to degrade and discolor synthetic dyes has also been experimented. It has been found that the degraded synthetic dyes by the use of enzymes underwent significant decomposition and that the structure of the dye had little impact on the extent of degradation (Forgacs, Cserháti et al. 2004). Currently, however, biological degradation techniques may not be very effective in eliminating

the potentially toxic components in dyes because commercial dyes have “been intentionally designed to resist aerobic microbial degradation” (Bouzaida et.al 2004).

Photocatalytic Methods Other than TiO2-mediated

Photocatalysis detoxification has been used as another alternative to detoxify polluted waters. Chemical oxidation detoxifies wastewater through the addition of an oxidizing reagent to oxidize the toxic components. Ultraviolet light can be added to accelerate the oxidation or create radicals which will aggressively oxidize the waste (LaGrega et. al 2001). Many semiconductors have been used as photocatalysts in reactions. Some catalysts include ZnO, WO_3, SnO_2, ZrO_2, CeO_2, CdS, and ZnS have been studied for the photocatalytic oxidation and discoloration of synthetic dyes (Neppolian et. al, 2002). Additionally, hydrogen peroxide, H_2O_2 has been used to effectively decolorize dye wastewater through photocatalysis and degrade certain dyes (Forgacs, Cserháti et al. 2004).

TiO2-mediated Photocatalysis

Many semiconductors have been used as photocatalysts in reactions. However, titanium dioxide is most commonly used due to the fact that it is chemically stable, non-toxic, and cheap (Li, Jingyi et al. 2007). Moreover, it is the most successful photocatalysis to degrade a wide range of chemicals (Vincenzo and Augugliaro 2010).

Titanium Dioxide Photocatalytic Mechanism

The following series of reactions will take place during irradiation of TiO_2 (Augugliaro, Vincenzo et al. 2012) shown in Figure 1.

$$TiO_2 + h\nu \rightarrow TiO_2(e^-_{(CB)} + h^+_{(VB)}) \quad (1)$$

$$OH^- + h^+_{(VB)} \rightarrow {}^\bullet OH \quad (2)$$

$$O_2 + e^-_{(CB)} \rightarrow {}^\bullet O_2^- \quad (3)$$

$${}^\bullet O_2^- + H^+ \rightarrow {}^\bullet HO_2 \quad (4)$$

$$2{}^\bullet HO_2 \rightarrow O_2 + H_2O_2 \quad (5)$$

$$H_2O_2 + {}^\bullet O_2^- \rightarrow OH^- + {}^\bullet OH + O_2 \quad (6)$$

Figure 1: Photocatalytic mechanism of titanium dioxide (Augugliaro, Vincenzo et al. 2012)

When TiO_2 is exposed to UV light ($h\nu$) with a wavelength of less than 390 nm, the radiation is absorbed and transformed into chemical energy. During this process, the electrons move from the valence band to the conduction band (e^-_{CB}), creating a positive electron hole (h^+_{VB}). The now positive valence band is reactive enough to form a radical species with hydroxyl ions. Moreover, the negative conduction band is powerful enough to reduce oxygen molecules and form a radical oxygen species. The radical species ${}^\bullet O_2^-$, ${}^\bullet H_2O$ and ${}^\bullet OH$ are extremely reactive and will oxidize organic pollutants and other toxic chemicals to form water and carbon dioxide. (Khataee, Vatanpour et al. 2004)

Immobilized Titanium Dioxide

There are several obstacles that arise while using a TiO_2-aqueous suspension system. After treatment, the TiO_2 particles would need to be separated from the solution. Another drawback is that the ultraviolet light would not be able to strongly penetrate the solution, due to the strong UV absorption of the TiO_2 particles. A solution to these disadvantages is to immobilize the photocatalyst (Lu, Max et al., 2013). Immobilizing the catalyst onto a solid support will eliminate the need to separate the particles from the effluent but it will also decrease the surface area of the catalyst (Aguedach, Abdelkahhar, et al. 2008).

According to Lu, Max, et al., nonwoven fabrics is an excellent support for titanium dioxide because it is flexible, cost-effective, and lightweight. Moreover, silicon dioxide (SiO_2) is commonly used as a binder to adhere the photocatalyst. There are two major methods to adding TiO_2 to nonwoven paper. These processes include: wet-end addition and size-press treatment. In wet-end addition, the risk of agglomerates is very high although it will ensure a complete coverage of the paper. In size-press treatment, dry paper is saturated with TiO_2 while running through a size press which is two rolls that press the paper as it passes through them (Vincenzo and Augugliaro 2010; Brander, Thorn 1997).

Current Uses

The use of TiO_2-mediated photocatalysis is an emerging technology. Currently there are several plants to treat wastewater using this method. For example, a solar photocatalytic wastewater plant was constructed 2000 in Madrid, Spain. It was the first industrial solar detoxification treatment plant and uses slurries of TiO_2 to aid in the photodegradation of pollutants. The plant treats 1 m^3 of wastewater with 21 solar photoreactors with a total surface area of 100 m^2. The photoreactors are shown below in Figure 2 (Vincenzo and Augugliaro 2010; Lu, Max et al., 2013).

Figure 2: Solar photoreactors at the wastewater treatment plant in Madrid, Spain. (Lu, Max et al. 2013)

The reactors are operated in batch mode and a mixture of wastewater and TiO_2 slurry will continuously circulate until the desired level of degradation is reached. The treated water and slurry then flow into a sedimentation tank where the catalyst gathers at the bottom of the tank. The catalyst exits the bottom and enters a filtration tank before being reused. (Vincenzo and Augugliaro 2010; Lu, Max et al., 2013)

In Spain there is also a continuous stirring photoreactor tank to degrade free cyanide ions in power plant wastewater. However, this was only a pilot plant. The reactor contained immersed UV lamps and the catalyst used was TiO_2 supported on aluminum oxide (Al_2O_3). In Canada, several photocatalytic reactors for water treatment have been produced using (a) immobilized TiO_2 on a fiberglass mesh, (b) suspended TiO_2 and artificial irradiation, and (c) suspended TiO_2 and simulated solar irradiation (Vincenzo and Augugliaro 2010).

Dye Degradation Kinetics

A Langmuir-Hinshelwood approach was selected to calculate the degradation rates of each of the solutions. This approach states that

$$r = \frac{dC}{dt} = k\theta = -\frac{kKC}{1 + KC}$$

Where:

r—Degradation rate

k—Degradation rate constant

θ—Occupation coverage of adsorption sites

K—Adsorption equilibrium constant (ration between adsorption and desorption rate constants $K = {k_{ads}}/{k_{des}}$

C—equilibrium concentration (after adsorption)

t—time

Since at low concentrations kC≪1, the term KC can be assumed to be negligible, therefore reducing the model to:

$$ln\frac{C}{C_o} = -k_{app} * t$$

This integrated reaction rate equation follows a first-order kinetics where C_o is the initial concentration of the dye solution. The apparent rate constant k_{app} contains both the degradation rate constant k and the adsorption equilibrium constant K (Pons, et al, 2013). Since the exact concentration of the specific dyes present in each of the dye mixtures could not be determined as they are proprietary information of the companies, the ratio of the adsorptions obtained from UV-visible spectroscopy was used to evaluate the kinetics of the sample using the equation 1 below.

Equation 1: Langmuir-Hinshelwood Kinetics

$$ln\frac{A}{A_o} = -k_{app} * t$$

It was assumed that the concentrations and the absorptions were directly proportional, making Equation 2 valid.

Equation 2: Color Removal Efficiency

$$CR\ (\%) = \left(1 - \frac{A}{A_o}\right) * 100$$

Rate of Dye Degradation on TiO2-Mediated Photocatalysis

The rate of degradation relates to the probability of the •OH radicals forming on the catalyst surface to the probability of •OH radicals reacting with dye molecules (Konstantinou and Albanis, 2003). There are several factors that affect the rate of photodegradation: initial dye concentration, reaction intermediates, irradiation time, and the pH of the solution (So et al., 2002).

Effects of initial dye concentration

At high dye concentrations, the generation of •OH radicals on the TiO_2 surface is reduced since the active sites of the catalyst are covered by dye ions. It also reduces the efficiency of the catalytic reaction because the presence of intermediates formed upon photodegradation of the parental dye increases (So et al., 2002). Previous studies have shown these intermediates may include aromatics, aldehydes, ketones, and organic acids (d' Hennezel et al., 1998; Tanaka et al., 2000). Additionally, at a high dye concentration, a significant amount of UV may be absorbed by the dye molecules rather than the TiO2 particles. Therefore the efficiency of the photocatalytic reaction is reduced because the concentrations of •OH and O2•− decrease due to the lack of electrons in the conduction band (Mills et al., 1993).

Effects of UV-Visible irradiation time

The amount of discoloration and photodegradation increases with increase in UV-Visible irradiation time. However, as the reaction time increases, the reaction rate decreases since it follows apparent first-order kinetics (Ollis et. al, 1991). The reactant and the intermediate products of the photocatalytic reaction may compete with each other for degradation by the radical species present in the solution.

Effects of pH

The pH has several effects on the efficiency of dye degradation through photocatalysis because it influences the adsorption of dye molecules onto the catalyst surfaces (So et al., 2002).

The point of zero charge (pzc) or the isoelectric point of the TiO2 is close to pH 6.8 (Poulius and Tsachpinis, 1999). Thus, according to electrochemical equilibrium, in acidic media, pH < pH_{pzc}, and the TiO2 surface is positively charged (Konstantinou and Albanis, 2003). Under these conditions, the degradation of the dye occurs through direct oxidation, which induces the adsorption of the organic compounds on the TiO_2 surface. Upon adsorption, "charge transfer from the aromatic rings to the positive valence hole could take place" (Tang and Huang, 1995). Hydroxide ions could be formed when the highly electrophilic groups such as hydroxyl (See Appendix A for specific dye structures) dissociate from the aromatic and they may be further oxidized into radical species (Tang and Huang, 1995).

In addition, at a low pH, the electrons conduction band may aid in the degradation of the dyes (Konstantinou and Albanis, 2003) because they facilitate the formation of the • O_2^- and • HO_2 radical species, as can be seen from the mechanism illustrated in Figure 1.

In alkaline media, pH >pH_{pzc}, and hydroxide ions are the dominant species (Konstantinou and Albanis, 2003). Therefore, under neutral and basic conditions, photodegradation occurs through indirect oxidation. These conditions favor the hydroxyl radical formation in the positive valence holes, thereby enhancing the degradation rate of the dye molecules (So et al., 2002).

Analytical Techniques

UV-Visible Spectroscopy

UV-visible spectroscopy is an important tool used in our analysis of the hair dye wastewater treatment. Spectroscopy refers to the use of absorption or emission of energy to analyze the contents of a sample. If the energy of passing through the sample matches the energy required to excite an electron, the electron will jump to a higher orbital. During this process, some of the energy from the UV-visible light will be absorbed by the sample. This energy is directly proportional to a wavelength of UV-visible light through the equation: $\lambda=h*c/\Delta E$ where λ refers to the wavelength, h Planck's constant, c the speed of light, and ΔE is the amount of energy absorbed by the electron. The wavelength at which this occurs and the amount absorbed is recorded (Reusch "Visible and Ultraviolet Spectroscopy").

In UV-Visible spectroscopy a beam of visible and ultra violet light passes through a cuvette containing the sample to be analyzed. First, a beam is passed through a cuvette containing only the solvent. This beam should not have undergone any absorption and its intensity is defined as I_0. After this baseline is defined, the sample can be analyzed. The intensity of the beam exiting the sample, defined as I, is less than that of the exiting beam of the solvent due to absorption by the sample. Absorbance is calculated by the equation: $A= (\log I_0)/I$ and is calculated by the spectrometer. From the data given by the spectrometer, absorbance is plotted on the y-axis versus the wavelength on the x-axis (Reusch, "UV-Visible Spectroscopy).

Spectrometer at the LGRP, ENSIC

The spectrometer available in the LGRP laboratory at ENSIC is a Secoman Anthelie UV visible light advanced spectrophotometer. The light source of this spectrometer is a pre-adjusted halogen lamp for the visible light and a pre-adjusted deuterium lamp for the ultra violet light. The cuvette used analyze the sample was a one-cm^2 quartz cuvette (Secoman).

Non-Purgeable Organic Carbon and Total Nitrogen

Wastewater is typically characterized by parameters such as total organic carbon (TOC) and total nitrogen (TN) (Roig, Gonzalez et al. 1999). The Environmental Protection Agency has recognized organic carbon matter as a hazardous substance in drinking water due to its ability to react with chlorine and form carcinogenic hydrocarbon compounds. The color, taste, and odor of drinking water are also dependent upon organic matter. It is therefore controlled and monitored in drinking water systems. Nitrogen compounds which can occur in wastewater as organic or inorganic are also of considerable concern (Roig, Gonzales et al. 1999). These compounds may cause eutrophication of an ecosystem, which causes toxic algae blooms (Stenholm, Holmstrom et al. 2008).

From a toxicological standpoint, TOC analysis is an appropriate method for evaluating the decontamination of polluted waters since it includes all residual carbon-containing compounds (Lacheb et al., 2002) after a certain treatment, in this case, TiO_2-mediated photocatalysis. TOC is measured by oxidizing the carbon in the sample, thereby forming carbon dioxide. In this analysis no separation occurred between inorganic and organic carbon. The carbon content measured is referred to as non-purgeable organic carbon (NPOC) meaning that the carbon content found signifies both the organic and inorganic carbon in the sample (Bisutti, Hilke et al. 2004; Volk, Christian 2002).

NPOC and TN Analyzer at the LRGP, ENSIC

The NPOC was measured in ENSIC using a TOC Analyzer Combustion Catalytic Oxidation/NDIR Method Model built by Shimadzu. This model used high temperature combustion by heating the sample to 680^{o}C to oxidize the carbon. According to Volk, Christian et al., dry combustion guarantees total oxidation of carbon and is therefore considered to be the most effective method. The amount of carbon dioxide present is measured through non-dispersive infrared absorption and is proportional to the amount of organic carbon and inorganic carbon in the sample (Bisutti, Hilke et al. 2004; Volk, Christian 2002).

The total nitrogen was measured at ENSIC using the TOC-V_{CPN} instrument with the TNM-1 accessory installed. This equipment measured the total nitrogen using oxidative combustion through thermal decomposition, similar to the method used to oxidize the carbon. The samples were catalytically combusted to 720 ^{o}C to oxidize the nitrogen by oxidative pyrolysis. Next, the nitrogen oxide reacts with ozone to form metastable nitrogen dioxide (Stenholm, Holmstrom et al. 2008). At this point, chemiluminescence was used to detect the metastable nitrogen dioxide as it degrades in the sample after combustion (Shimadzu).

Composition of Commercial Hair Dyes

The commercial hair dyes that were tested had different ingredients and compositions. The color dyes in each mixture were identified and they are listed in Appendix A with their respective structures and CAS numbers. The following dye ingredients present in the final commercial products tested (except for the hennas) are all non-oxidative, meaning they are semi-permanent and wash off after a certain number of rinses.

Although they all different dyes responsible to give them their characteristic final color, all the commercial products had the following ingredients in common: Cetearyl alcohol, distearoylethyl hydroxyethylmonium methosulfate, ceteareth-20, citric acid, and methyl paraben. The structure, CAS numbers, and molecular weight for these compounds can be found in Appendix A.

Cetearyl Alcohol

According to the International Journal of Toxicology (IJT), cetearyl alcohol proved only slightly toxic when administered orally at doses of 5 g/kg and greater. When a cream containing 3.0% cetearyl alcohol was applied to the skin of New Zealand albino rabbits, only mild irritation was observed. Additionally, in a human skin sensitization study of a cream containing 3.0% cetearyl alcohol, none of the subjects had positive reactions. The journal concluded that cetearyl alcohol is safe as a cosmetic ingredient (IJT,1988).

Distearoylethyl Hydroxyethylmonium Methosulfate

The International Nomenclature of Cosmetic Ingredients (INCI) defines its function as an antistatic agent and hair conditioner (Special Chem, 2014). However, no further information regarding its safety was found.

Ceteareth-20

The International Nomenclature of Cosmetic Ingredients (INCI) defines its function as a cleansing and emulsifying agent (Special Chem, 2014). However, no further information regarding its safety was found.

Citric Acid

Due to its low toxicity, citric acid has a great worldwide demand mainly in the pharmaceutical and food industries. Other applications of citric acid can be found in detergents and cleaning products, cosmetics and toiletries (Soccol et al., 2006).

Methyl Paraben

Methyl paraben is a stable, non-volatile compound that has been used as an antimicrobial preservative in foods, drugs and cosmetics for over 50 years (Soni, 2002). Acute toxicity studies in rats, rabbits, dogs and cats indicate that methyl paraben is non-toxic by both oral and parenteral routes. In addition, they indicate that methyl paraben is readily absorbed from the gastrointestinal tract, metabolized and excreted. Dermal toxicity of a hair-dressing product containing 0.2% methyl paraben was tested in three male and three female albino rabbits methyl paraben

and was found to be non-irritating. Methyl paraben is neither carcinogenic nor mutagenic. Therefore, it was concluded that methyl paraben is safe for cosmetic use (Soni, 2002).

HC Yellow No. 2

HC Yellow No. 2 is used in concentrations up to 1%. When tested at a concentration of 10% in solution in guinea pigs, it was observed that the compound was only a minor ocular and skin irritant. HC Yellow No. 2 proved non-mutagenic in assays using four *S. typhimurium* strains. Therefore, the American College of Toxicology (ACT) concluded that HC Yellow No. 2 is safe for use in hair dyes at concentrations up to 3% (ACT, 1994).

HC Yellow No. 4

HC Yellow No. 4 is used in concentrations that range from 0.1% to 1.0%. When tested in guinea pigs, HC Yellow No. 4 did not produce noticeable skin irritation. HC Yellow No. 4 proved mutagenic in several assays, but no evidence of carcinogenesis was found in oral or dermal studies. Therefore, it is concluded that HC Yellow No. 4 is safe as a hair colorant (Bergfeld,1998).

Basic Yellow 57

The maximum concentration of Basic Yellow 57 on the head is 2.0%. At a maximum test concentration of 10%, Basic Yellow 57 proved to be a skin irritant. Basic Yellow 57 was tested for the three genotoxicity endpoints: gene mutation, structural and numerical chromosomal aberrations (SCCS, 2010). When tested *in vitro* using bacteria and mammalian cells, the dye did not induce gene mutations (SCCS, 2010).

Acid Green 25

Acid Green 25 is allowed to be present in the final cosmetic product at a maximum concentration of 0.3%. When applied in a 10 % solution and above, Acid Green 25 exhibited low irritating effects. It tested negative for mutagenicity; it did neither induce gene mutations in bacteria nor in cultured mammalian cells. In addition, Acid Green 25 does not induce structural chromosome aberrations (SCCP, 2005).

Basic Orange 51

No current uses or maximum allowable concentrations in cosmetics are reported.

HC Blue 15

No current uses or maximum allowable concentrations in cosmetics are reported.

Basic Blue 99

Basic Blue 99 is used at concentrations ranging from 0.004% to 2%, and its dermal absorption is low in both rats and humans. The Cosmetic Ingredient Review Expert Panel determined that Basic Blue 99 lacks any carcinogenic potential when used in hair dyes. The Panel concluded that Basic Blue 99 is safe as a hair dye ingredient when used at the allowable concentrations (Alan, 2007).

Brilliant Blue FCF

The only information in the literature regards its use as a food coloring, not as a hair dye.

Basic Violet 2

No current uses or maximum allowable concentrations in cosmetics are reported. The only Basic Violets found in the literature are basic Violet 1, 3, and 4.

Acid Violet 43

Acid Violet 43 is considered a coal tar ingredient which might incur in skin irritation in any given individual. The maximum allowable concentration is 1%. In a short-term dermal toxicity study using guinea pigs and rabbits, no significant local skin reactions were observed. Acid Violet 43 was not genotoxic in bacterial assays, and was deemed non-carcinogenic when applied to mouse skin at a 1% concentration (Fiume, 2001).

Materials & Methodology

Dyes

Both permanent and semi-permanent commercial hair dyes were studied under TiO_2-mediated photocatalysis. The *La Fiche* and *Star Gazer* dyes were all semi-permanent. Both the Moroccan and the Tunisian hennas are permanent dyes because of their oxidative properties (*Henna,* 2010 and Henna for Hair, 2005). Table 1 below summarizes the different brands used with the specific dye colors. Appendix A contains the complete list of ingredients pertaining to each commercial hair dye.

TABLE 1: HAIR DYES USED BY BRAND AND COLOR

Brand	Color
La Fiche	Apple Green
Directions	Fire
	Fluorescent Glow
	Lagoon Blue
Star Gazer	Violet
Henna	Moroccan
	Tunisian

Gels

5 g of the *La Fiche—Directions* and *Stargazer* hair dye gels were dissolved up to 1 L of solution using DI or tap water and with the aid of a magnetic stirrer. This amount proved sufficient for two experimental runs.

Henna

The henna, unlike the other dyes, comes in a powder form. In this work, their solutions were prepared using distilled water only. To prepare a solution; 500 mL of distilled water was heated to a temperature of 30°C. When this temperature was reached, 1 g of the henna powder was introduced to the water and the solution was kept magnetically stirred for 15 minutes. Finally, the solution was filtered using Cora (TM) Koffiefilters N°4 to minimize the presence of particles that could possibly clog the photocatalytic reactor.

Titanium Dioxide Catalyst

Millenium PC-500, the titanium dioxide powder, was immobilized by means of a silica-based binder on a mat based on cellulose fibers. (Ahlstrom Research & Services, Pont-Eveque, France). MilleniumPC-500 consists of of approximately 97% anatase and 3% rutile, both forms of titanium dioxide powder. It has a primary particle size of 5-10 nm (Qourzal et al., 2012). Only one sheet of this photocatalytic paper was employed during all the experiments.

Photocatalytic Reactor

The photocatalytic reactor used in the experimental runs is shown in Figure 3 (Pons et.al 2013). A peristaltic pump takes the dye solution from the reservoir to the top of the reactor. The solution then covers the catalyst bed and the outlet is collected back in the reservoir, and the cycle is repeated for 24 hours.

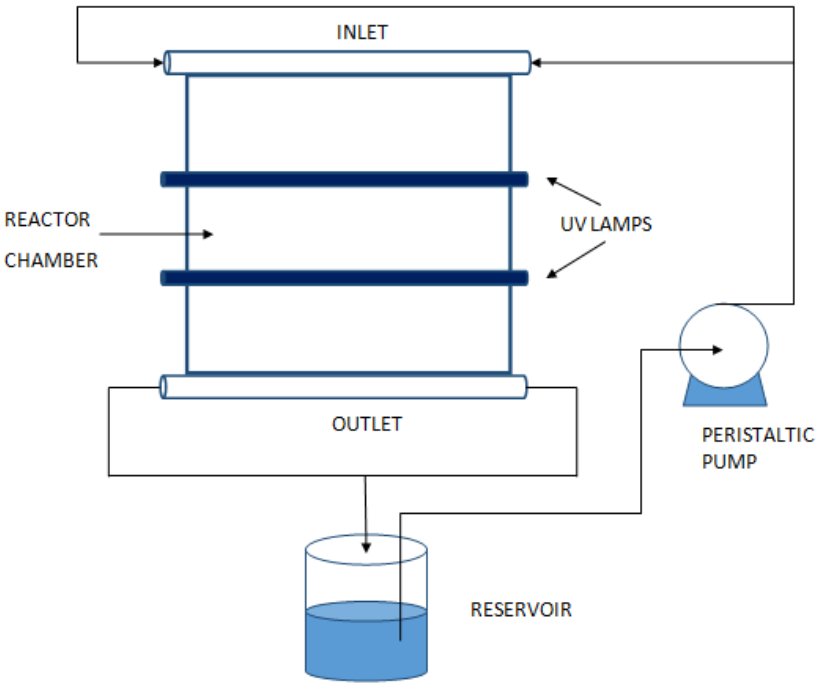

FIGURE 3: SKETCH OF PHOTOCATALYTIC REACTOR USED IN ENSIC.

The lab-built reactor used to perform the photocatalytic reactions is shown in Figure 4 (Pons, et al, 2013). The angle of the reactor is set to 37° to achieve a homogenous distribution on the solution onto the catalytic paper (Pons, et al, 2013). Two UV Lamps, (F15T8, BLB 15W, Duke, Essen, Germany) emitting around 365 nm, are positioned parallel to the reactor to provide the artificial irradiation. To ensure sufficient oxygenation, the reservoir was open to air and the outlet tubes were kept from being in the sample (Pons, et al, 2013).

FIGURE 4: PHOTOCATALYTIC REACTOR LOCATED IN THE LGRP LABORATORY AT ENSIC (PONS ET AL. 2014)

At the start of each experimental run, the reactor was washed with distilled water for about 15 minutes prior to each experimental run. Then, the dye solution (initial volume = 500 mL) was run through the reactor for about 15 minutes with the UV lights turned off at a rate of 110 mL/min. After the new dye solution seemed to have covered the reactor's surface almost evenly, a sample was taken, and then the UV lights were turned on, this time being t = 0. Samples of approximately 8 mL were collected periodically every 0.5 hours until discoloration of the solution was reached. In addition, two 50 mL samples of solution were collected in glass vials both at the beginning and the end of the experiment for total organic carbon (TOC) and total nitrogen testing. The photocatalytic reaction was allowed to run for 24 hours. Between each different hair dye, the reactor was cleansed for one day using distilled water. The tests were run in duplicate.

pH

For each experimental run, the pH of the samples at t = 0 and t = 24h was recorded using the Hach pH meter. Approximately 25 mL of the solution was used, and the pH meter was introduced in the sample. The pH was read until the Hach instrument indicated stabilization of the reading. The pH tests were performed in duplicate to ensure reproducibility of the results.

UV-Visible Spectroscopy

UV visible spectroscopy was performed on all the samples taken from the solution using the Secoman Anthelie Light UV Spectrometer. The sample was introduced in a 10 mm quartz cuvette, and the baseline for all the analyses was

distilled water. The UV-visible spectral analysis was performed over the range of 200-600 nm. After the samples were analysed, the remaining volume of each was returned to the solution reservoir to minimize volume loss.

Non-Purgeable Organic Carbon (NPOC) and Total Nitrogen (TN)

The 50 mL samples that were collected at t = 0 and t = 24 h were used for TOC and TN testing. The NPOC was measured in ENSIC using a TOC Analyzer Combustion Catalytic Oxidation/NDIR (TOC-V_{CPN}) Method Model built by Shimadzu. The total nitrogen was also measured at ENSIC using the TOC-V_{CPN} instrument with the TNM-1 accessory installed. The techniques used by these pieces of equipment were previously explained in the background.

Toxicity

The lettuce (L.sativa L.) test was performed to determine the toxicity of each of the dyes tested, both at the initial and final stage of the photocatalytic reaction. A positive and a negative control were also performed for the lettuce toxicity test. The positive controls used Vittel and Crystalline water, while the negative control used Vittel water with sodium chloride at a concentration of 5 g/L. Each sample was tested in an individual glass container. Two layers of absorbent paper were placed at the bottom of the glass jars, and then 2 mL of each sample was added to the container. Twelve lettuce seeds were evenly distributed on the absorbent paper, and the glass jar was then covered with aluminum foil. Four small holes were pierced on the foil, and the covered glass jar was then placed in a sealed plastic bag. All the containers were kept in a laboratory cabinet for five days at room temperature.

On the fifth day, the number of germinated seeds was counted and the length of the germinated seed (sum of the radicle and hypocotyl lengths) was measured for each sample. This measurement is indicated by L_{sample}. This value was used to determine the relative toxicity of each of the samples, as compared to that of pure water (positive control), and salt water (negative control). The relative toxicity, RT, is given by Equation 3.

Equation 3: Relative Toxicity

$$RT = \frac{L_{posit\_control} - L_{sample}}{L_{posit\_control} - L_{negat\_control}}$$

The relative toxicity of pure water is assumed to be 0, while the relative toxicity for salt water is assumed to be 1. The relative toxicities for each of the dyes at t=0 and t=24h were subtracted to determine the change in toxicity, ΔRT. This is shown in Equation 4.

Equation 4: Change in Toxicity

$$\Delta RT = RT_{final} - RT_{initial}$$

Therefore, a negative ΔRT would indicate a decrease of toxicity over time, while a positive ΔRT would indicate an increase in toxicity.

In addition to the relative toxicity the absolute germination index (AG) was also computed.

Equation 5: Absolute Germination Index (AG)

$$AG = \frac{N_{germ}}{N_{seed}}$$

N_{seed} is the number of seeds originally placed in the container (12 seeds) and N_{germ} is the number of germinated seeds in the tested sample (Pons, et al, 2013).

Toxicity Estimation of Dyes using T.E.S.T.

The dye molecules pertinent to each dye mixture were drawn using the USEPA T.E.S.T. (Toxicity Estimation Software Tool) version 4.0.1 (2012), which provided 2D descriptors for each of the molecules' structure. The simulation method used was consensus, and the endpoints tested were the following: Fathead minnow LC50 (96hr), Daphnia magna LC50 (48hr), T. Pyriformis IGC50 (48hr), Oral rat LD50, Bioaccumulation factor, Developmental toxicity, and Mutagenicity.

Results and Discussion

UV-Visible Spectroscopy

UV-Visible spectroscopy was taken for each commercial hair dye solutions using both DI and tap water. Two runs were performed for each dye in each type of water and samples were collected over a span of 24 hours. The averaged absorption data for each dye solution are shown in Appendix B. A comparison of each commercial dye for initial and final values between DI and tap water are shown in Appendix C. The UV-Vis data were averaged together and the data at t = 0 hours for the dyes dissolved in DI water are shown below in Figure 5. As shown, all of the dyes share an adsorption peak at a wavelength of about 253 nm. Fluorescent Glow, Fire, and Apple Green share an absorption peak at a wavelength of around 440 nm. Furthermore, Fire and Violet share a similar absorption peak around a wavelength of approximately 540 nm.

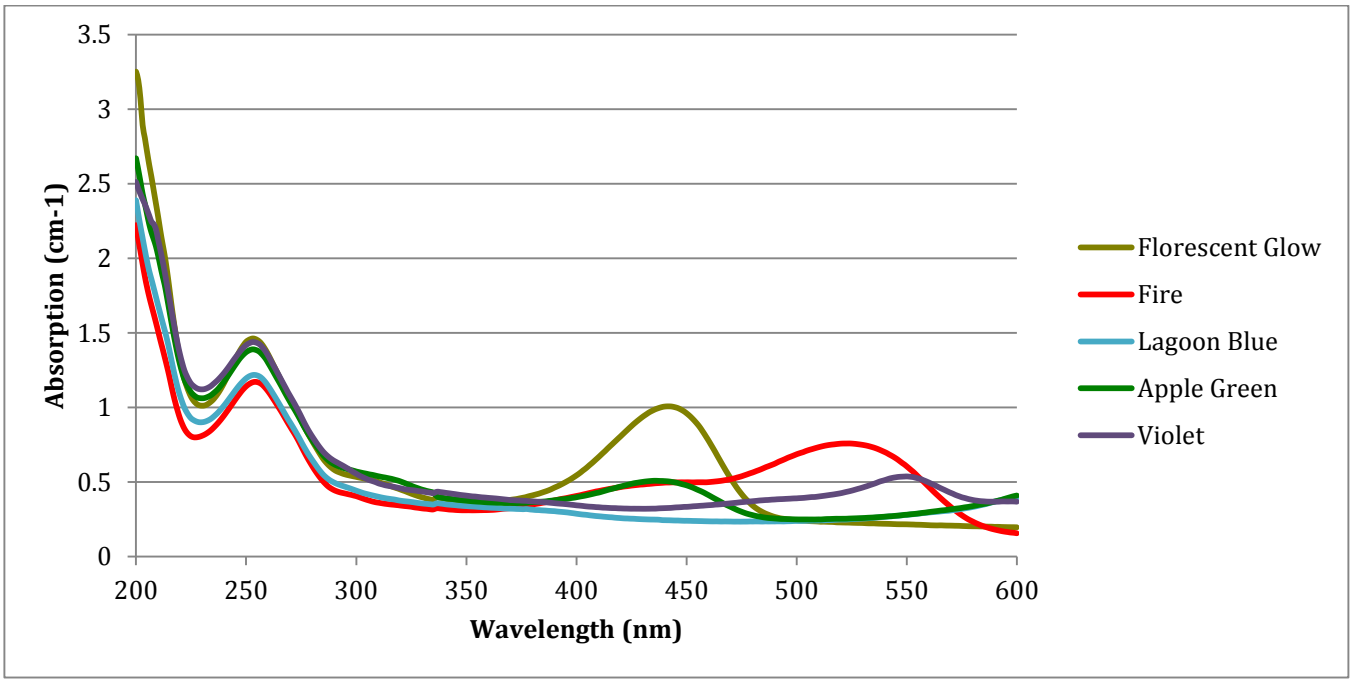

FIGURE 5: COMPARISON OF ABSORPTION VALUES FOR COMMERCIAL DYES IS DI WATER AT T=0 H.

As mentioned previously in the background, the ingredients present in these commercial dyes were cetearyl alcohol, distearoylethyl hydroxyethylmonium methosulfate, ceteareth-20, citric acid, and methyl paraben. Comparing the absorbance values shown in Figure 4 to values found in the literature (Tsourounaki et al., 2012 and Dhahir, 2013)), the peak at 253 nm corresponds to methyl paraben.

Table A.1 Appendix a lists the specific dyes present in each commercial product. The peak at 440 nm may correspond to HC Yellow 4, which is found in Fluorescent Glow, Fire, and Apple Green. However, this peak is more noticeable

for Fluorescent Glow and Apple Green than for Fire. This may be due to the presence of Basic Yellow 40 in both of these dyes.

The peak at 540 nm may correspond to either Basic Violet 2 or Acid Violet 43, which are both present in Fire and Violet. Broad variations at this peak can be due to the different concentrations of these dyes in the final commercial product.

The averaged UV-visible spectroscopy data taken at t = 0 hours for tap water are shown in Figure 6. The dyes dissolved in tap water share similar absorption peaks at the same wavelengths to the dyes dissolved in DI water. However, the absorption values are slightly lower. It is also important to note that in tap water, all of the commercial dyes share a slight peak at wavelength at approximately 290 nm. This could be due to the fact that there are compounds present in tap water that are not present in DI water such as metallic ions, organic, and inorganic compounds (EPA, 2013).

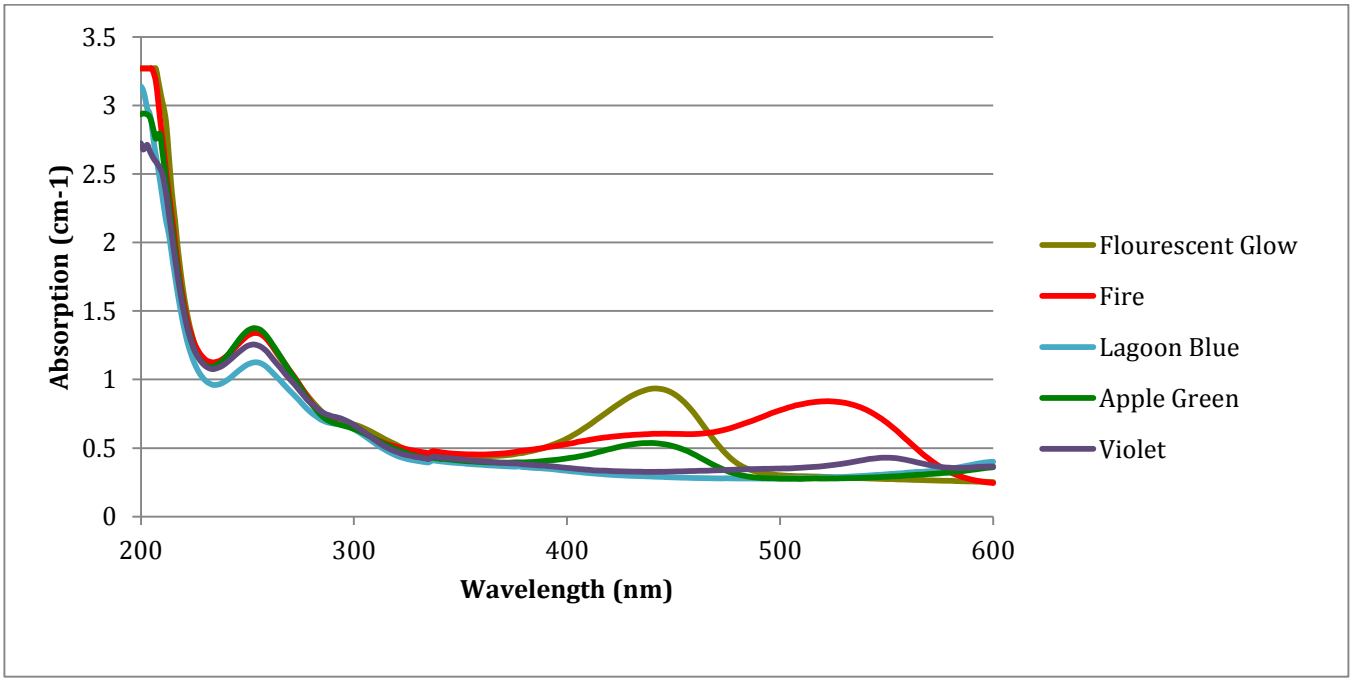

FIGURE 6: COMPARISON OF ABSORPTION VALUES FOR COMMERCIAL DYES IN TAP WATER AT T=0 H.

The UV-visible spectroscopy data taken at t = 24 hours for the commercial dyes dissolved in DI water are shown in Figure 7. As shown, Fluorescent Glow yielded the lowest absorption values at the end of the experiment, whereas Apple Green yielded the highest. Moreover, Apple Green and Violet exhibit a slight increase in absorption at a wavelength of about 335 nm, possibly corresponding to the presence of Basic Blue 99 or Brilliant Blue FCF.

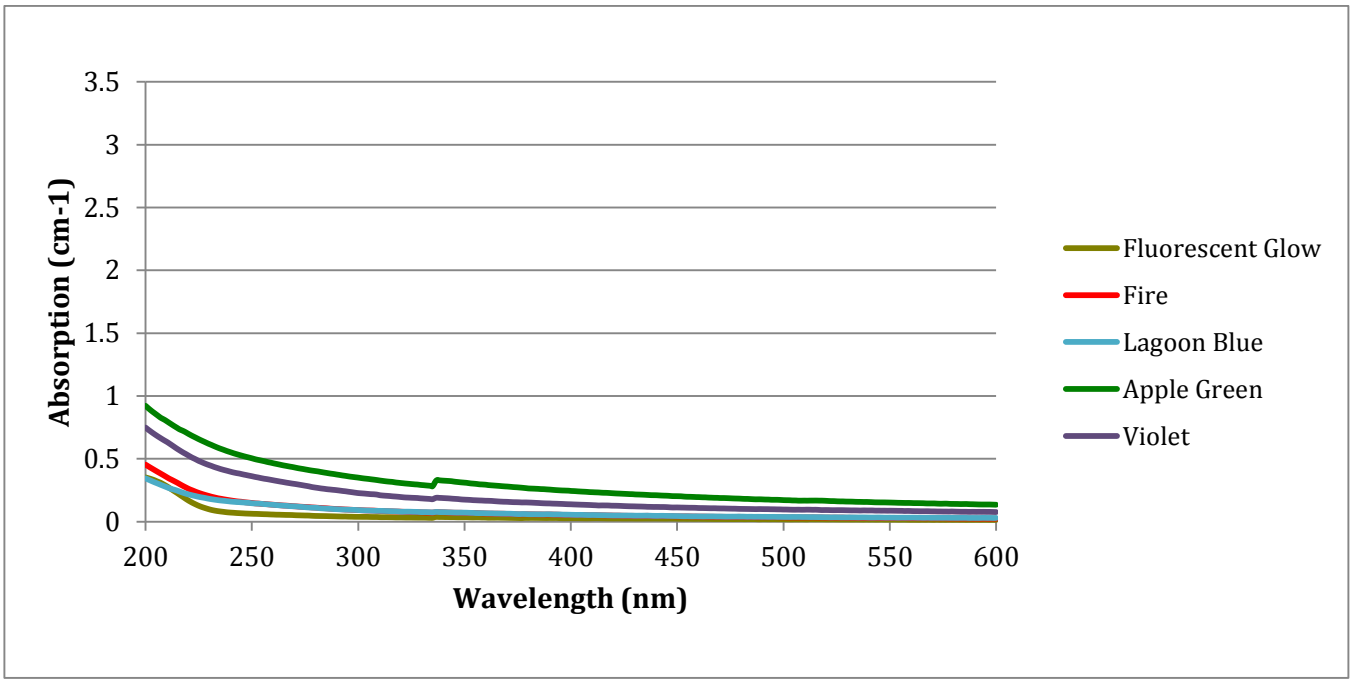

FIGURE 7: COMPARISON OF ABSORPTION VALUES FOR DYES IN DI WATER AT T=24 H.

The UV-Visible spectroscopy data for the commercial dyes dissolved in tap water at a time of t = 24 hours is shown below in Figure 8. The commercial dyes dissolved in tap water exhibit higher absorption values at lower wavelengths when compared to the final absorption values of the dyes dissolved in DI water. As previously mentioned, this could be due to the fact that there are compounds present in tap water that are not present in DI water. The slight peak at 335 nm visible in the DI water runs is not noticeable at the tap water run. In contrast to the run with DI water, Fluorescent Glow yielded the highest absorption values in tap water, whereas Lagoon Blue yielded the lowest.

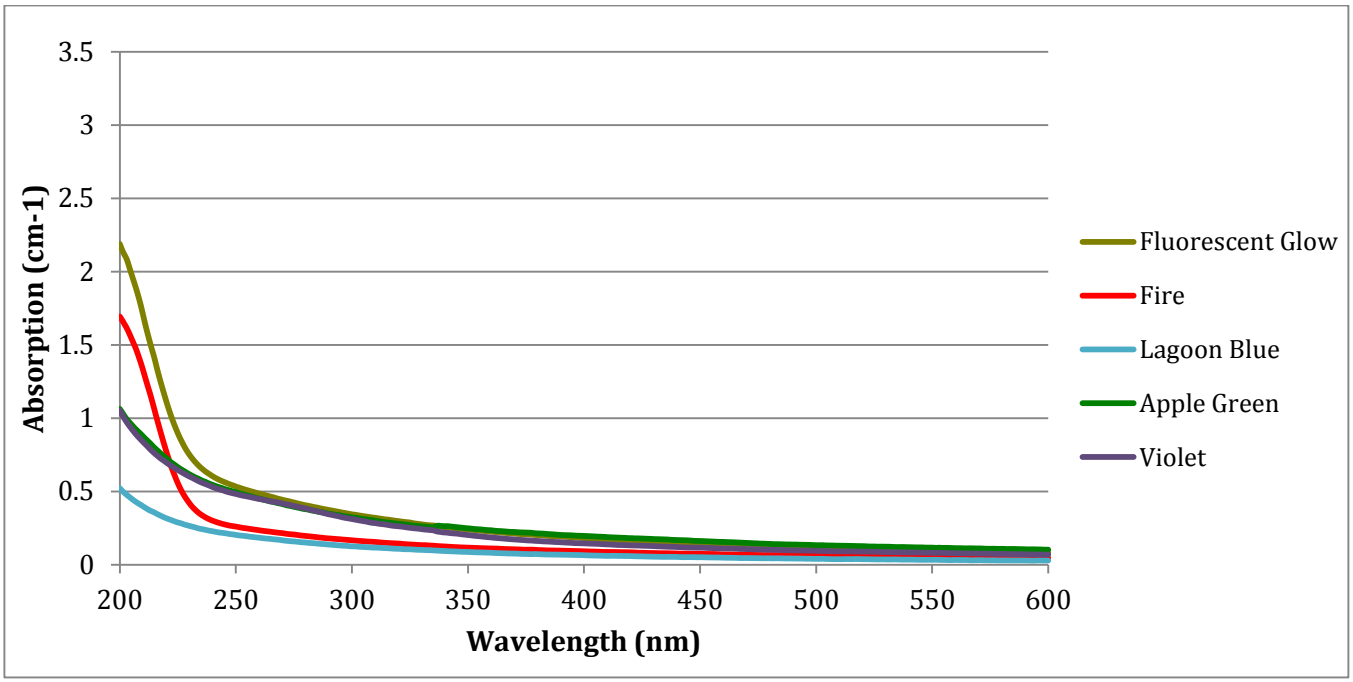

FIGURE 8: COMPARISON OF ABSORPTION VALUES FOR DYES IN TAP WATER AT T = 24 H.

The two henna dyes tested were only studied using DI water. The UV-Visible absorption data at t=0 hours and t=24 hours are shown in Figure 9. Both of the henna dyes had absorption values higher than could be recorded by the spectrometer until a wavelength of approximately 325 nm. They also yielded a slight absorption peak at a wavelength of about 450 nm. Moreover, both of the dyes resulted in similar absorption values at t=24 hours. Lawsone is the main ingredient in henna (See Appendix A for structure). The slight peak at approximately 275 nm still visible at t=24 h might correspond to this ingredient, and its dominant presence might explain its unrecorded absorption. Even though the hennas are oxidative and differ in composition to the commercial hair dyes, the absorption data proves how TiO_2-mediated photocatalysis is effective in decolorizing both substances.

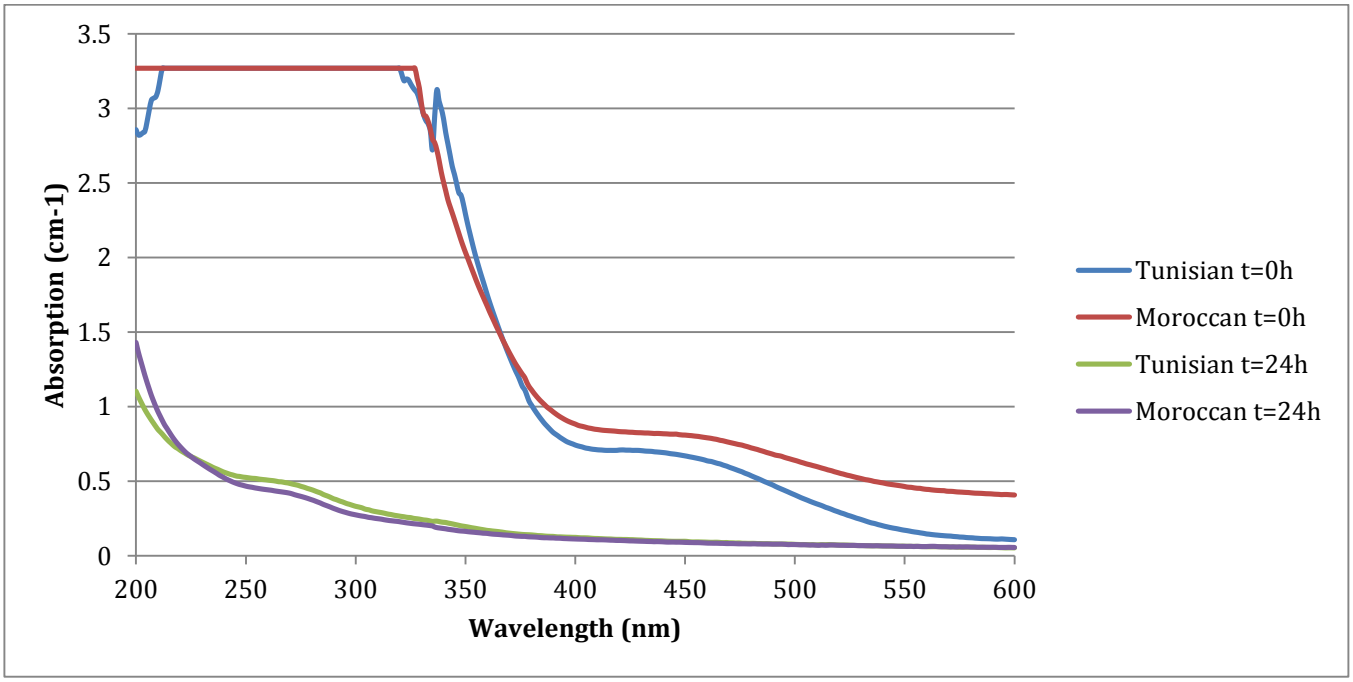

FIGURE 9: COMPARISON OF MOROCCAN AND TUNISIAN HENNA IN DI WATER.

Absorption Peaks

The absorption peaks of the commercial dyes that were recorded at the wavelengths of approximately 253 nm, 443 nm, and 540 nm from the UV-visible spectroscopy data were further analyzed. Figure 10 plots the degradation of the absorption peak occurring at 253 nm for the commercial dyes mixed in DI water versus time.

All of the commercial dyes shared a peak at this wavelength corresponding to methyl paraben. The peaks for each dye degraded in a similar logarithmic pattern. Initially, Fluorescent Glow obtained the highest absorption, 1.146 cm^{-1}, while Fire had the lowest, 1.169 cm^{-1}. After 24 hours, Lagoon Blue yielded the lowest absorption value, 0.143 cm^{-1}, while Apple Green yielded the highest, 0.492 cm^{-1}. It is also interesting to note that the average absorption value for Apple Green at t= 5 hours, 0.388 cm^{-1}, is actually less than the absorption value at t = 24 hours. This does not follow the trend of the other commercial dyes in which the final absorption value corresponds to the lowest value. Between 5 and 7 hours the degradation of Apple Green is decreasing, however, possibly at some point between 7 and 24 hours the dye molecules began to accumulate instead of degrading. There is insufficient data to make any conclusive statements or hypotheses.

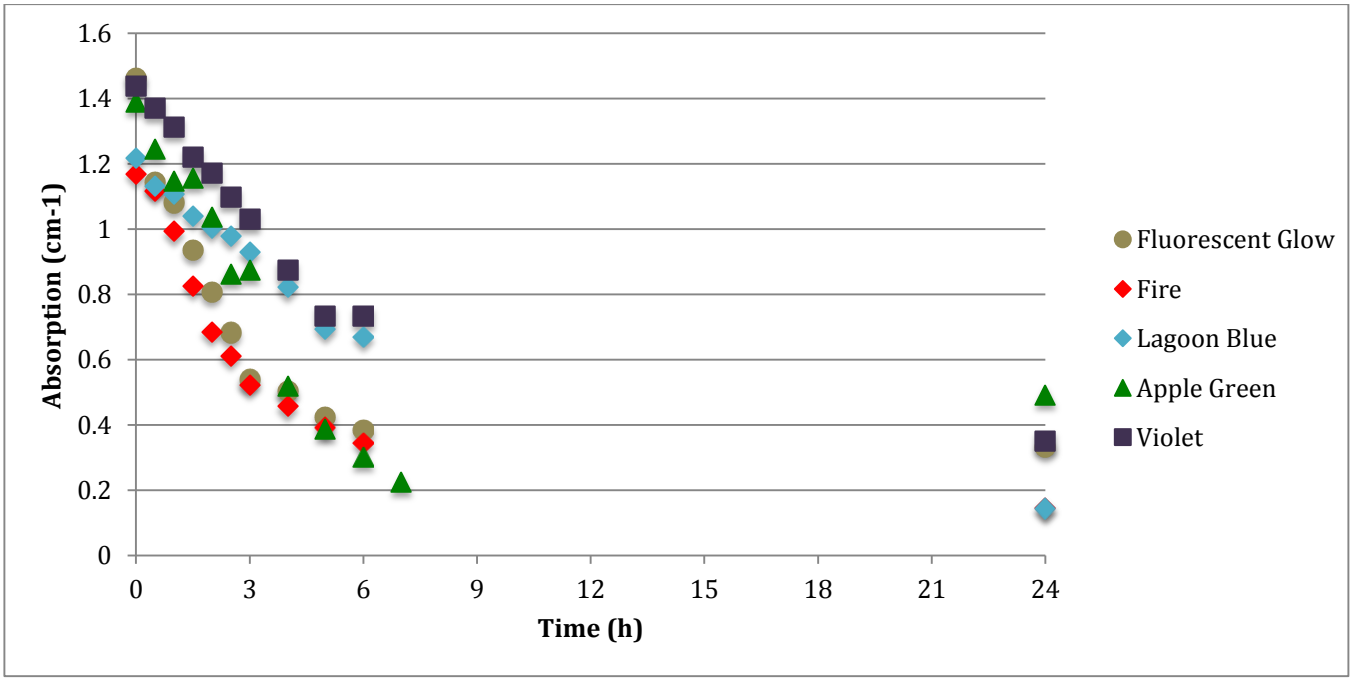

FIGURE 10: UV-VISIBLE SPECTROSCOPY ABSORPTION VALUES FOR COMMERCIAL DYES MIXED IN DI WATER WITH AN ABSORPTION PEAK AT A WAVELENGTH OF APPROXIMATELY 253 NM.

The degradation of the maximum absorption peak at a wavelength of about 253 nm recorded over time for the commercial dyes mixed in tap water are shown in Figure 11.

Compared to the dyes dissolved in DI water, the dyes in tap water yielded slightly higher absorption values at the end of the 24-hour period. However, initially, Fire, Apple Green, and Fluorescent Glow all had the highest absorption value of approximately 1.37 cm^{-1} while Lagoon Blue had the lowest absorption value at 1.125 cm^{-1}. These values follow a smoother logarithmic pattern as compared to the dyes dissolved in DI water. Lagoon Blue resulted in the lowest final absorption value of 0.198 cm^{-1} and Apple Green had the highest final absorption value, 0.582 cm^{-1}. Again, the final absorption of Apple Green was higher than absorption values between 5 and 7 hours.

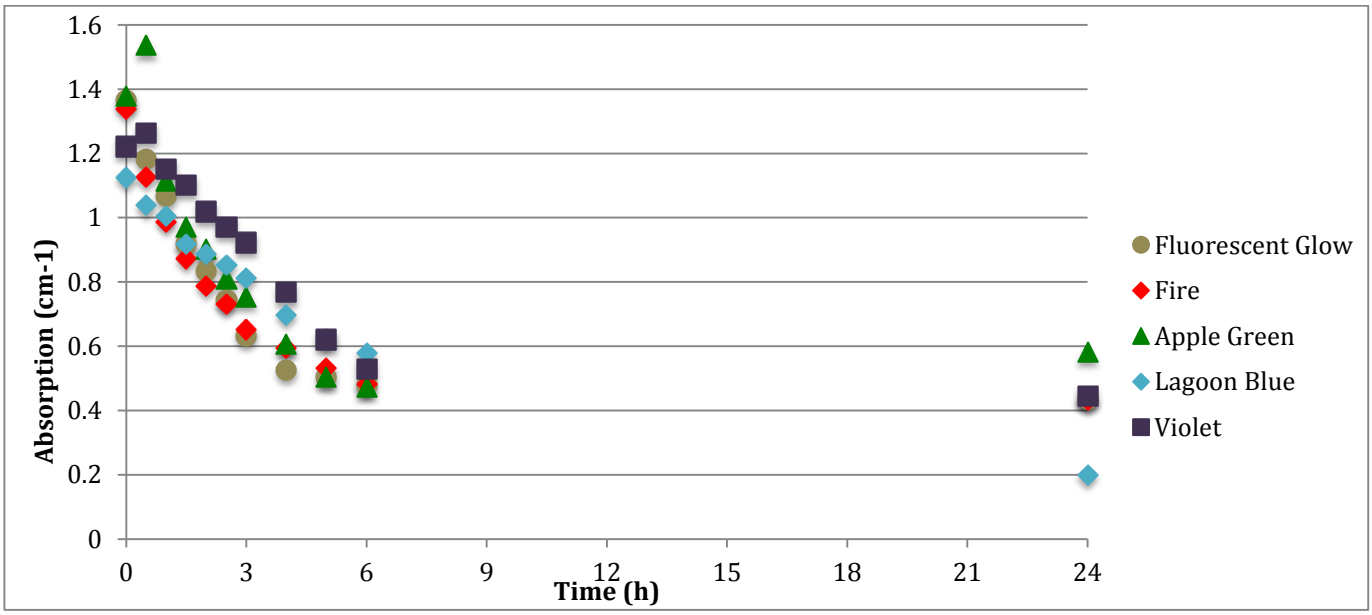

FIGURE 11: UV-VISIBLE SPECTROSCOPY ABSORPTION VALUES FOR COMMERCIAL DYES MIXED IN TAP WATER WITH AN ABSORPTION PEAK AT A WAVELENGTH OF APPROXIMATELY 253 NM.

The absorption values for the commercial dyes that share an absorption peak at a wavelength of approximately 443 nm are presented in Figure 12. The dyes that exhibited a peak at this wavelength include Fluorescent Glow, Fire, and Apple Green, and may correspond to HC Yellow 4. The discoloration of the 443 nm peak also followed a logarithmic pattern. At t = 0 hours, all three dyes had an absorption of about 0.51 cm^{-1}. Fire yielded the lowest final absorption value of approximately 0.046 cm^{-1}, possibly due to the lack of Basic yellow 40, which is present in both Fluorescent Glow and Apple Green. Apple Green yielded the highest final absorption value of 0.212 cm^{-1}. Similar to the previous peak, Apple Green yielded lower absorption values between a time of 4 hours and 7 hours than at 24-hours.

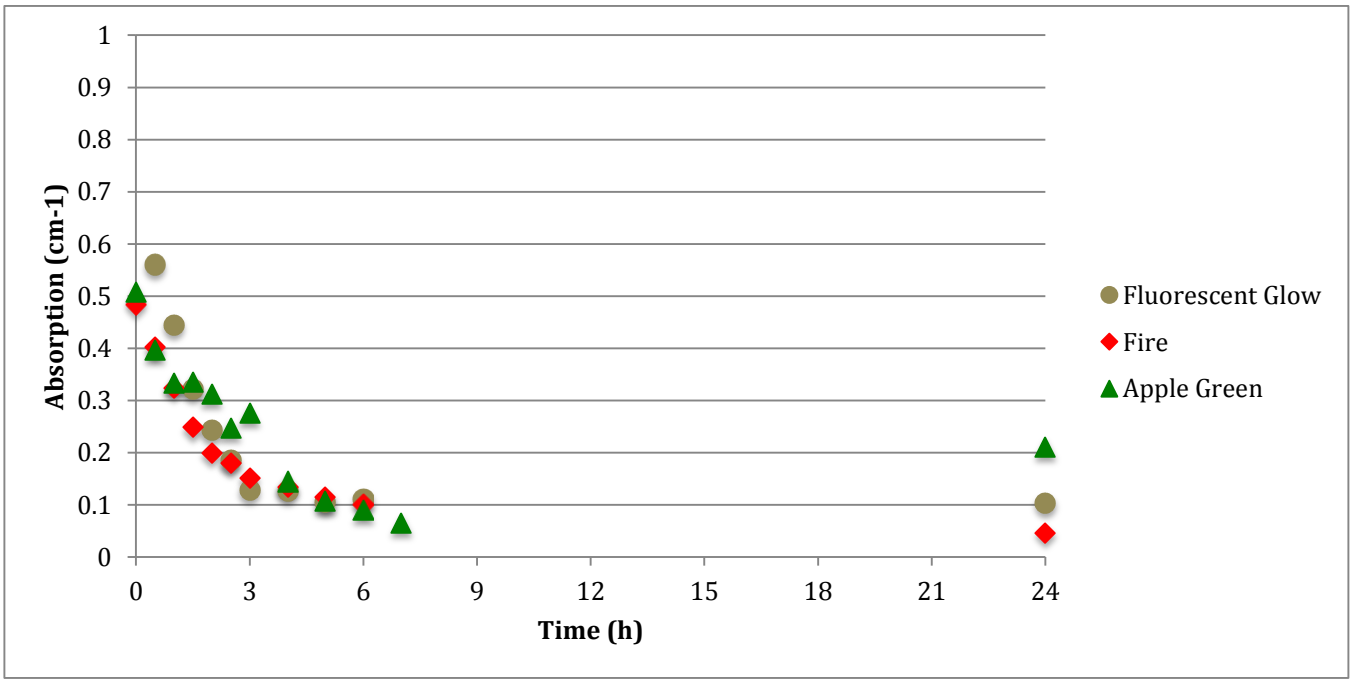

FIGURE 12: UV-VISIBLE SPECTROSCOPY ABSORPTION VALUES FOR COMMERCIAL DYES MIXED IN DI WATER WITH AN ABSORPTION PEAK AT A WAVELENGTH OF APPROXIMATELY 443 NM.

The absorption data for the commercial dyes dissolved in tap water at the wavelength of 443 nm are shown in Figure 13. Again, the data displays a smoother curve compared to the data of the dyes mixed in DI water. However, the starting absorption values of the dyes are not similar to one another, in contrast to those shown in Figure 11. Fluorescent Glow had the highest starting absorption value of 0.933 cm^{-1}, while Fire had the lowest value, 0.595 cm^{-1}. Moreover, the final absorption values for tap water are very similar between the dyes, yielding a value of approximately 0.19 cm^{-1}.

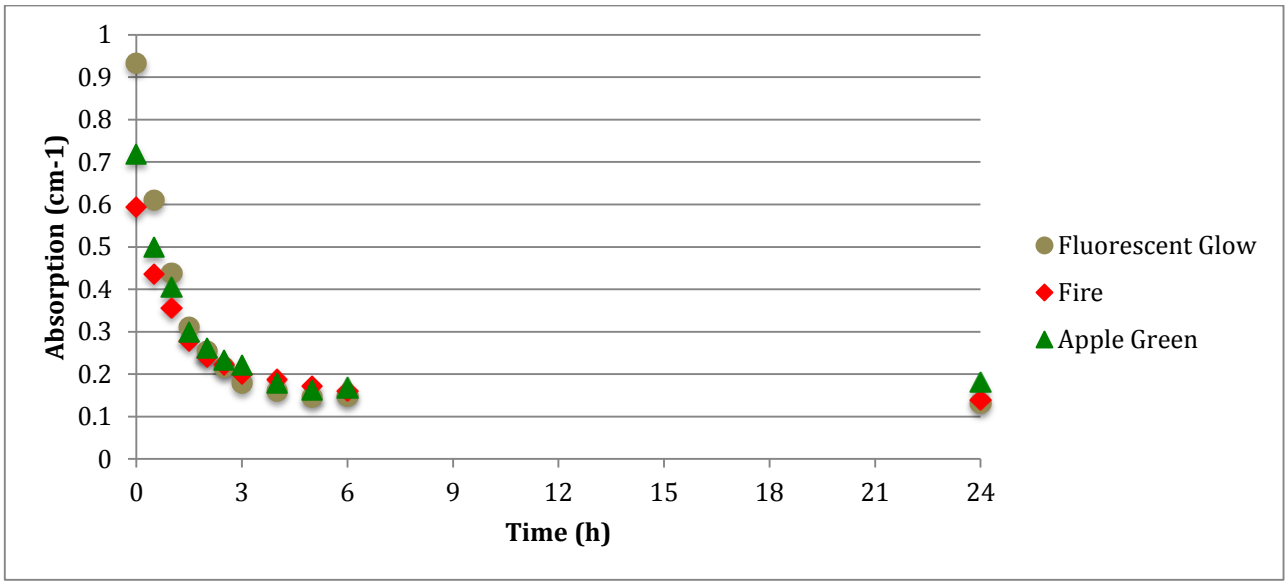

FIGURE 13: UV-VISIBLE SPECTROSCOPY ABSORPTION VALUES FOR COMMERCIAL DYES MIXED IN TAP WATER WITH AN ABSORPTION PEAK AT A WAVELENGTH OF APPROXIMATELY 443 NM.

Figure 14 shows the absorption data for the commercial dyes in DI that have a peak at approximately 540 nm. The dyes that exhibit a peak at this wavelength are Fire and Violet, and may correspond to the presence of Basic Violet 2, Acid Violet 43, or both. According to Ballarin, et al., the absorption value of 542.6 nm corresponds to Basic Red 51 (Ballarin, 2011). This dye, as can be seen in Appendix A, is present in Fire only. However, the other dyes present in Violet might also be responsible for this close absorption peak. At 540 nm, Fire displayed a higher absorption value, 0.758 cm^{-1} than Violet, 0.538 cm^{-1}. However, at the end of the experiment, Fire yielded a lower final absorption value of 0.032 cm^{-1}, compared to Violet's 0.088 cm^{-1}.

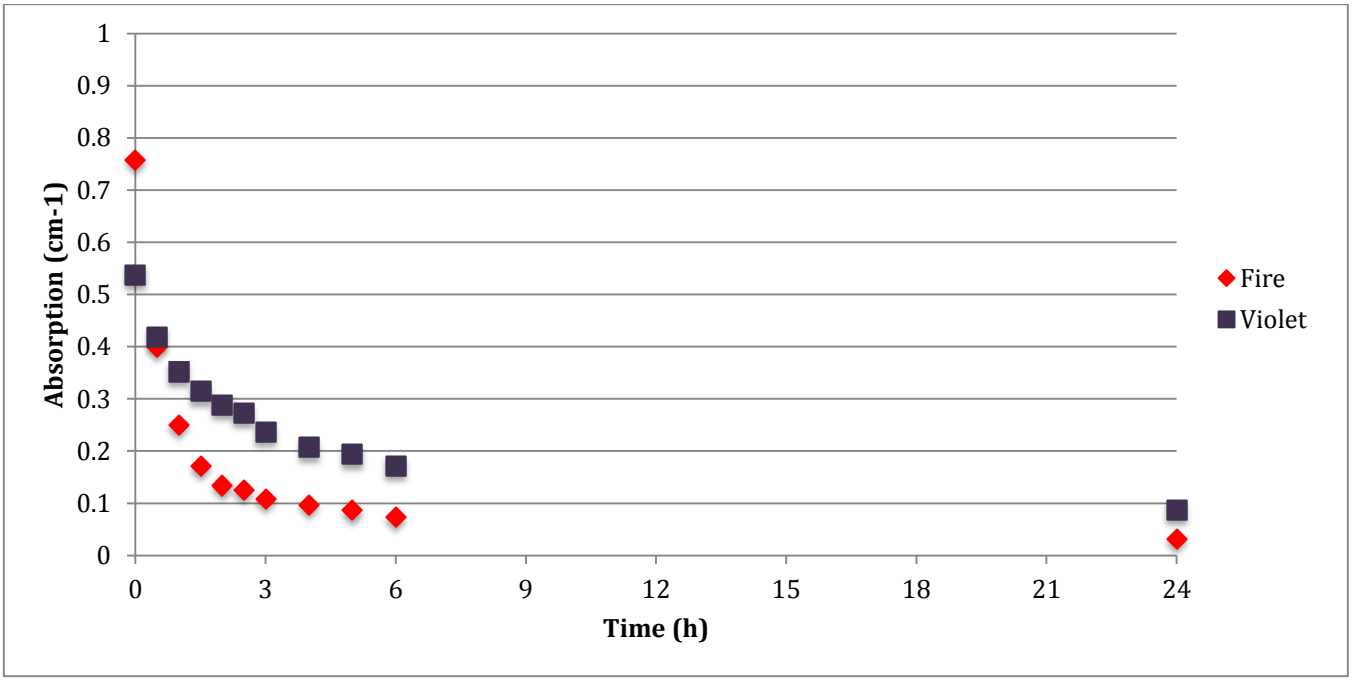

FIGURE 14: UV-VISIBLE SPECTROSCOPY ABSORPTION VALUES FOR COMMERCIAL DYES MIXED IN DI WATER WITH AN ABSORPTION PEAK AT A WAVELENGTH OF APPROXIMATELY 540 NM.

The absorption values at 540 nm for both the Fire and the Violet dyes dissolved in tap water are plotted in Figure 15. Both Fire and Violet follow the same trend as observed in DI water. Initially, Fire obtained an absorption value of 0.84 cm^{-1} which was higher than Violet's 0.451 cm^{-1}. Nevertheless, the final absorption values at this peak were roughly the same for both the dyes, approximately 0.1 cm^{-1}.

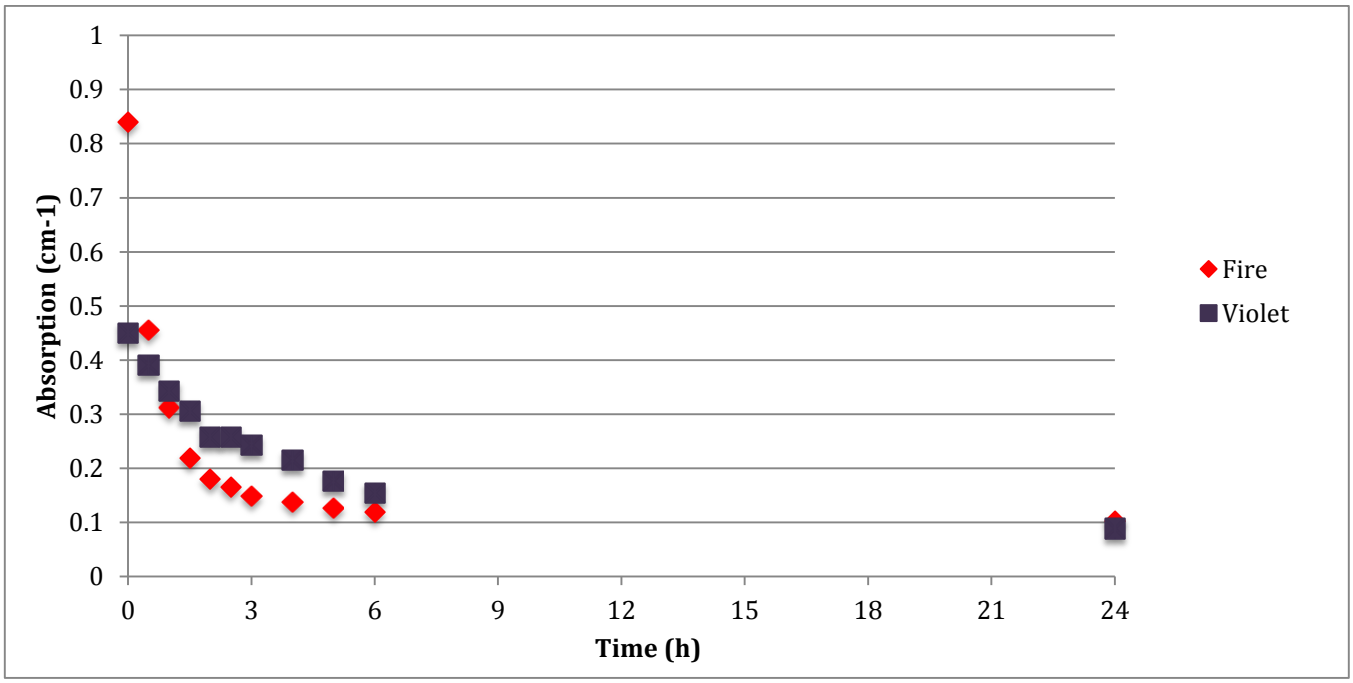

FIGURE 15: UV-VISIBLE SPECTROSCOPY ABSORPTION VALUES FOR COMMERCIAL DYES MIXED IN TAP WATER WITH AN ABSORPTION PEAK AT A WAVELENGTH OF APPROXIMATELY 540 NM.

Color Removal Efficiency

The color removal efficiency was analyzed at each absorption peak from the averaged UV-visible spectroscopy data. This efficiency was calculated from Equation 2 previously shown in the background:

$$CR\ (\%) = \left(1 - \frac{A}{A_o}\right) * 100$$

The color removal efficiencies over time for commercial dyes in DI water with an absorption peak at a wavelength of approximately 253 nm are plotted in Figure 16.

As shown, Fluorescent Glow achieved the highest color removal efficiency, 95.8%, and also discolored the fastest. Despite having a relatively high rate of color removal, Apple Green had the lowest color removal efficiency, 64.8%, at the end of the 24 hours. Although Violet had a higher rate of color removal compared to Lagoon Blue during the 6 hour period of data collection, as shown by its steeper slope, at the end of the 24 hours it had a lower color removal efficiency, 75.8%, than Lagoon Blue, 88.2%, which had the same final color removal efficiency as Fire. It is also important to note that Apple Green's final color removal efficiency is lower than its color removal efficiencies between 3.5 and 6 hours. However, without sufficent data between 6 and 24 hours, no conclusions can be made.

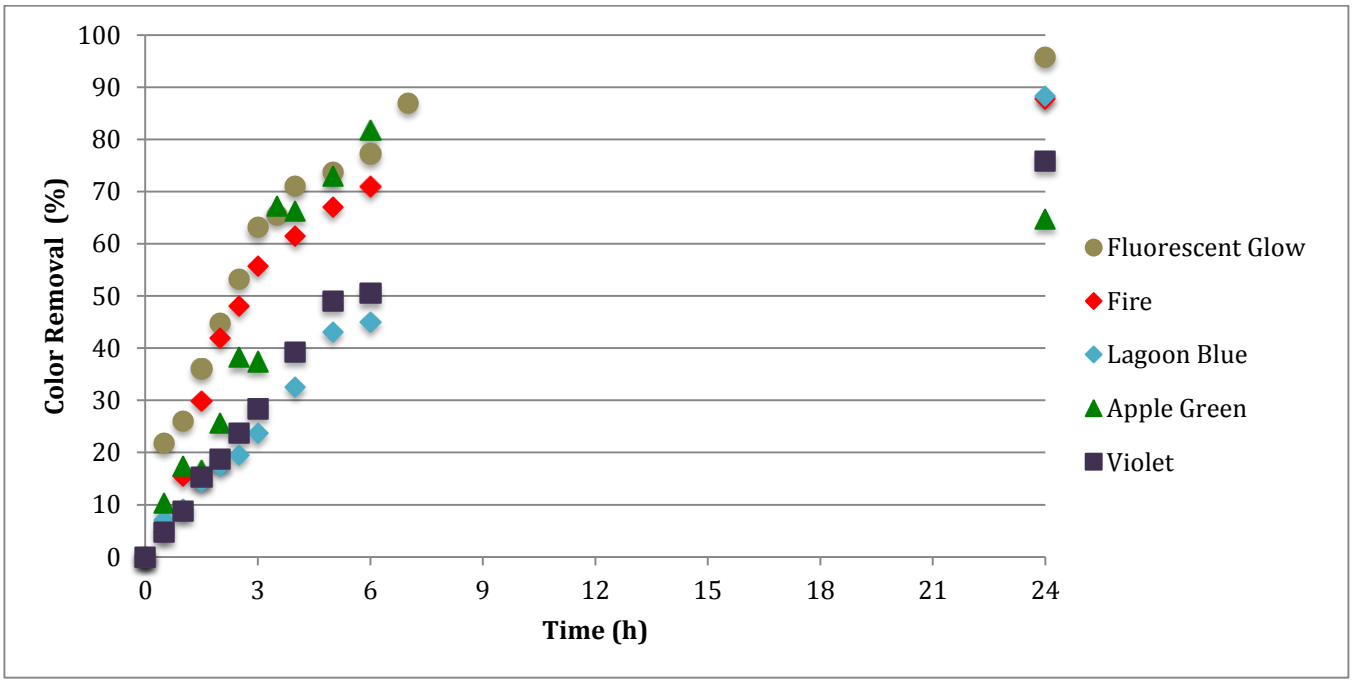

FIGURE 16: COLOR REMOVAL EFFICIENCY OVER TIME FOR COMMERCIAL DYES IN DI WATER WITH AN ABSORPTION PEAK AT A WAVELENGTH OF APPROXIMATELY 253 NM.

The color removal efficencies for the commercial dyes dissolved in tap water with an absorption peak at approximately 253 nm are displayed in Figure 17. Each of the dyes dissolved in tap water behaved differently than when dissolved in DI water. Even though Fluorescent Glow had a higher rate of removal for the first 6 hours of the experiment, Lagoon Blue had the highest color removal efficiency with a value of 81.8%. Apple Green had the lowest color removal efficiency with a value of, 57%. Fire, Violet, and Fluorescent Glow had color removal efficiency values of 67.7%, 63.5%, and 63%, respectively. Again, Apple Green yielded the lowest color removal efficiency despite having a relatively high color removal rate.

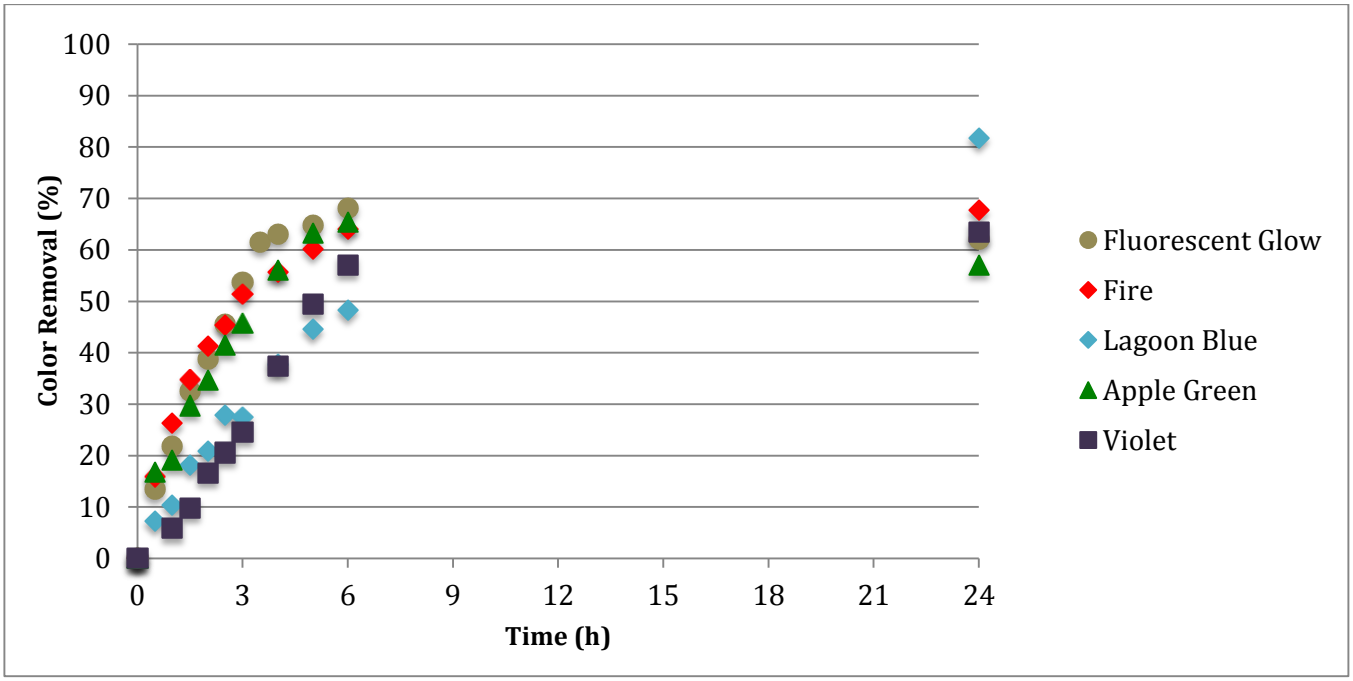

FIGURE 17: COLOR REMOVAL EFFICIENCY OVER TIME FOR COMMERCIAL DYES IN TAP WATER WITH AN ABSORPTION PEAK AT A WAVELENGTH OF APPROXIMATELY 253 NM.

Figure 18 presents the color removal efficiencies for the commercial dyes in DI water with an absorption peak at a wavelength of approximately 440 nm. These dyes that exhibit a peak at this wavelength include Fluorescent Glow, Fire, and Apple Green. Similar to the color removal efficiency at wavelength 253 nm, at 440 nm Fluorescent Glow resulted in the highest color removal efficiency with a value of 97.4%, while Apple Green resulted in the lowest, with a color removal of 58.6%. Fire yielded a color removal efficiency of 90.4%. Again, the color removal at t= 24 hours for Apple Green is lower than its color removal than between 3.5 and 6 hours.

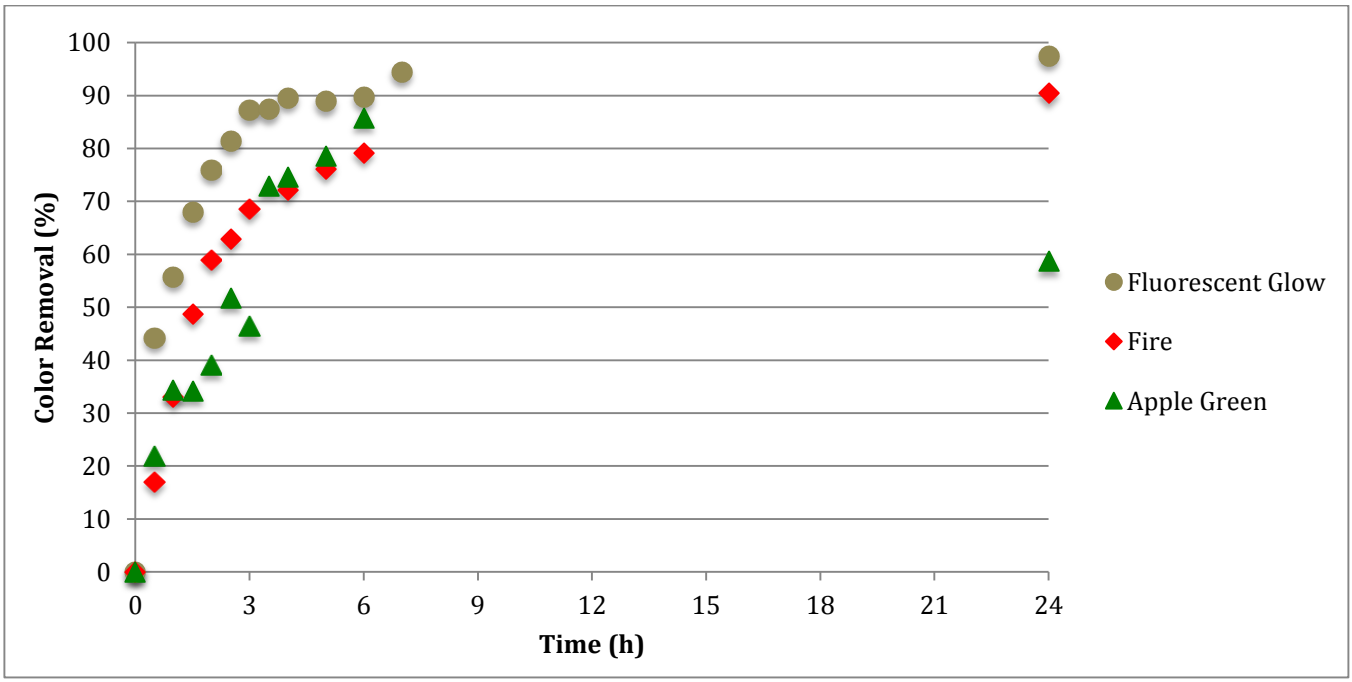

FIGURE 18: COLOR REMOVAL EFFICIENCY OVER TIME FOR COMMERCIAL DYES IN DI WATER WITH AN ABSORPTION PEAK AT A WAVELENGTH OF APPROXIMATELY 440 NM.

The color removal efficiencies for commercial dyes mixed in tap water at a wavelength of approximately 440 nm are plotted in Figure 19. Compared to the dyes dissolved in DI water at the same wavelength, the dyes dissolved in tap resulted in lower color removal efficiencies with the exception of Apple Green. Fluorescent Glow resulted in the highest color removal efficiency with a value of 83.9%, while Apple Green resulted in the lowest, with a color removal of 74.4%. Fire yielded a color removal efficiency of 76.7%. The presence of other species in the tap water may be responsible for the observed decrease of color removal efficiency when compared to the values from DI water.

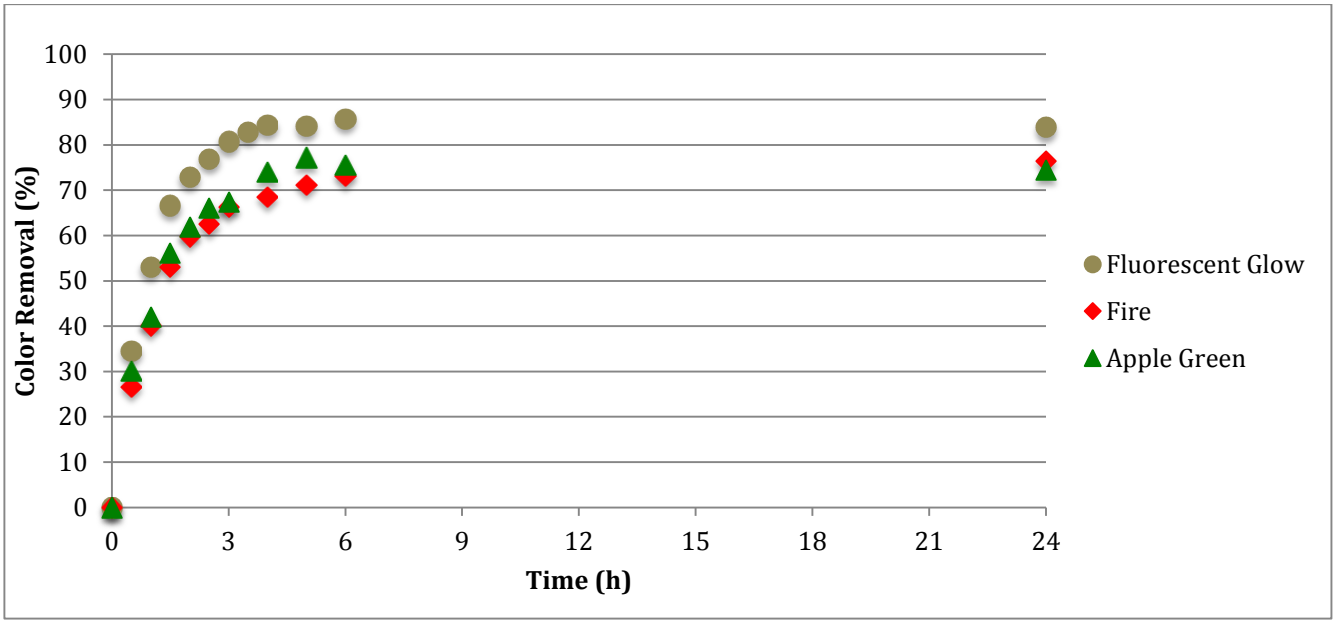

FIGURE 19: COLOR REMOVAL EFFICIENCY OVER TIME FOR COMMERCIAL DYES IN TAP WATER WITH AN ABSORPTION PEAK AT A WAVELENGTH OF APPROXIMATELY 440 NM.

The color removal efficiencies for Fire and Violet mixed in DI water at a wavelength of approximately 540 nm versus time are plotted below in Figure 20. At this wavelength, Fire yielded a higher color removal efficiency of 95.7 % than Violet, which had a color removal efficiency of 84%.

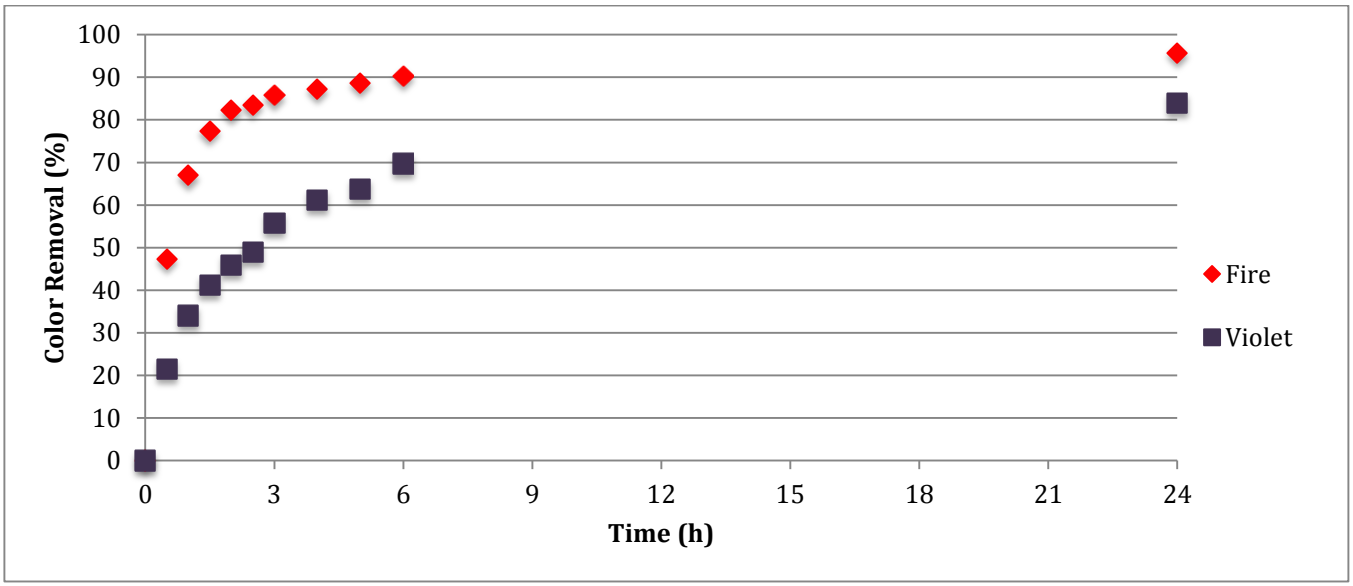

FIGURE 20: COLOR REMOVAL EFFICIENCY OVER TIME FOR COMMERCIAL DYES IN DI WATER WITH AN ABSORPTION PEAK AT A WAVELENGTH OF APPROXIMATELY 540 NM.

The color removal efficiencies for Fire and Violet dissolved in tap water at the same wavelength are displayed in Figure 21. Again, Fire resulted in a higher color removal efficiency, 87.7%, than Violet, 80.4%. However, compared to the DI water mixture, the dyes dissolved in tap water resulted in lower color removal efficiencies.

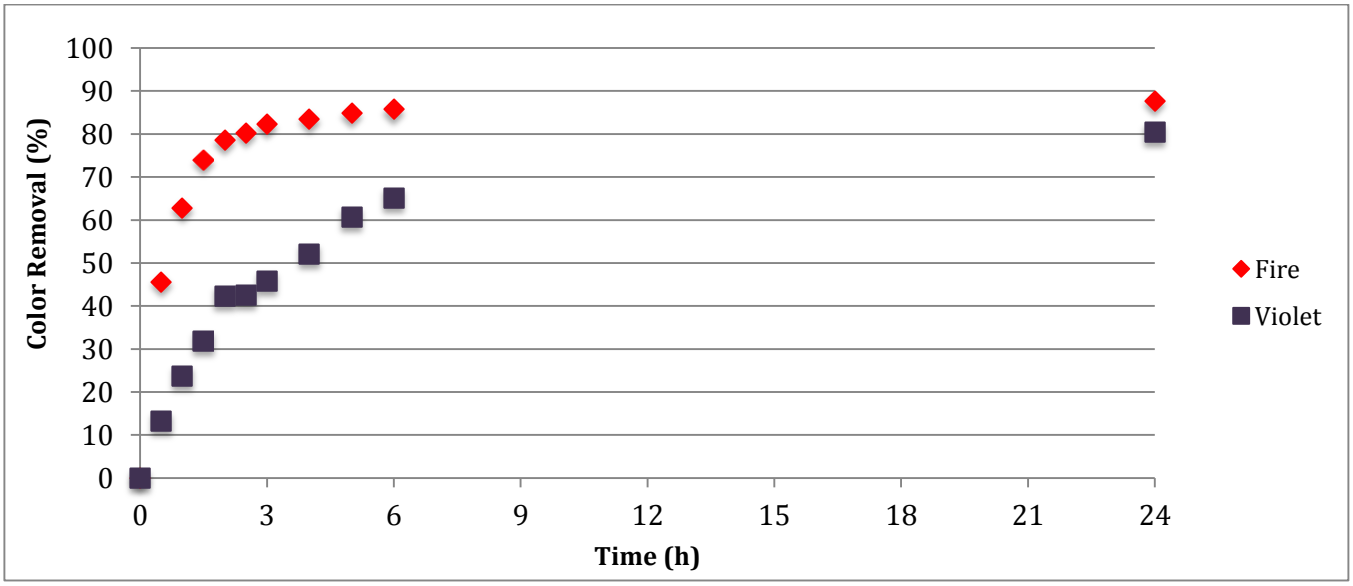

FIGURE 21: COLOR REMOVAL EFFICIENCY OVER TIME FOR COMMERCIAL DYES IN TAP WATER WITH AN ABSORPTION PEAK AT A WAVELENGTH OF APPROXIMATELY 540 NM.

Kinetics

The kinetics for the different absorption peaks were evaluated using the Langmuir-Hinshelwood approach derived in the background section. The detailed kinetic graphs for the different absorption peaks of the dyes are included in Appendix D, in addition to a Table D.1 which summarizes this data. The apparent rate constants, k_{app} , was calculated from Equation 1 shown below:

$$ln\frac{A}{A_o} = -k_{app} * t$$

Figure 22 shows the k_{app} for the five commercial dyes tested at a wavelength of approximately 253 nm. In solutions using DI water, the dye that resulted in the highest rate constant was Florescent Glow, with a value of 0.3042 h^{-1}. Apple Green had the lowest value, 0.219 h^{-1}. For tap water, the dye that resulted in the highest rate constant was again Fluorescent Glow, with a value of 0.2651 h^{-1} and the one with the lowest k_{app} was Apple Green with a value of -0.226 h^{-1}. As mentioned previously, the negative rate constants may indicate that there was accumulation or possible generation of organic compounds instead of the desired degradation. However, more studies would have to be performed as the current data is inconclusive. In all cases, except for the Lagoon Blue and Violet, the k_{app} for the runs using DI water were higher than the runs using tap water. This might indicate that the photocatalytic reaction is enhanced by the more acidic conditions when dissolving the dyes in DI water. Appendix F shows the pH values for each experimental run, the average pH for DI water being around 3-4 and that for tap water being close to 7-7.5 due to the presence of buffering agents. Under these acidic conditions, as previously discussed in the background sections, it is presumed that the main photocatalytic path is through direct oxidation, through which charge transfer between the TiO_2 molecules and the organic compounds occurs at the positive electron holes. Additionally, the conductive electron band is a major oxidizer in this path, producing other radical species that might have aided the photocatalytic reaction.

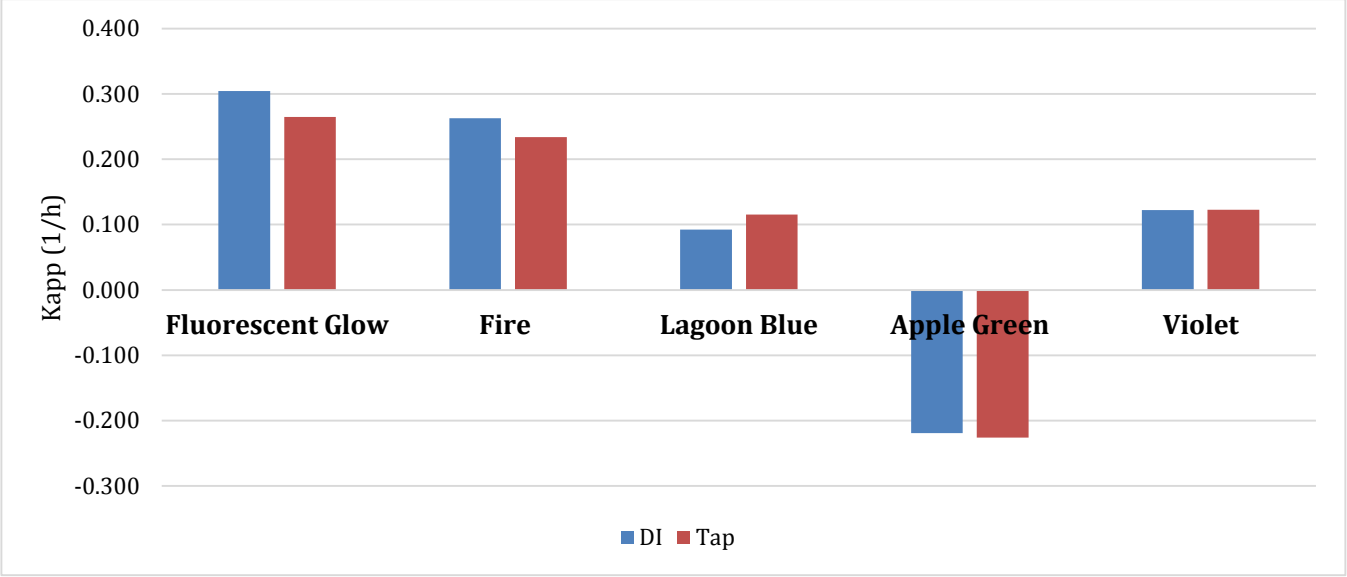

FIGURE 22. APPARENT RATE CONSTANTS FOR THE COMMERCIAL DYES IN BOTH DI AND TAP WATER AT 253 NM.

Figure 23 shows the k_{app} of the degradations of the absorption peaks for Fluorescent Glow, Fire, and Apple Green at a wavelength of 440 nm. In solutions using DI water, the dye that resulted in the highest rate constant was Florescent Glow, with a value of 0.5479 h^{-1}. Apple Green had the lowest value, 0.2179 h^{-1}. For tap water, the dye that resulted in the highest rate constant was again Fluorescent Glow, with a value of 0.4473 h^{-1} and the one with the lowest k_{app} was Apple Green with a value of -0.2637 h^{-1}.

A similar trend is observed as compared to the k_{app} values at a wavelength of 253 nm: The k_{app} values for the DI water samples are higher for both the Fluorescent Glow and Apple Green, while the k_{app} for Fire using DI and tap water are very similar. This correlates to the previous assumption that a lower pH enhances the rate of the photocatalytic reaction through direct oxidation. In addition, the rate of degradation using DI water might be greater because there are less species (e.g., various organics, inorganics, and metallic ions) that would compete for the active sites in the TiO_2 molecules and for the oxidative radical species in solution.

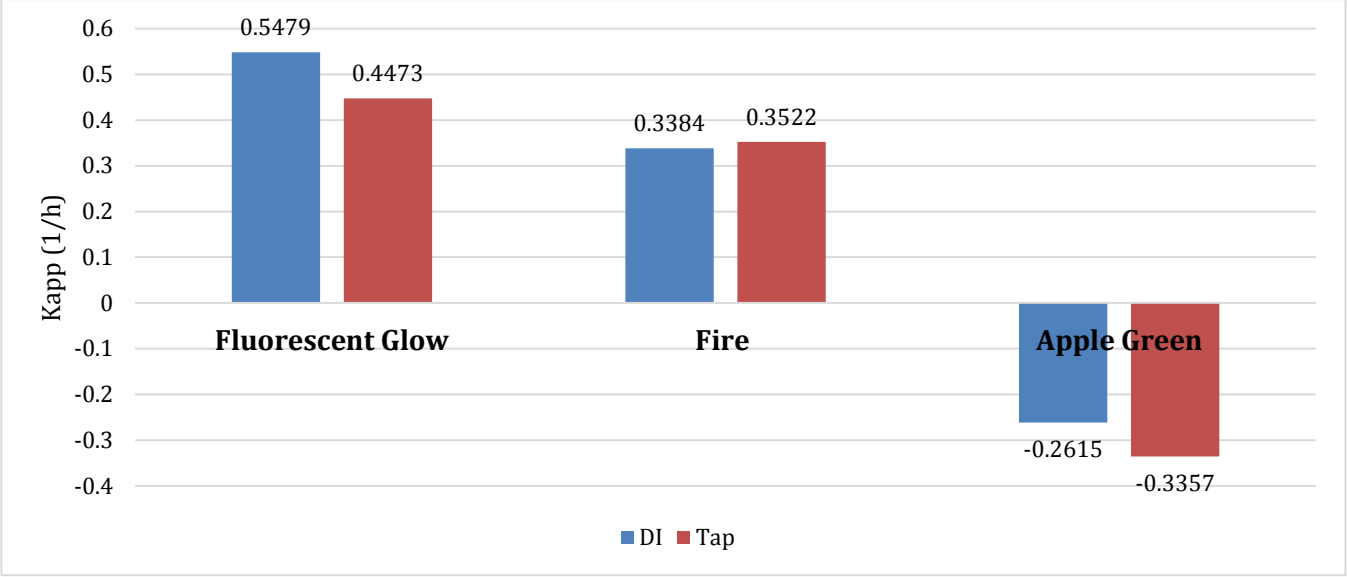

FIGURE 23. APPARENT RATE CONSTANT FOR THREE COMMERCIAL DYES AT 440 NM

Only two dyes exhibited absorption peaks at a wavelength of approximately 540 nm, Fire and Violet as Figure 24 shows below. In solutions using DI water, the dye that resulted in the higher rate constant was Fire, with a value of 0.4953 h^{-1}. Violet had the lower value, 0.2509 h^{-1}. For tap water, the dye that resulted in the higher rate constant was again Fire, with a value of 0.5220 h^{-1} and the one with the lower k_{app} was Violet with a value of -0.2057 h^{-1}.The k_{app} for Fire in tap water was slightly higher than at DI water, but the values are still in close proximity to each other. The k_{app} for Violet was higher at DI water, following the general trend observed at the 253 nm and 440 nm peaks.

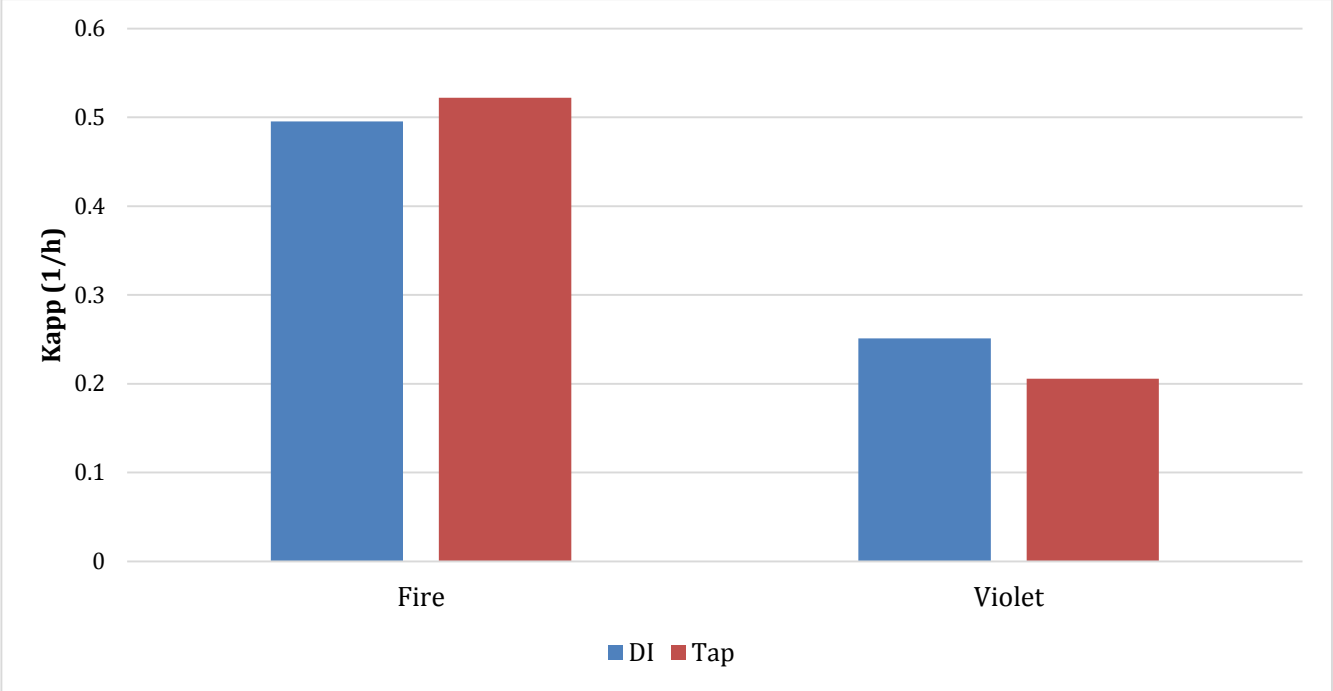

FIGURE 24. APPARENT RATE CONSTANT FOR FIRE AND VIOLET AT 540 NM

Of all the commercial products, Fluorescent Glow was the one with the highest kinetic rate constants at both 253 nm and 440 nm. This might be due to the fact that Fluorescent Glow is the product with the least number of dyes in its chemical composition (See Table A.1 in Appendix A). When compared to the other products, Fluorescent Glow has the least number of total bonds and functional groups (See Table A.2 in Appendix A). This reduced number of organic compounds present in solution possibly enhance the kinetics of the photocatalytic reaction, therefore resulting in higher k_{app} values.

Figure 25 presents the k_{app} for the Moroccan and the Tunisian hennas. Both experiments were run using DI water only. Even though the powders are produced from henna plants, the Moroccan and Tunisian henna displayed four different absorption peaks. The differences in peaks may be due to different compositions due to quality of the henna plant, production methods, etc. The Moroccan henna displayed absorption on the highest and lowest wavelength, with the value of the rate constants also being higher than those for the Tunisian henna. However, in this case, these results cannot be assumed reproducible because the experiments were run only one time.

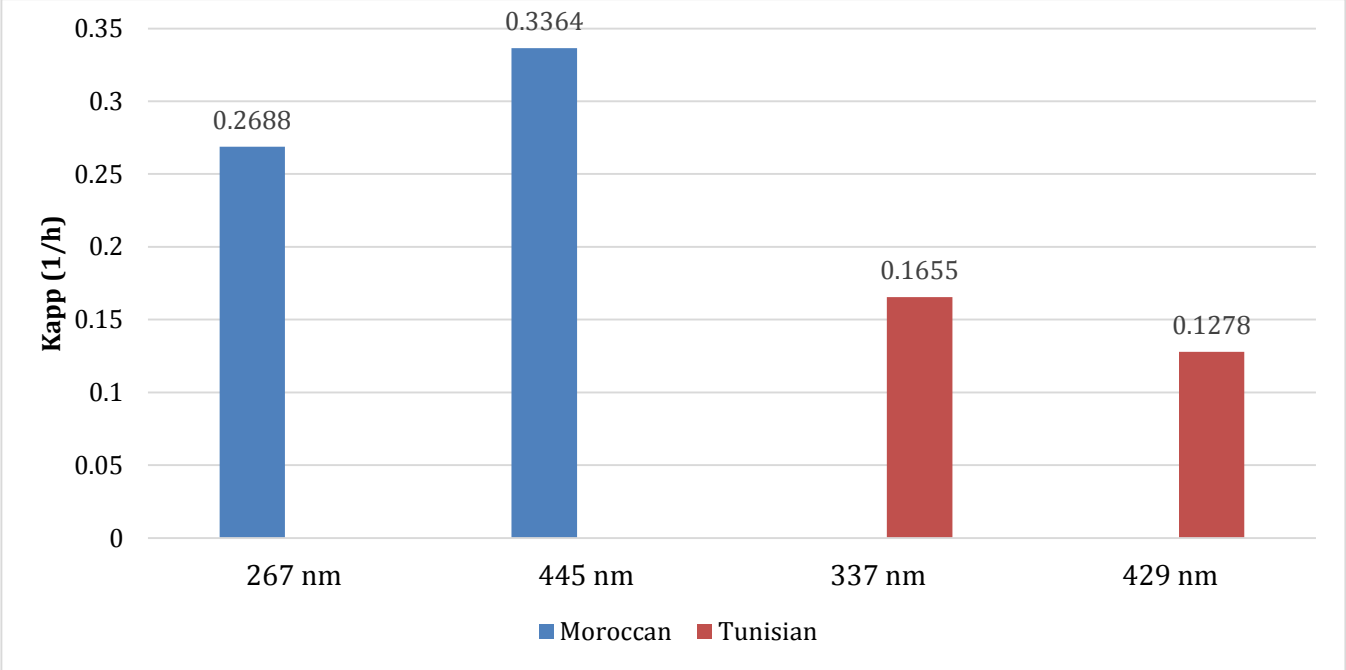

FIGURE 25. APPARENT RATE CONSTANT FOR THE MOROCCAN AND THE TUNISIAN HENNA

Mineralization

Table 2 shows the final carbon and nitrogen yield percent for the other commercial dyes tested. These yields were calculated by dividing the final nitrogen or carbon by the initial amount present, respectively, in the sample. Therefore, the lower the yields, the better the photodegradation of the dye molecules in solution. Appendix E shows the carbon and nitrogen mineralization data for each experimental run.

TABLE 2. AVERAGE YIELD % FOR TOTAL CARBON AND TOTAL NITROGEN

Commercial Dye	Carbon	Nitrogen
Fluorescent Glow in DI Water	9.10	100.57
Fluorescent Glow in Tap Water	33.00	105.06
Fire in DI Water	11.17	50.98
Fire in Tap Water	37.64	106.42
Moroccan Henna in DI Water	12.08	38.80
Lagoon blue in DI Water	9.26	53.58
Lagoon blue in Tap Water	42.14	30.20
Apple Green in DI Water	3.49	38.75
Apple Green in Tap Water	11.96	47.06
Violet in DI Water	4.91	49.99
Violet in Tap Water	62.96	126.48
Tunisian Henna in DI Water	12.24	76.16

Figure 26 shows the results of the Non-Purgeable Organic Carbon (NPOC) for all the experimental runs at the initial and final times. The experimental runs with the highest initial levels of organic carbon correspond to the Moroccan and the Tunisian hennas. These dyes had initial NPOC levels of approximately 324 mg C/L for the Moroccan henna and 301 mg C/L for the Tunisian henna. The final amount of carbon in these solutions were 39.1 and 36.7 mg C/L, respectively, resulting in final yields close to 12%. Even though the hennas exhibited the highest levels of initial carbon content, the solution that had the highest levels of carbon at the end of the 24-hour span was Lagoon Blue in Tap Water, with an average amount of 54.4 mg C/L and a yield of 42.1%. However, Violet in tap water exhibited the highest yield of all the solutions (62.96%), indicating it was least effective photocatalytic degradation.

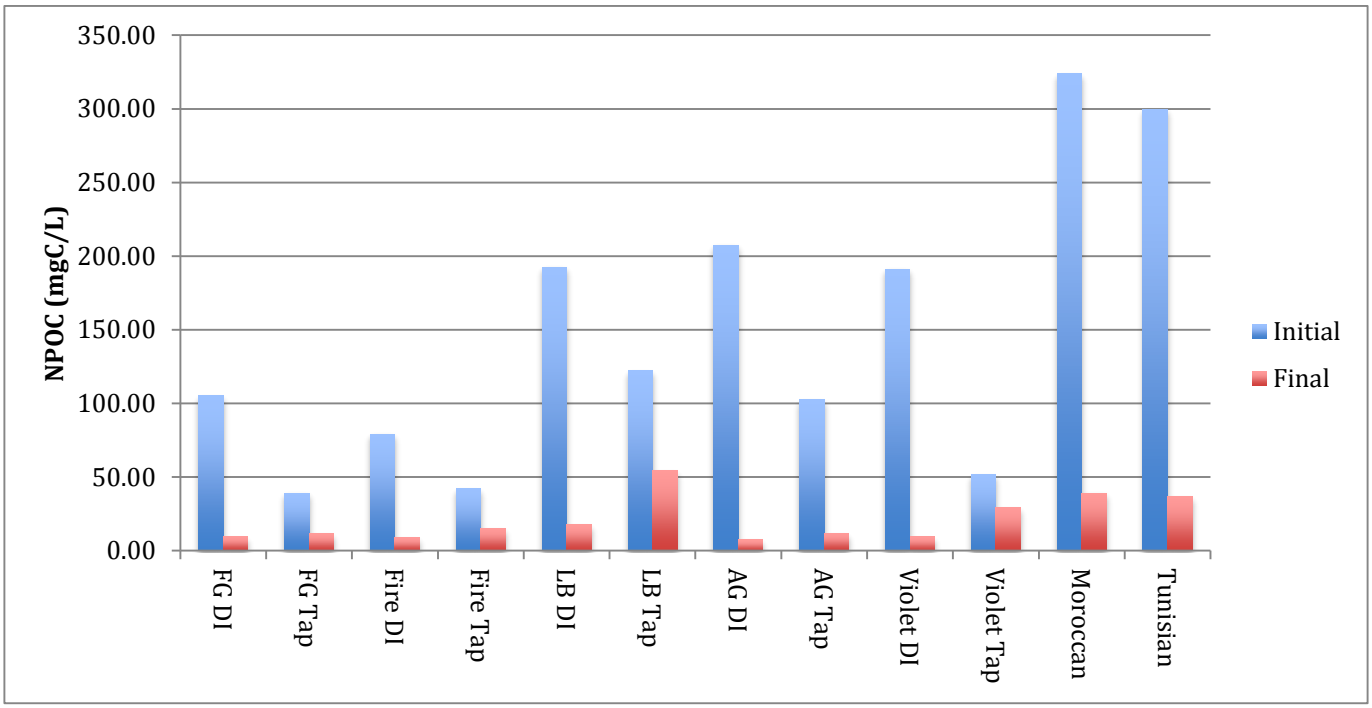

FIGURE 26: AVERAGED NON-PURGEABLE ORGANIC CARBON (NPOC) FOR EACH DYE IN DI AND TAP WATER

Fluorescent Glow (FG) in Tap water had the lowest initial carbon concentration of 39.2 mg C/L, and this might correlate to the fact that Fluorescent Glow possesses the least number of dyes in its composition (3 in total), as shown in Table A.1 in Appendix A. However, Apple Green (AG) had the lowest final carbon concentration of 7.44 mg C/L (a yield of 3.49%). Figure 25 shows how the initial levels of carbon are always higher for the solutions in DI water than in tap water. However, regardless of the carbon levels present initially, the solutions with DI water always yielded less carbon levels at the end of the photocatalytic reaction. The higher levels of carbon that resulted in DI water solutions contradict the assumption that tap water would show higher carbon levels because it has not been treated. However, the enhanced photocatalytic efficacy shown by solutions using DI water agrees with the previous results which state that possible competition by all the species present in tap water for active sites and radical species reduces the photodegradation level of the dyes.

Figure 27 shows the levels of Nitrogen present in the solutions and Appendix E shows the detailed and non-averaged data for each experimental runs. These levels range up to a level of approximately 4 mg N/L, which are significantly lower than the levels of carbon originally present in the solutions. The Moroccan henna exhibited the highest level of nitrogen in the original solution; with a value of 3.825 mg N/L. Lagoon Blue in DI water had the lowest initial nitrogen level with a value of 0.80 mg N/L. It also had the lowest final value with a nitrogen level of 0.45 mg N/L, with a yield of 53.58%. However, it was also the only case among the dye solutions in which the nitrogen yield was higher for the DI water than in tap water. Fire in tap water had the highest nitrogen levels after photocatalysis with a value of 3.02 mg N/L.

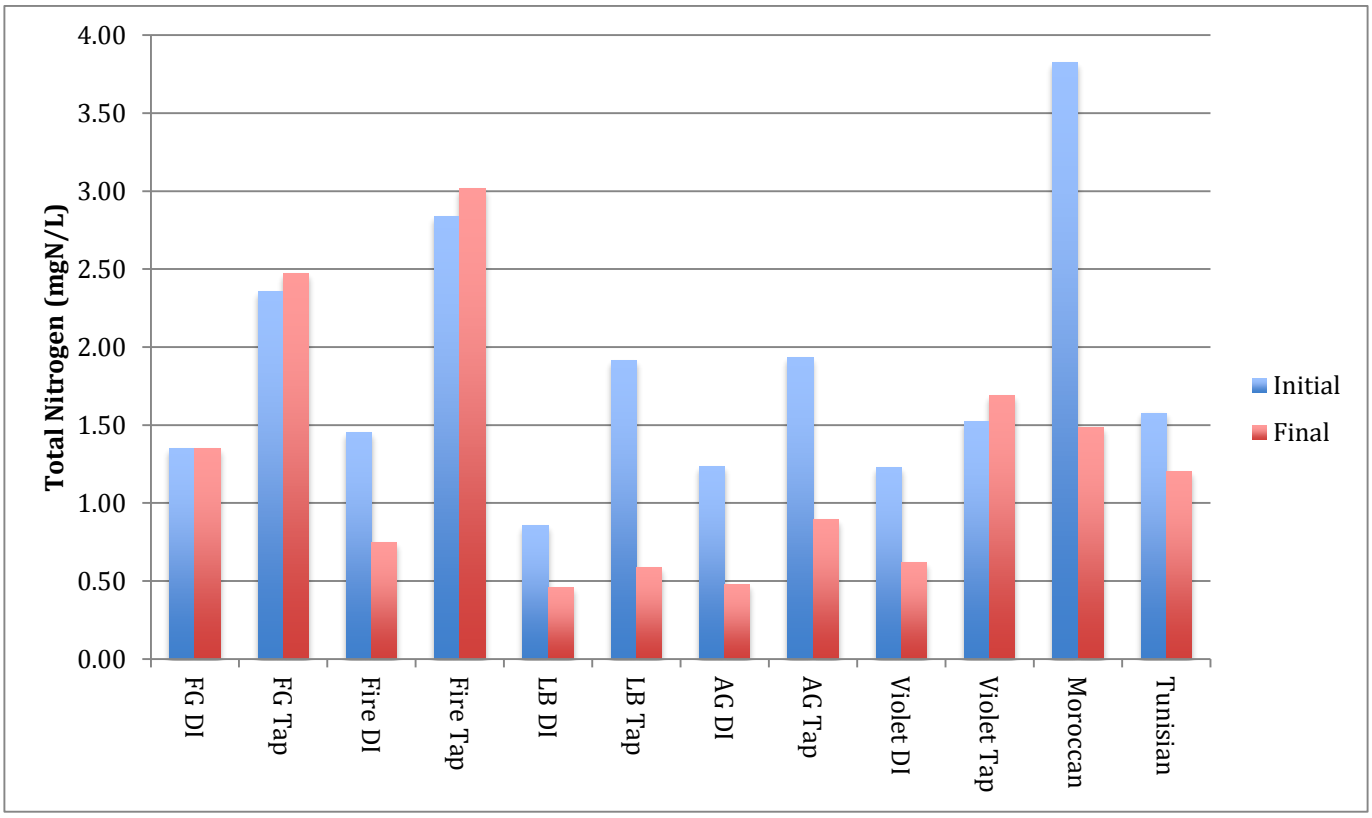

FIGURE 27: AVERAGED TOTAL NITROGEN FOR EACH DYE IN DI AND TAP WATER.

The experimental runs show a general trend decreasing levels of nitrogen in solution after photocatalysis. However, the solutions of Fluorescent Glow, Fire, and Violet in tap water show increased levels of nitrogen after photocatalysis and yields greater than 100% as shown in Table 2. As can be seen from the composition and functional dyes present in these commercial dyes, (see Appendix A) Fire, which presented the highest final nitrogen level also is the commercial product that contains the most dyes (8 in total). In addition, two of its dyes, Basic Orange 51 and Basic Red 51, are the ones that contain the greatest number of nitrogen bonds per molecule; 5 in total. Violet has 6 dyes present in its composition, one of them being Basic Yellow 51, which also has 5 nitrogen bonds per molecule. The increased nitrogen levels after the photocatalytic reaction might be due to the fact that

the initial Total Nitrogen reactor could not fully oxidize all the nitrogen molecules present in solution. After photodegradation of the dye molecules, these nitrogen bonds might have become more exposed therefore a higher quantity of them might have been oxidized in the final Total Nitrogen test, therefore yielding higher end values as shown in Figure 27.

Lettuce Test

The lettuce test was performed to determine the toxicity of the solutions before and after the TiO_2 mediated photocatalysis. The toxicity data for each experimental run is shown in Appendix G. Table 3 indicates two indexes the absolute germination index (AG) and the change in Relative Toxicity (ΔRT), which were used to assess the toxicity levels of each of the dye solutions. The RT uses the lengths of the radicle, while the AG accounts for the number of seeds. As previously discussed in the background, the change in relative toxicity is obtained by the following equation:

$$\Delta RT = RT_{final} - RT_{initial}$$

Therefore, a positive ΔRT would indicate an increase in toxicity and a negative ΔRT would indicate a decrease in toxicity. The relative toxicity values range from 0.0 to 1.0, in which zero corresponds to innocuous substances (in this case, the Vittel and Crystalline water controls). Moreover, a value of 1.0 indicates the substance is toxic.

It was assumed that after the reaction, the organic compounds present in the solutions would be oxidized; therefore, the solutions would result in lower toxicity levels at the end of the 24 hour period. However, Fluorescent Glow and Apple Green all exhibited increased relative toxicity levels in both DI and tap water, with ΔRT values of 0.1 and 0.2, respectively. This might be due to a possible formation of other organic compounds that could potentially be more harmful than the ones originally present in the solution. Even though both solutions indicated increased in their toxic levels, the tap water solution increase was higher, possibly because of the additional organic and metallic compounds. Lagoon Blue exhibited a decrease in toxicity for DI water (-0.2) but an increase in toxicity in the tap water solution (0.2), following the trend from the previous dyes. Fire, Violet, and the Moroccan Henna both exhibited decreased toxicity levels with negative ΔRT for both DI and tap water solutions. Violet showed a higher decrease in toxicity in the DI water solution than in the tap water solution, the values being -0.5 and -0.2, respectively. In contrast, for Fire, the higher decrease in toxicity was observed for tap water (-0.5) rather than DI water (-0.2).

As discussed in the background, the AG is the ration of the number of seeds that germinated after 5 days to the original number of seeds. Fluorescent Lagoon Blue, and the Moroccan henna, all dissolved in DI water, resulted in the highest absolute germination index (1.0) for both their initial and final solutions, indicating that all the seeds originally planted germinated. This contradicts the assumption that the initial solutions would have less germinated

seeds because of the increased toxicity prior to photocatalysis. However, the RT accounts for this by measuring the radicle length and comparing it to controls. It can also be observed that the AG is higher for the solutions prepared using DI water than those that used tap water. It can be assumed that the additional compounds present in tap water increase the solutions' toxicity, hindering the lettuce seeds' growth.

TABLE 3. TOXICITY INDEXES FOR ALL THE DYE SOLUTIONS

		AG	RT	ΔRT
Fluorescent Glow Distilled Water	Initial	1.0	0.0	0.1
	Final	1.0	0.1	
Fluorescent Glow Tap Water	Initial	0.9	0.2	0.1
	Final	0.8	0.3	
Fire Distilled Water	Initial	1.0	0.1	-0.2
	Final	0.9	-0.1	
Fire Tap Water	Initial	0.9	0.1	-0.5
	Final	0.9	-0.4	
Lagoon Blue Distilled	Initial	1.0	-0.1	-0.2
	Final	1.0	-0.3	
Lagoon Blue Tap	Initial	0.7	0.3	0.2
	Final	0.9	0.5	
Apple Green Distilled	Initial	1.0	0.2	0.2
	Final	0.9	0.4	
Apple Green Tap	Initial	0.9	0.3	0.2
	Final	0.8	0.5	
Violet Distilled	Initial	0.8	0.5	-0.5
	Final	1.0	0.0	
Violet Tap	Initial	0.8	1.3	-0.2
	Final	0.9	1.1	
Moroccan Henna Distilled	Initial	1.0	-0.3	-0.2
	Final	1.0	-0.5	
Controls	Positive Vittel	1.0	0.0	
	Crystalline	0.9	0.0	
	Negative Vittel + NaCl	0.9	1.0	

Conclusions and Recommendations

The systems that were analyzed in this work presented a certain degree of complexity due to the several ingredients present in the commercial dye mixtures and their unknown concentrations. Nonetheless, all the dyes exhibited the similar wavelength peak at 253 nm, and when compared to literature values, it can be assumed it corresponds to methyl paraben, a safe antimicrobial that has been approved safe for use in cosmetics and other applications. However, further research is encouraged to correctly identify the peaks at approximately 440 nm and 540 nm that were also observed in the absorbance data from the UV-Vis spectrometer.

The absorption values and the degradations rate constants observed in tap water were lower than those at DI water. This possibly suggests that the additional species present in tap water, such as organics, inorganics, and metallic ions, serve as competing species against the dye molecules for the catalytic active sites or for oxidization by the radical species present in solution. Additionally, tap water continually exhibited lower levels of carbon and nitrogen photocatalytic degradation and increased levels of toxicity when compared to DI water. This can be attributed to the possible presence of secondary reactions with the additional components present in tap water that may form other toxic by-products. Further research should be pursued in order to identify and characterize the possible secondary reactions present in tap water as this system will resemble most closely that of household wastewater and make findings more applicable to current water treatment facilities. Another reason for the higher degradation rate constants observed in DI water might be a possible higher efficacy of direct photocatalysis, favored in acidic conditions, over indirect photocatalysis. Further research can investigate both catalytic paths to create conditions that might enhance photocatalytic applications.

It is also suggested that more data points for TOC/TN analyses are included for time periods other than at the initial and the final stages of the photocatalytic reaction. This will contribute to a better characterization of the mineralization kinetics and of the secondary reactions that might occur in the system.

Generally, photocatalysis was effective in significantly reducing the levels of organic carbon and nitrogen in the samples. Even though some yields were high, average mineralization results showed that more than 40% of the organic compounds present in the samples were degraded by photocatalysis. If this level of degradation correlates at a plant scale, a significant portion of these molecules could be removed, therefore reducing the amount that is being discharged into the environment and leading to lower human health and ecological risks.

Works Cited

ACT. "Final Report on the Safety Assessment of Hc-Yellow no-2."*JOURNAL OF THE AMERICAN COLLEGE OF TOXICOLOGY*13.3 (1994): 157-66. Print.

Aguedach, Abdelkahhar, et al. "Influence of Ionic Strength in the Adsorption and during Photocatalysis of Reactive Black 5 Azo Dye on TiO2 Coated on Non Woven Paper with SiO2 as a Binder." *Journal of hazardous materials* 150.2 (2008): 250. Print.

Alan, F., and Cosmetic Ingredient Review Expert Panel. "Final Report on the Safety Assessment of Basic Blue 99."*International journal of toxicology* 26 Suppl 2.Supplement 2 (2007): 51-. Print.

Augugliaro, Vincenzo, et al. "Overview on Oxidation Mechanisms of Organic Compounds by TiO.Sub.2 in Heterogeneous Photocatalysis." *Journal of Photochemistry & Photobiology, C: Photochemistry Reviews* 13.3 (2012): 224. Print.

Ballarin, B., et al. "Effect of Cationic Charge and Hydrophobic Index of Cellulose-Based Polymers on the Semi-permanent Dyestuff Process for Hair." *International journal of cosmetic science* 33.3 (2011): 228-33. Print.

Bergfeld, WF, et al. "Final Report on the Safety Assessment of HC Yellow no. 4." *INTERNATIONAL JOURNAL OF TOXICOLOGY* 17 (1998): 39-70. Print.

Bouzaida, I., et al. "Heterogeneous Photocatalytic Degradation of the Anthraquinonic Dye, Acid Blue 25 (AB25): A Kinetic Approach." *Journal of Photochemistry & Photobiology, A: Chemistry* 168.1 (2004): 23-30. Print.

Bisutti, Isabella, Ines Hilke, and Michael Raessler. "Determination of Total Organic Carbon – an Overview of Current Methods." *Trends in Analytical Chemistry* 23.10 (2004): 716-26. Print.

Brander, James, et al. *Surface Application of Paper Chemicals*. Dordrecht: Springer Netherlands, 1997. Print.

ChemBlink Database of Chemicals from around the World. ChemBlink, 2014. Web. 18 Feb. 2014. <http://www.chemblink.com/ >.

ChemicalBook---Chemical Search Engine. ChemicalBook, 2008. Web. 18 Feb. 2014. <http://www.chemicalbook.com/>.

Cooper, Karen. "Total Organic Carbon Analysis." *Biopharm* (2001): 49. Print.

Dhahir, Saadiyah. "Spectrophotometric Determination of Methyl Paraben in Pure and Pharmaceutical Oral Solution". *Advances in natural science (2013): 1715-7862*, 6(4), p.69

d'Hennezel, O., P. Pichat, and DF Ollis. "Benzene and Toluene Gas-Phase Photocatalytic Degradation Over H2O and HCL Pretreated TiO2: By-Products and Mechanisms." JOURNAL OF PHOTOCHEMISTRY AND PHOTOBIOLOGY A-CHEMISTRY118.3 (1998): 197-204. Print.

Dye|World Dye Variety. Dye|World Dye Variety, n.d. Web. 18 Feb. 2014. <http://www.worlddyevariety.com/>.

Epling, Gary A., and Chitsan Lin. "Photoassisted Bleaching of Dyes Utilizing TiO2 and Visible Light." *Chemosphere* 46.4 (2002): 561-70. Print.

Fabbri, D., P. Calza, and AB Prevot. "Photoinduced Transformations of Acid Violet 7 and Acid Green 25 in the Presence of TiO2 Suspension." *JOURNAL OF PHOTOCHEMISTRY AND PHOTOBIOLOGY A-CHEMISTRY*213.1 (2010): 14-22. Print.

Fiume, M. Z., and Cosmetic Ingredient Review Expert. "Final Report on the Safety Assessment of Acid Violet 43."*International journal of toxicology* 20 Suppl 3.Supplement 3 (2001): 1-. Print.

Forgacs, Esther, Tibor Cserháti, and Gyula Oros. "Removal of Synthetic Dyes from Wastewaters: A Review." *Environment international* 30.7 (2004): 953-71. Print.

Glaze, W. H., Kang, J. W. & Chapin, D. H. The chemistry of water treatment processes involving ozone, hydrogen peroxide and UV-radiation. *Ozone: Sci. Eng.* 9, 335–352 (1987).

Global Chemical Network. Zhejiang NetSun Co., Ltd., n.d. Web. 18 Feb. 2014. <http://www.chemnet.com/>.

Henna. Wiley, 2010. Print.

Henna for Hair. Retrieved from web April 17, 2014. <http://www.hennaforhair.com/faq/>.

IJT. “Final Report on the Safety Assessment of Cetearyl Alcohol, Cetyl Alcohol, Isostearyl Alcohol, Myristyl Alcohol, and Behenyl Alcohol” International Journal of Toxicology. (1988) vol. 7 no. 3 359-413

http://ijt.sagepub.com/content/7/3/359.abstract

Khataee, A. R., V. Vatanpour, and A. R. Amani Ghadim. "Decolorization of C.I. Acid Blue 9 Solution by UV/Nano-TiO2, Fenton, Fenton-Like, Electro-Fenton and Electrocoagulation Processes: A Comparative Study." *Journal of Hazardous Materials* 161.2-3 (2009): 1225-33. Print.

Konstantinou, IK, and TA Albanis. "TiO2-Assisted Photocatalytic Degradation of Azo Dyes in Aqueous Solution: Kinetic and Mechanistic Investigations - A Review." *APPLIED CATALYSIS B-ENVIRONMENTAL* 49.1 (2004): 1-14. Print.

Lachheb, Hinda, et al. "Photocatalytic Degradation of various Types of Dyes (Alizarin S, Crocein Orange G, Methyl Red, Congo Red, Methylene Blue) in Water by UV-Irradiated Titania."*Applied Catalysis B, Environmental* 39.1 (2002): 75-90. Print.

LaGrega, Michael D., Phillip L. Buckingham, and Jeffery C. Evans. *Hazardous waste management*. New York: McGraw-Hill, 2001. Print.

Li, Jingyi, et al. "Photodegradation of Dye Pollutants on One-Dimensional TiO 2 Nanoparticles Under UV and Visible Irradiation." *Journal of Molecular Catalysis. A, Chemical* 261.1 (2007): 131-8. Print.

Lu, Max, and Pierre Pichat. *Photocatalysis and Water Purification: From Fundamentals to Recent Applications*. DE: Wiley-VCH, 2013. Print.

MILLS, A., RH DAVIES, and D. WORSLEY. "Water-Purification by Semiconductor Photocatalysis." *CHEMICAL SOCIETY REVIEWS* 22.6 (1993): 417-25. Print.

Neppolian, B., Choi, H. C., Sakthivel, S., Arabindoo, B., & Murugesan, V. (2002). Solar light induced and TiO2 assisted degradation of textile dye reactive blue 4.*Chemosphere, 46*(8), 1173-1181. doi:10.1016/S0045-6535(01)00284-3

Ollis, D., et al. "Photocatalyzed Destruction of Water Contaminants."*Environmental Science and Technology* 25.9 (1991): 1522-9. Print.

Pons, M.N., et al. "Comparison of Photocatalytic Degradation of Dyes in Relation to their Structure." *Environmental Science and Pollution Research* 20.6 (2013): 3570-81. Print.

Poulios, I., and I. Tsachpinis. "Photodegradation of the Textile Dye Reactive Black 5 in the Presence of Semiconducting Oxides." *JOURNAL OF CHEMICAL TECHNOLOGY AND BIOTECHNOLOGY* 74.4 (1999): 349-57. Print.

Qourzal, S., et al. "Heterogeneous Photocatalytic Degradation of 4-Nitrophenol on Suspended Titania Surface in a Dynamic Photoreactor." *FRESENIUS ENVIRONMENTAL BULLETIN*21.7A (2012): 1972-81. Print.

Reusch, William. "UV-Visible Spectroscopy." *Visible and Ultraviolet Spectroscopy*. Michigan State University, 05 May 2013. Web. 12 Feb. 2014. < http://www2.chemistry.msu.edu/>.

Reusch, William. "Visible and Ultraviolet Spectroscopy." *Visible and Ultraviolet Spectroscopy*. Michigan State University, 05 May 2013. Web. 12 Feb. 2014. < http://www2.chemistry.msu.edu/>.

Roig, B., C. Gonzalez, and O. Thomas. "Measurement of Dissolved Total Nitrogen in Wastewater by UV Photooxidation with Peroxodisulphate." *Analytica Chimica Acta* 389.1 (1999): 267-74. Print.

SCCS (Scientific Committee on Consumer Safety). “Opinion on Basic Yellow 57.” European Commission (2010) <http://ec.europa.eu/health/scientific_committees/consumer_safety/docs/sccs_o_020.pdf>.

SCCP (Scientific Committee on Consumer Products). “Opinion on Acid Green 25.” European Commission (2005) <http://ec.europa.eu/health/ph_risk/committees/04_sccp/docs/sccp_o_009.pdf>.

So, C. M., et al. "Degradation of Azo Dye Procion Red MX-5B by Photocatalytic Oxidation." *Chemosphere* 46.6 (2002): 905-12. Print.

Soccol, CR, et al. "New Perspectives for Citric Acid Production and Application." *FOOD TECHNOLOGY AND BIOTECHNOLOGY* 44.2 (2006): 141-9. Print.

Soni, M. G., et al. "Evaluation of the Health Aspects of Methyl Paraben: A Review of the Published Literature." *Food and Chemical Toxicology* 40.10 (2002): 1335-73. Print.

SpecialChem4Cosmetics. “Ceteareth-20.” Retrived from web: April 20, 2014 <http://www.specialchem4cosmetics.com/services/inci/ingredient.aspx?id=2434>.

SpecialChem4Cosmetics. “Distearoylethyl Hydroxyethylmonium Methosulfate.” Retrived from web: April 20, 2014 <http://www.specialchem4cosmetics.com/services/inci/ingredient.aspx?id=4365>.

Stenholm, A., S. Holmstrom, and A. Ragnarsson. "Total Nitrogen in Wastewater Analysis: Comparison of Devarda's Alloy Method and High Temperature Oxidation Followed by Chemiluminescence Detection." *JOURNAL OF ANALYTICAL CHEMISTRY* 64.10 (2009): 1047-53. Print.

Tanaka, Keiichi, Kanjana Padermpole, and Teruaki Hisanaga. "Photocatalytic Degradation of Commercial Azo Dyes." *Water Research* 34.1 (2000): 327-33. Print.

Tang, Walter Z., and C. P. Huang. "Photocatalyzed Oxidation Pathways of 2,4-Dichlorophenol by CdS in Basic and Acidic Aqueous Solutions." *Water Research* 29.2 (1995): 745-56. Print.

Tissue, Bryan M. "Ultraviolet and Visible Absorption Spectroscopy (UV-Vis)." *The Chemistry Hypermedia Project*. Virginia Tech, 2000. Web. 13 Feb. 2014. <http://www.files.chem.vt.edu/>.

Tsourounaki, K., Aroniada, G., and Psillakis, E. “Photodegradation of Methylparaben in Various Environmental Aqueous Solutions by 254 nm Irradiation.” Department of Environmental Engineering, Technical University of Crete (2012) <http://www.srcosmos.gr/srcosmos/showpub.aspx?aa=16478>.

Vincenzo, Augugliaro. *Clean by Light Irradiation: Practical Applications of Supported TiO2*. GB: Royal Society of Chemistry, 2010. Print.

Volk, Christian, et al. "Monitoring Dissolved Organic Carbon in Surface and Drinking Waters." *Journal of environmental monitoring : JEM* 4.1 (2002): 43-7. Print.

Appendices

The list of the individual experiments with their titles is listed below for reference to the individual experiments displayed in charts.

List of Experiments	
Solution	**Experiment No.**
Fluorescent Glow in DI Water	1
	2
	3
Fluorescent Glow in Tap Water	4
	5
Fire in DI Water	6
	7
Fire in Tap Water	8
	9
Moroccan Henna in DI Water	10
Lagoon Blue in DI Water	11
	12
Lagoon Blue inTap Water	13
	14
Apple Green in DI Water	15
	16
Apple Green in Tap Water	17
	18

Violet in DI Water	19
	20
Violet in Tap Water--Redo	21
Violet in Tap Water	22
	23
Tunisian Henna in DI Water	24

Appendix A: Ingredients and Characterization of the Dyes

TABLE A.1: DYE INGREDIENTS

	Fluorescent Glow	Fire	Lagoon Blue	Apple Green	Violet	Hennas
HC Yellow 2				X		
HC Yellow 4	X	X	X	X		
Basic Yellow 40	X			X		
Basic Yellow 57					X	
Acid Green 25 (CI61570)	X					
Basic Orange 31		X	X			
HC Blue 15		X	X	X		
Basic Blue 99 (CI 56059)		X	X	X	X	
Brilliant Blue FCF (42090)				X	X	
Basic Violet 2 (CI 42520)		X	X		X	
Basic Violet 13 (CI 42536)					X	
Acid Violet 43 (CI 60730)		X	X		X	
Basic Violet 16		X	X			
Basic Red 51		X	X			
Lawsone						X
Para-phenylenediamine ***may be present***						X

The following information for each of the functional groups present in the several dyes was obtained from the T.E.S.T. software

TABLE A.2: FUNCTIONAL GROUPS FOR EACH DYE

	Rings	Double bonds	Aromatic bonds	Carbon	Nitrogen	Oxygen	Halogen (other)	Phenol Groups	Benzene-like rings	MW
HC Yellow 2	1	1	6	8	2	3	0	0	1	183
HC Yellow 4	1	1	6	10	2	5	0	0	1	242.3
Basic Yellow 40	4	2	16	22	3	2	0	0	2	363
Basic Yellow 57	3	3	12	19	5	1	0	0	2	336.5
Acid Green 25 (CI61570)	5	18		28	2	8	2 Na 1 S	0		
Basic Orange 31	2	1	11	11	5	0	1*	0	1	216.3
HC Blue 15	3	4	12	23	2	0	2	0	2	397
Basic Blue 99 (CI 56059)	3	3	12	20	4	2	1	1	2	430
Brilliant Blue FCF (42090)	5	22		37	2	9	2 Na 3 S	0		
Basic Violet 2 (CI 42520)	3	4	12	22	3	0	0	0	2	328
Basic Violet 13 (CI 42536)	Data not available									
Acid Violet 43 (CI 60730)										
Basic Violet 16	3	2	12	22	3	0	1*	0	1	335.5
Basic Red 51	2	1	11	13	5	0	1*	0	1	244.4

TABLE A.3: INGREDIENT CHEMICAL COMPOSITIONS, MOLECULAR STRUCTURES, AND CAS NUMBERS

	Chemical Composition	Molecular Structure	CAS Number
HC Yellow 2	$C_8H_{10}N_2O_3$	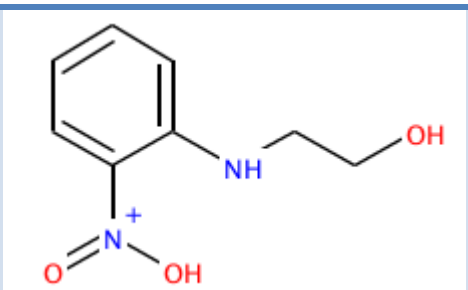	4926-55-0
HC Yellow 4	$C_{10}H_{15}N_2O_5$	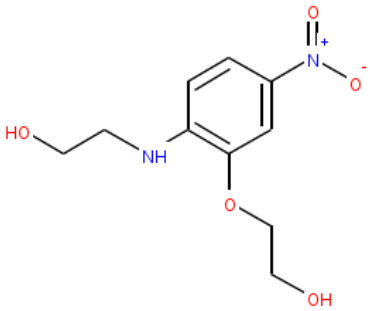	59820-43-8
Basic Yellow 40	$C_{23}H_{27}N_3O_6S$	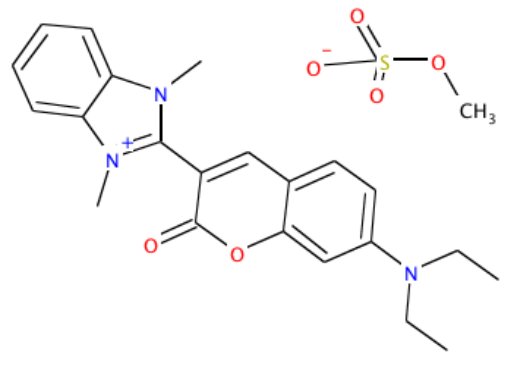	35869-60-4
Basic Yellow 57 (CI 12719)	$C_{19}H_{22}ClN_5O$	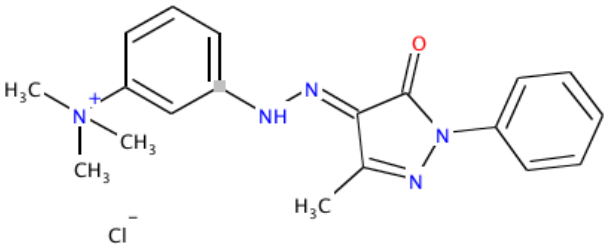	68391-31-1

	Chemical Composition	Molecular Structure	CAS Number
Basic Orange 31	$C_{11}H_{14}N_5Cl$	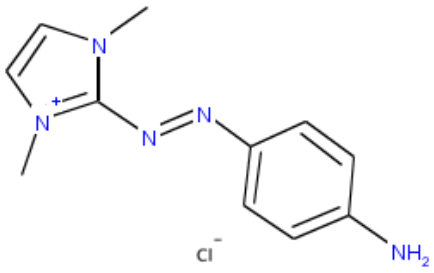	97404-02-9
HC Blue 15	$C_{23}H_{22}Cl_2N_2\,H_3O_4P$	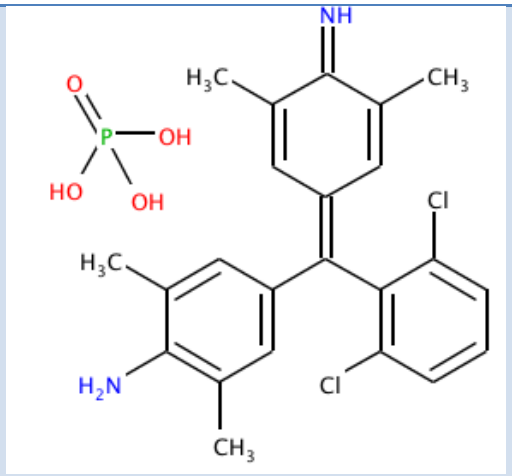	74578- 10-2
Basic Blue 99 (CI 56059)	$C_{19}H_{20}BrClN4O_2$	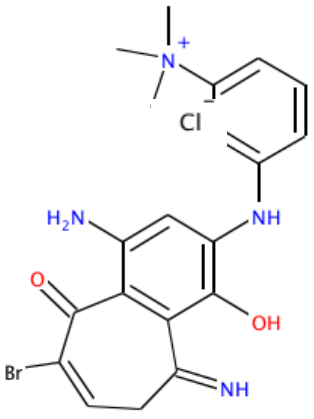	68123-13-7

Brilliant Blue FCF (CI 42090)	$C_{37}H_{34}N_2Na_2O_9S_3$	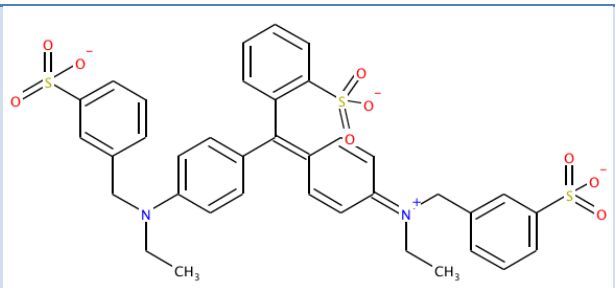	2650-18-2
Basic Violet 2 (CI 42520)	$C_{22}H_{24}ClN_3$	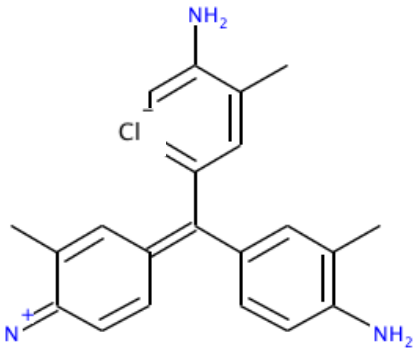	3248-91-7
Basic Violet 13 (CI 42536)	N/A	N/A	8004-88-4
Acid Violet 43 (CI 60730)	$C_{21}H_{14}NNaO_6S$	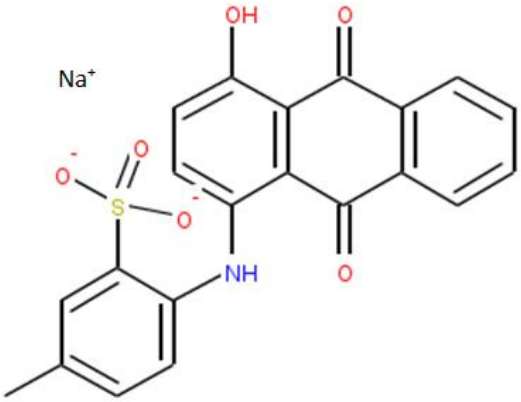	4430-18-6

Basic Violet 16	$C_{23}H_{29}ClN_2$	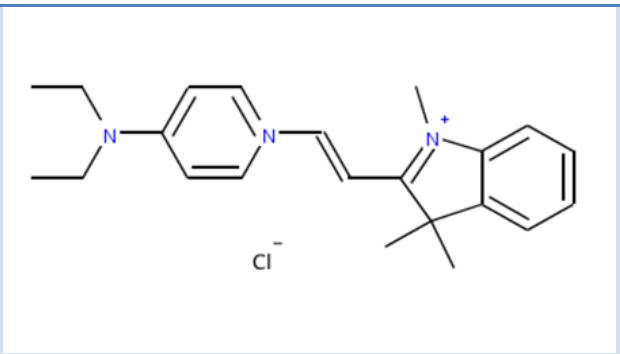	6359-45-1
Basic Red 51	$C_{13}H_{18}ClN_5$	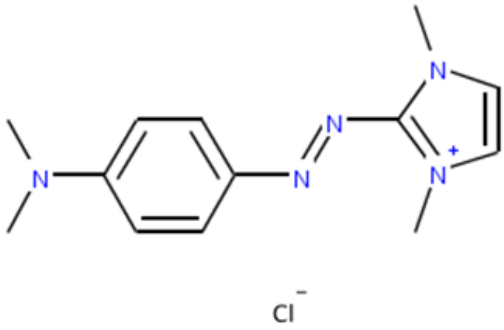	12270-25-6
Lawsone **2-Hydroxy-1,4-naphthoquinone**	$C_{10}H_6O_3$	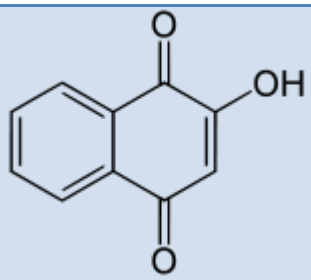	83-72-7
Para-phenylenediamine ***may be present***	$C_6H_8N_2$ 1,4-Diaminobenzene	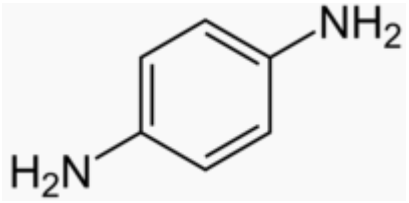	106-50-3

Appendix B: Averaged UV-Visible Spectroscopy Data

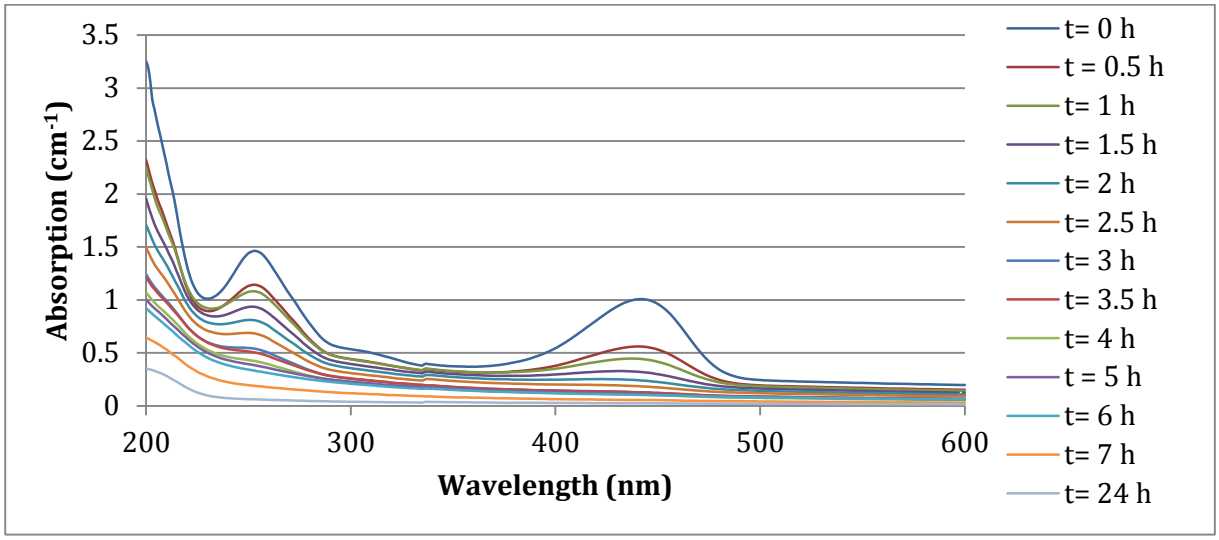

FIGURE B.1: AVERAGE UV-VISIBLE SPECTROSCOPY DATA OF FLUORESCENT GLOW IN DI WATER FROM EXPERIMENTS 2 AND 3.

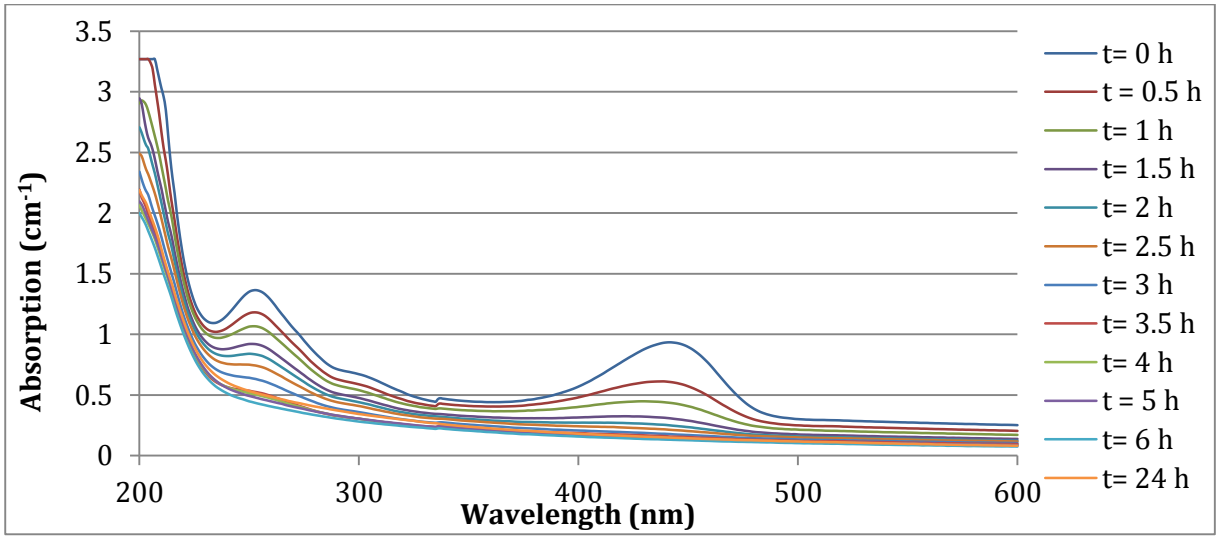

FIGURE B.2: AVERAGE UV-VISIBLE SPECTROSCOPY DATA OF FLUORESCENT GLOW IN TAP WATER FROM EXPERIMENTS 4 AND 5.

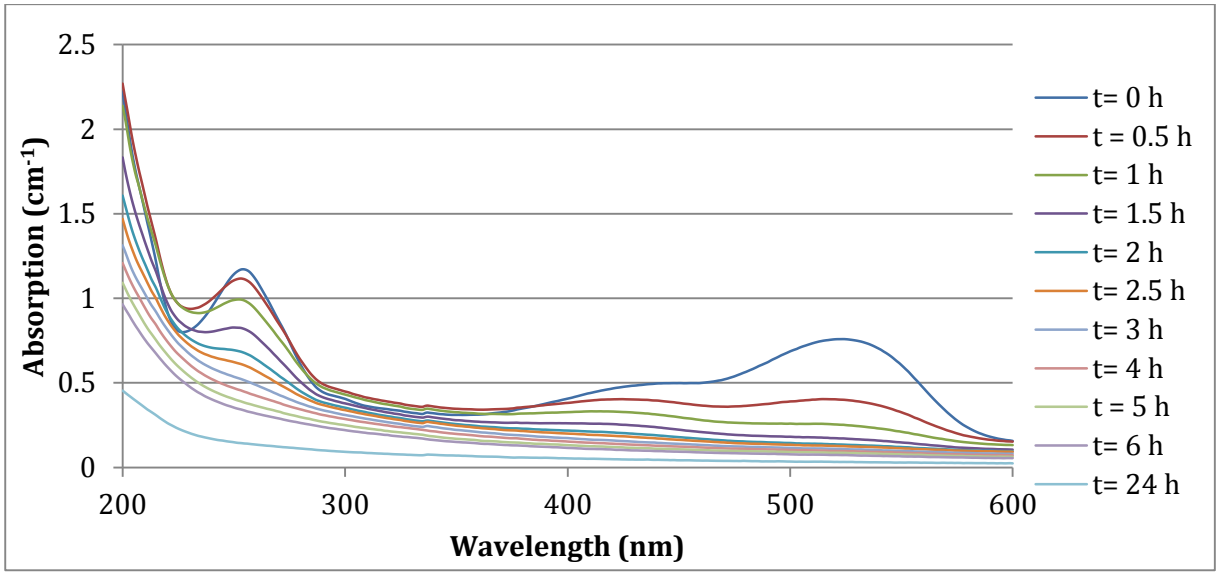

FIGURE B.3: AVERAGE UV-VISIBLE SPECTROSCOPY DATA OF FIRE IN DI WATER FOR EXPERIMENTS 6 AND 7.

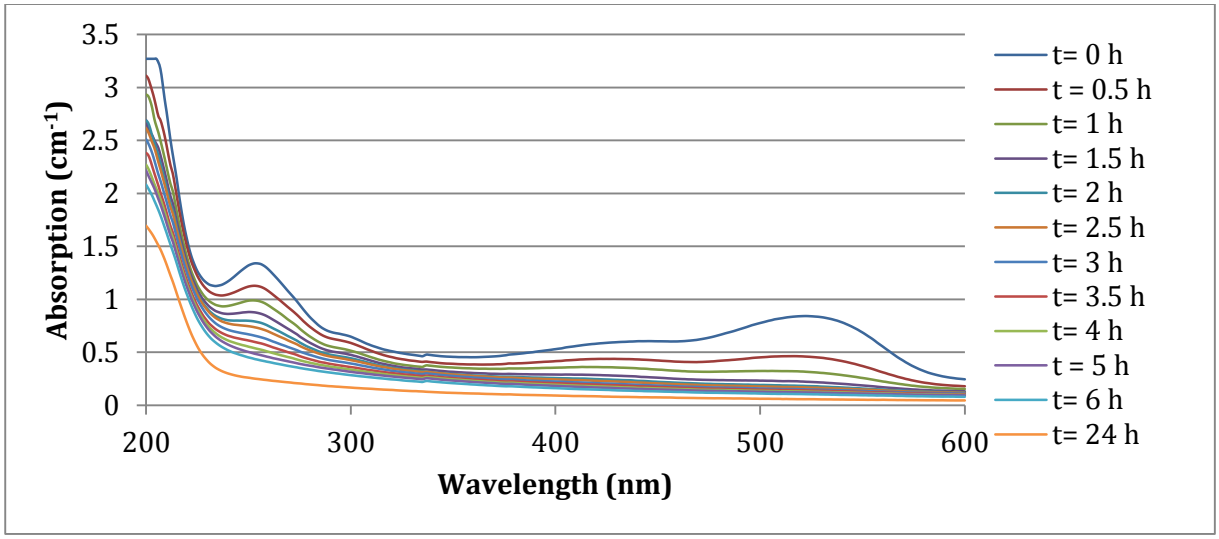

FIGURE B.4: AVERAGE UV-VISIBLE SPECTROSCOPY DATA OF FIRE IN TAP WATER FOR EXPERIMENTS 8 AND 9.

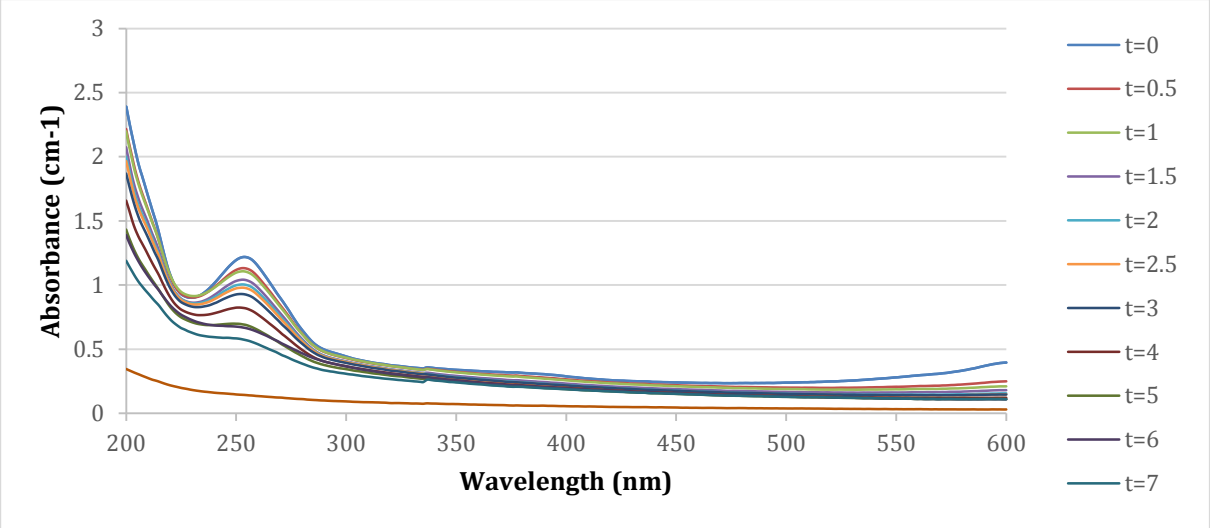

FIGURE B.5: FIGURE 8: AVERAGE UV-VISIBLE SPECTROSCOPY DATA OF LAGOON BLUE IN DI FOR EXPERIMENTS 11 AND 12.

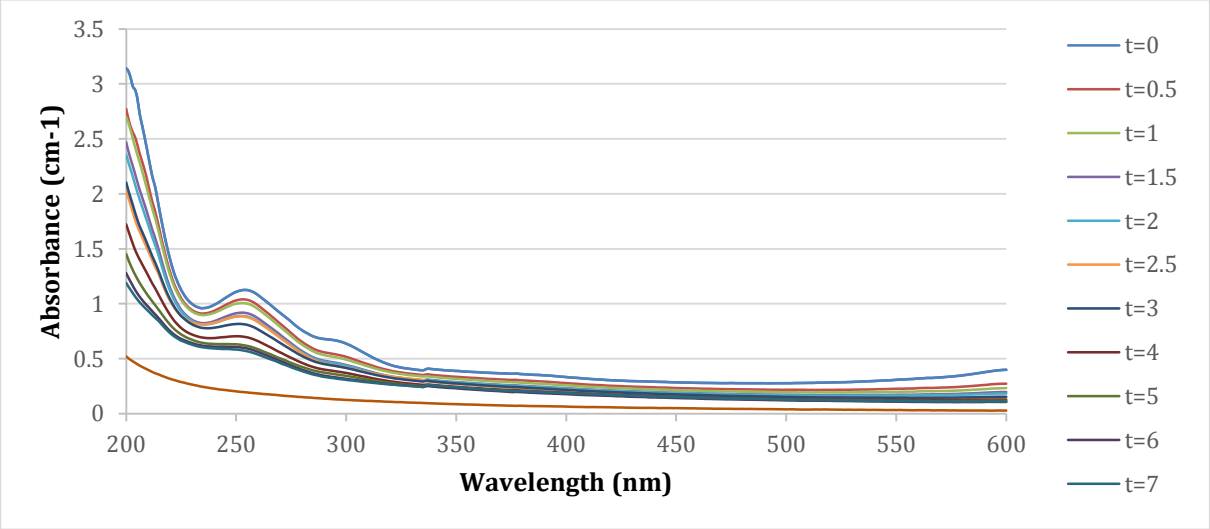

FIGURE B.6: AVERAGE UV-VISIBLE SPECTROSCOPY DATA OF LAGOON BLUE IN TAP WATER FOR EXPERIMENTS 13 AND 14.

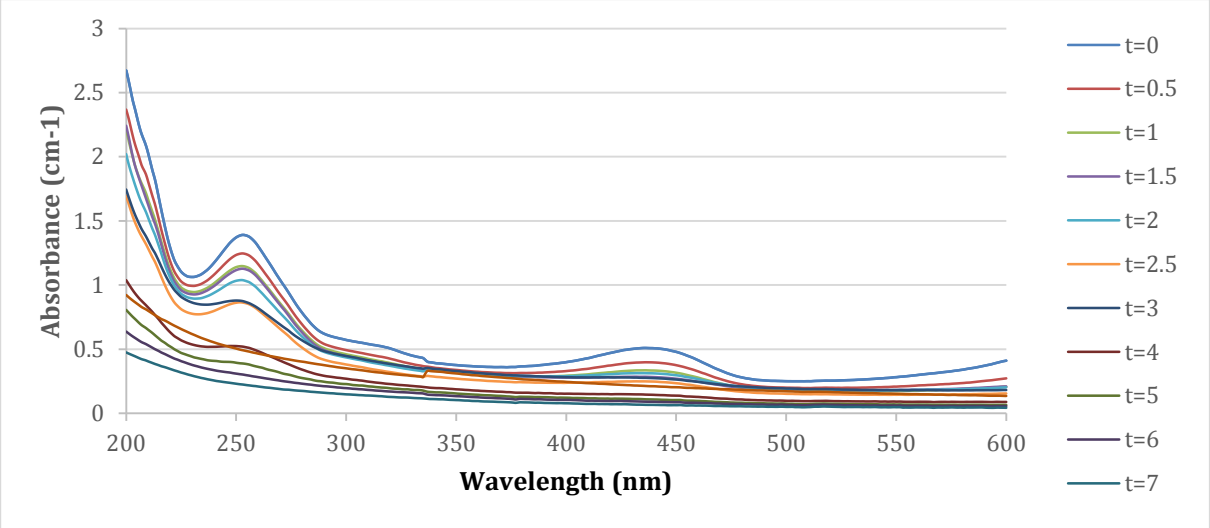

FIGURE B.7: AVERAGE UV-VISIBLE SPECTROSCOPY DATA OF APPLE GREEN IN DI FOR EXPERIMENTS 15 AND 16.

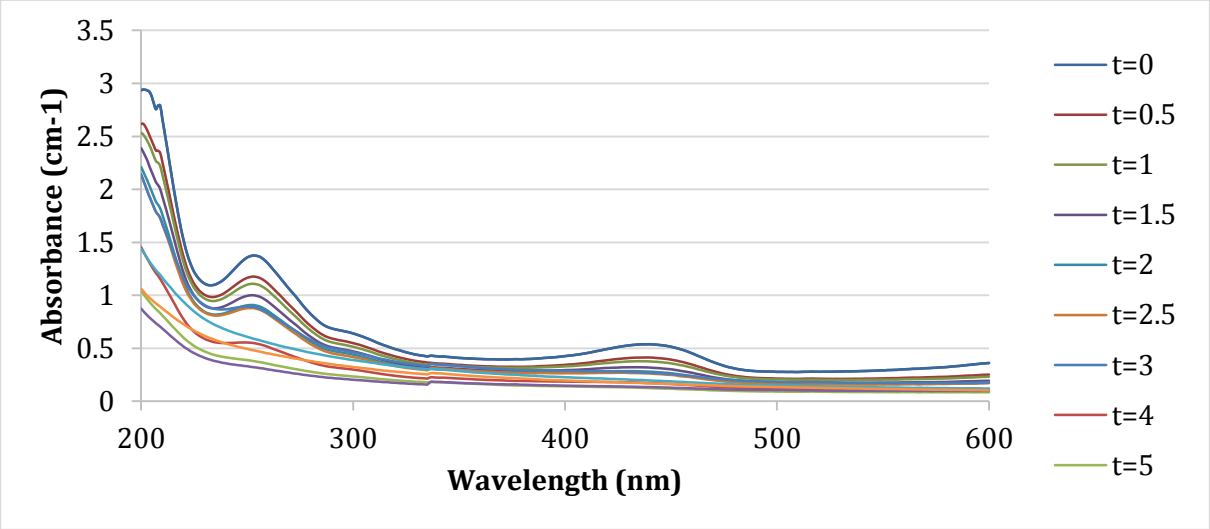

FIGURE B.8: AVERAGE UV-VISIBLE SPECTROSCOPY DATA OF APPLE GREEN IN TAP WATER FOR EXPERIMENTS 17 AND 18.

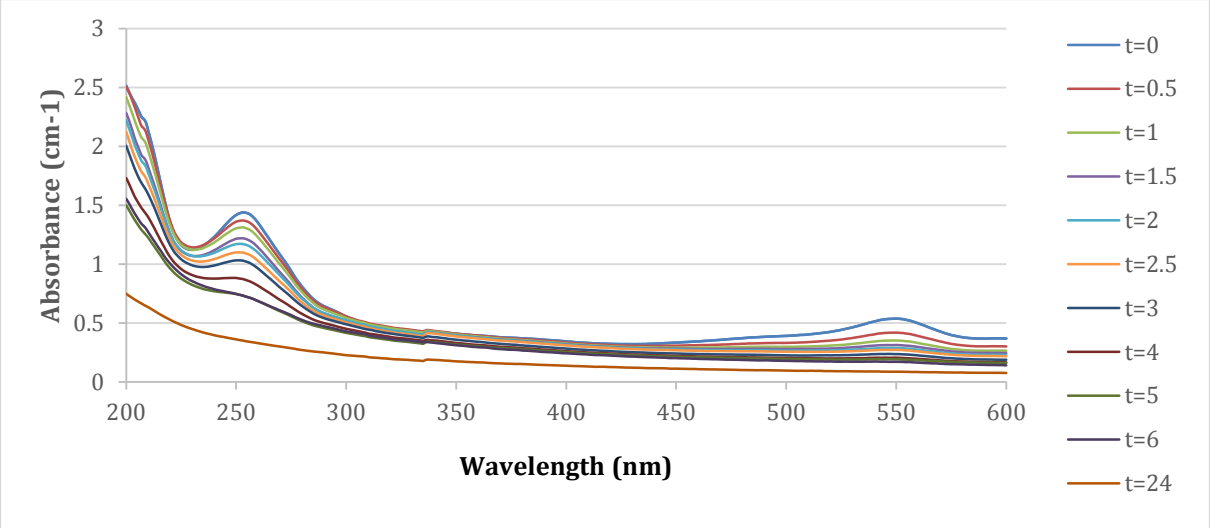

FIGURE B.9: AVERAGE UV-VISIBLE SPECTROSCOPY DATA OF VIOLET IN DISTILLED WATER FOR EXPERIMENTS 19 AND 20.

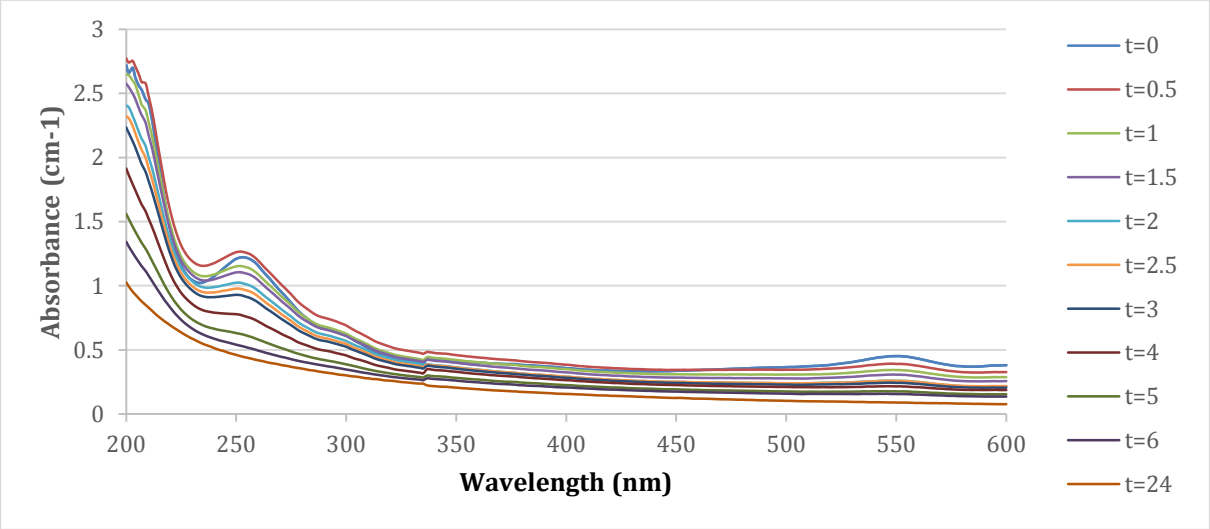

FIGURE B.10: AVERAGE UV-VISIBLE SPECTROSCOPY DATA OF VIOLET IN TAP WATER FOR EXPERIMENTS 21 AND 23.

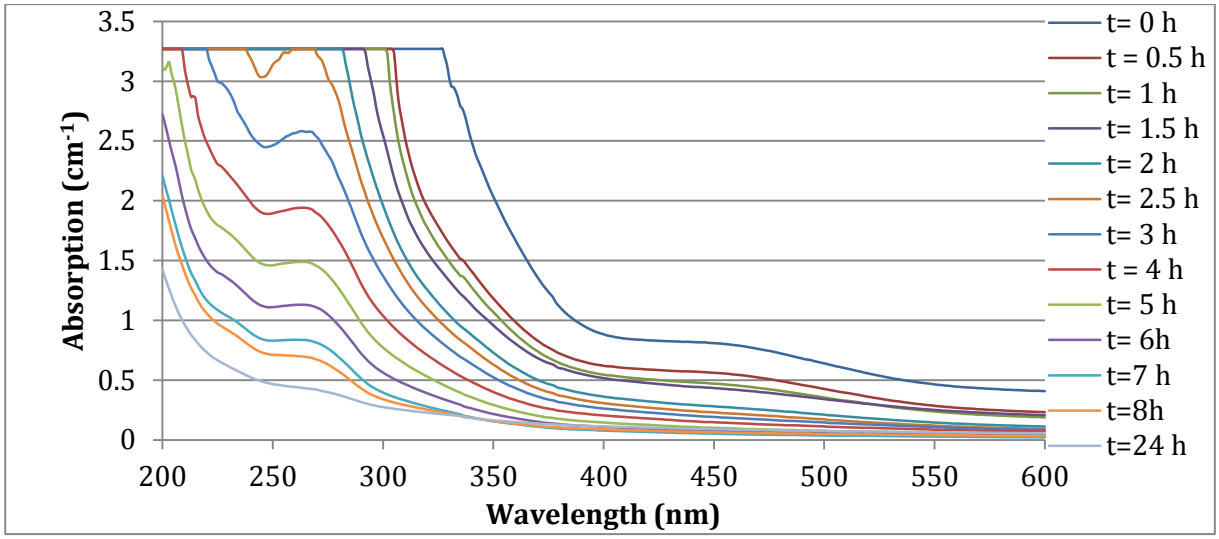

FIGURE B.11: UV-VISIBLE SPECTROSCOPY DATA FOR MOROCCAN HENNA IN DI WATER IN EXPERIMENT 10.

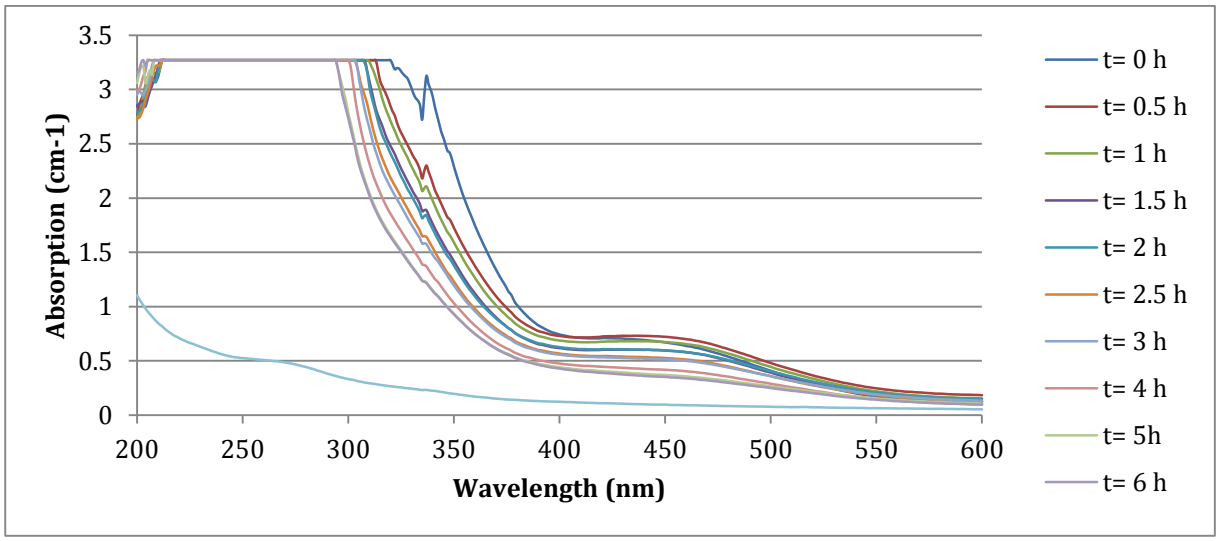

FIGURE B.12: UV-VISIBLE SPECTROSCOPY DATA FOR TUNISIAN HENNA IN DI WATER FOR EXPERIMENT 24.

Appendix C: DI vs Tap UV-Visible Spectroscopy Data Comparison

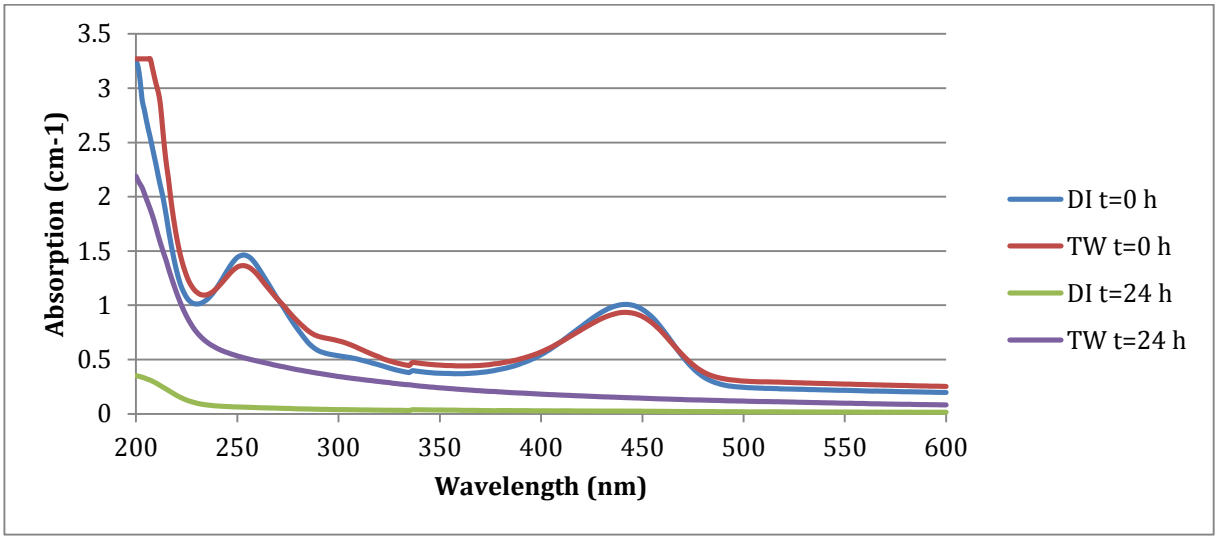

FIGURE C.1: DI VS TW COMPARISON FOR FLUORESCENT GLOW

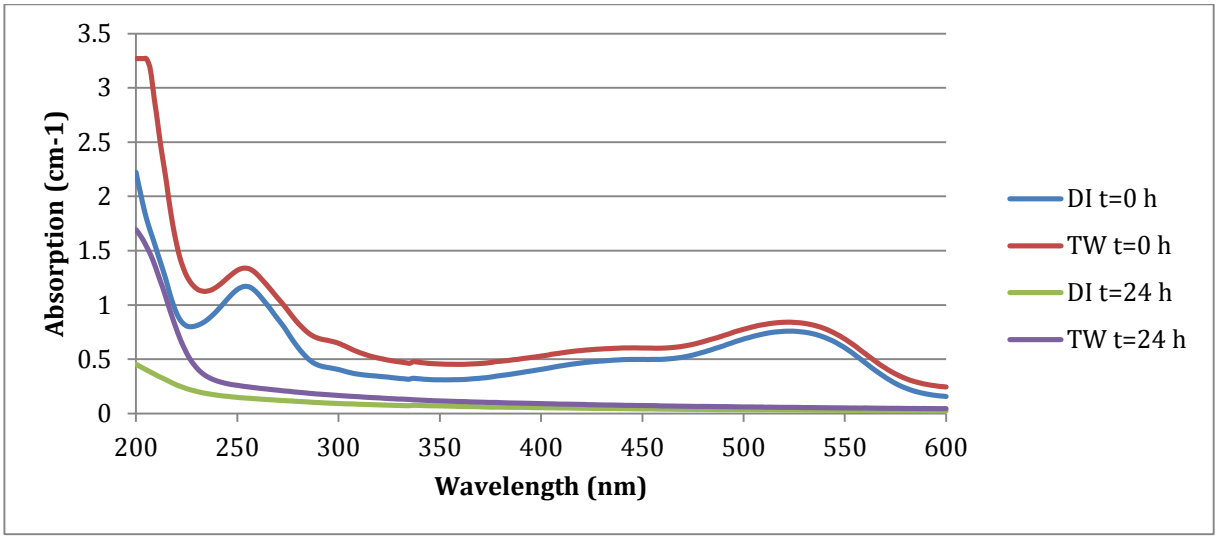

FIGURE C.2: DI VS. TAP WATER COMPARISON FOR FIRE

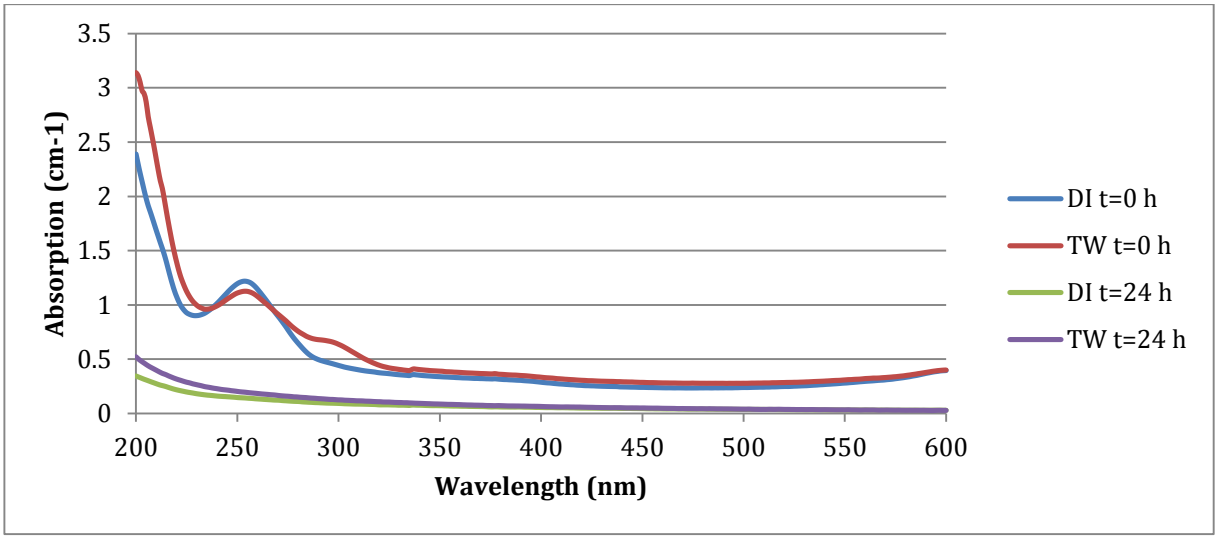

FIGURE C.3: DI VS. TAP WATER COMPARISON FOR LAGOON BLUE

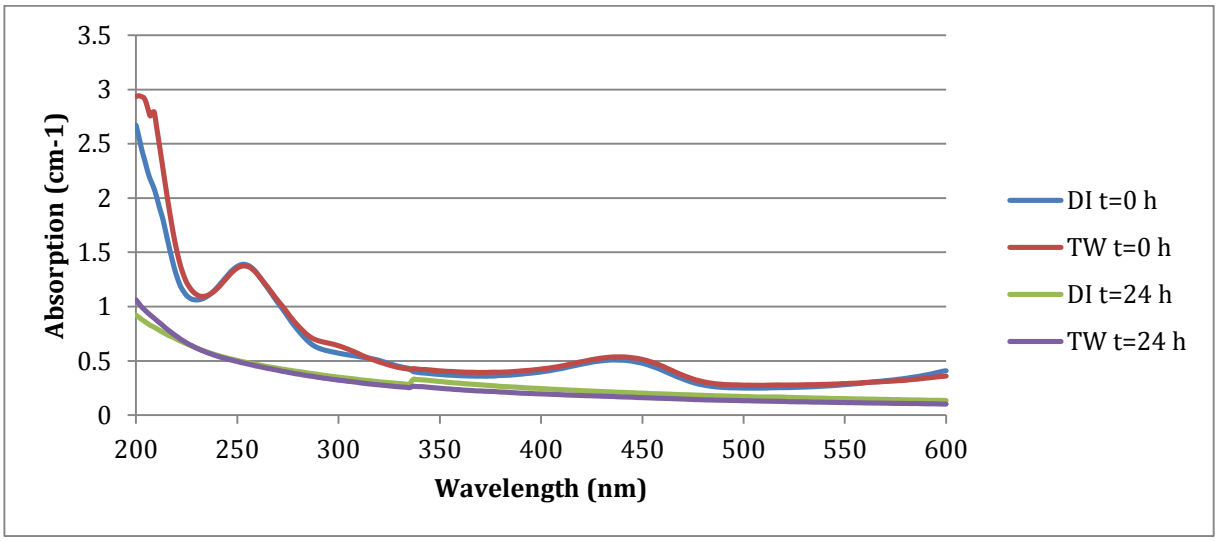

FIGURE C.4: DI VS. TAP WATER COMPARISON FOR APPLE GREEN

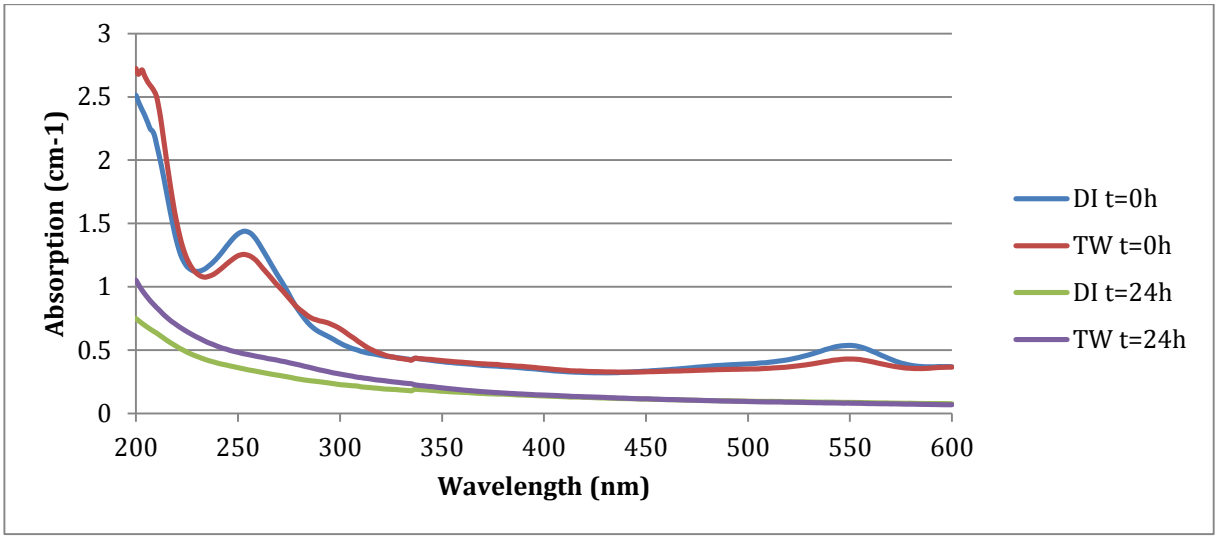

FIGURE C.5: DI VS. TAP WATER COMPARISON FOR VIOLET

Appendix D: Kinetics

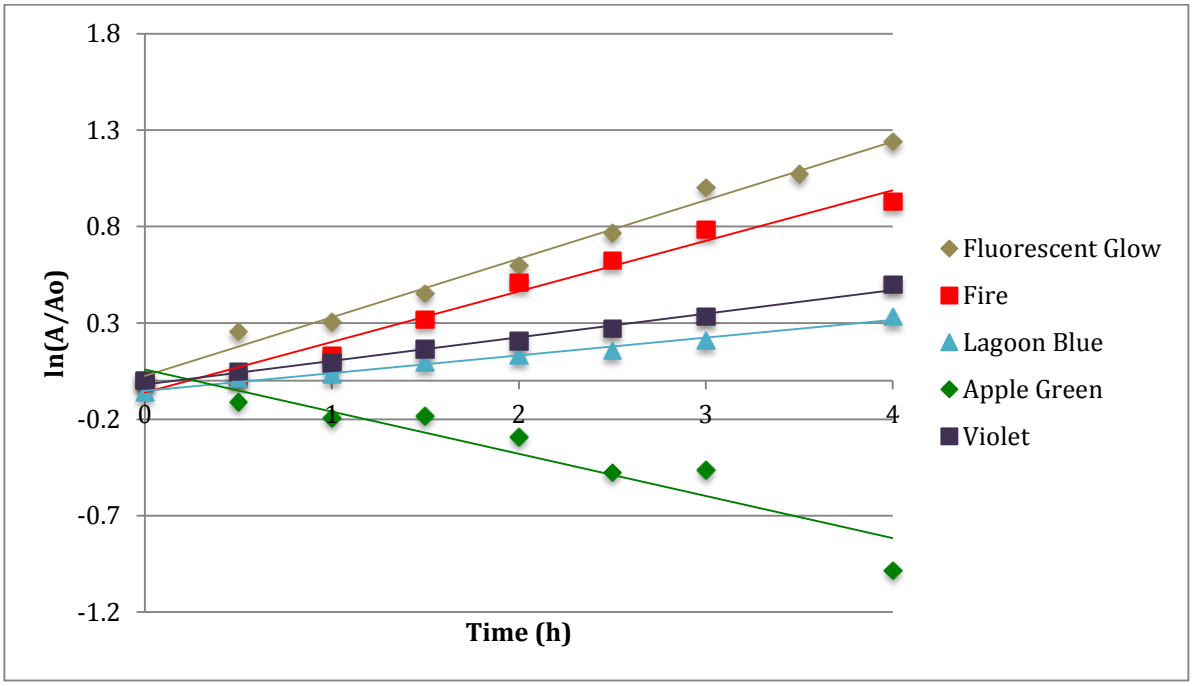

FIGURE D.1: KINETICS DATA FOR COMMERCIAL DYES IN DI WATER WITH AN ABSORPTION PEAK AT A WAVELENGTH OF APPROXIMATELY 253 NM.

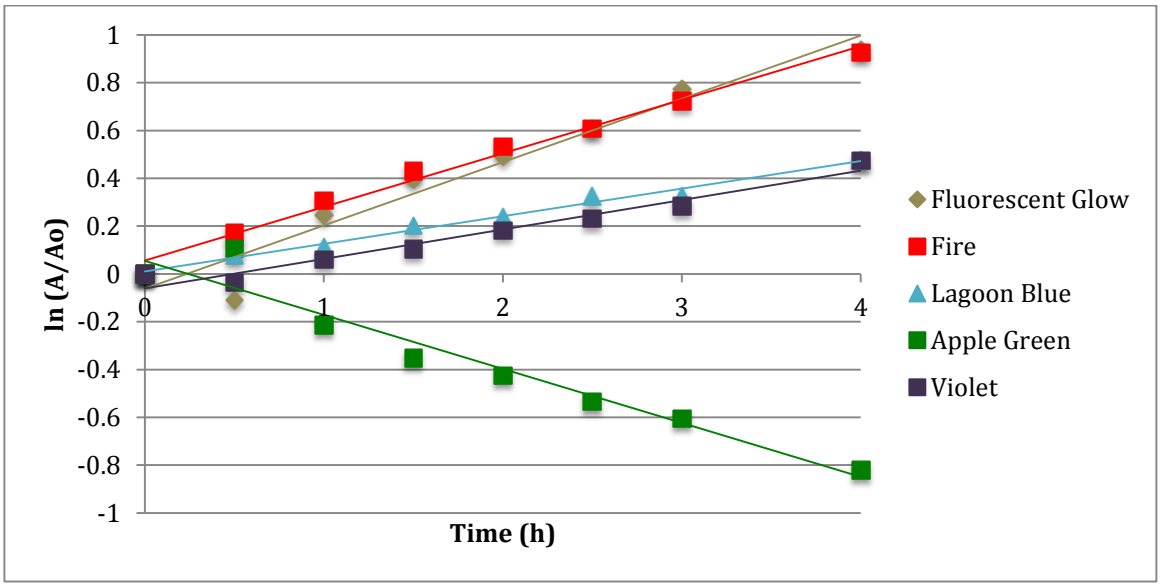

FIGURE D.2: KINETICS DATA FOR COMMERCIAL DYES IN TAP WATER WITH AN ABSORPTION PEAK AT A WAVELENGTH OF APPROXIMATELY 253 NM.

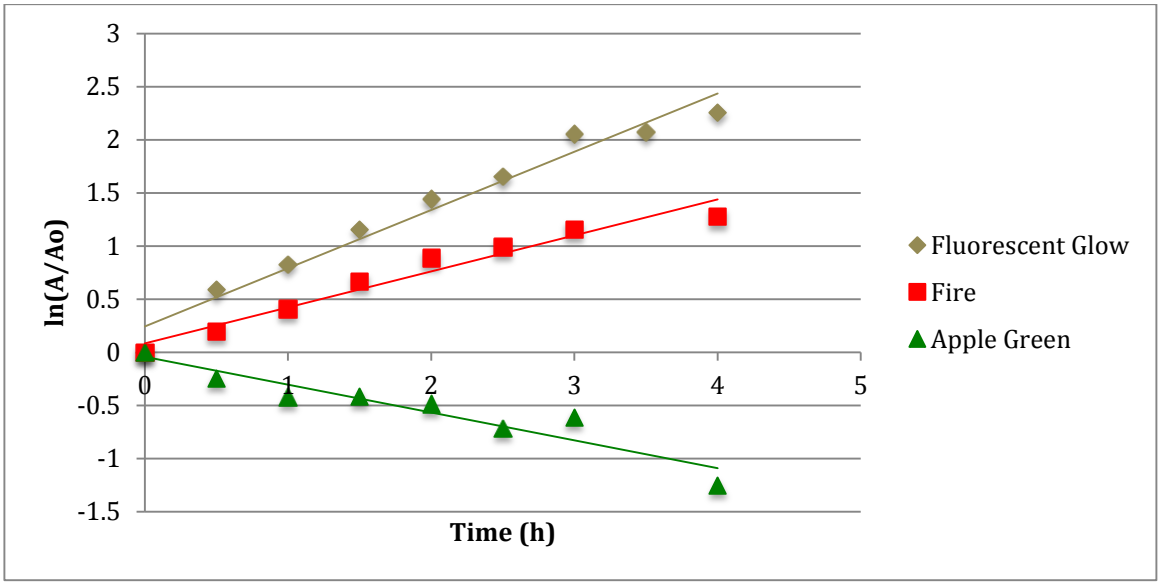

FIGURE D.3: KINETICS DATA FOR COMMERCIAL DYES IN DI WATER WITH AN ABSORPTION PEAK AT A WAVELENGTH OF APPROXIMATELY 443 NM.

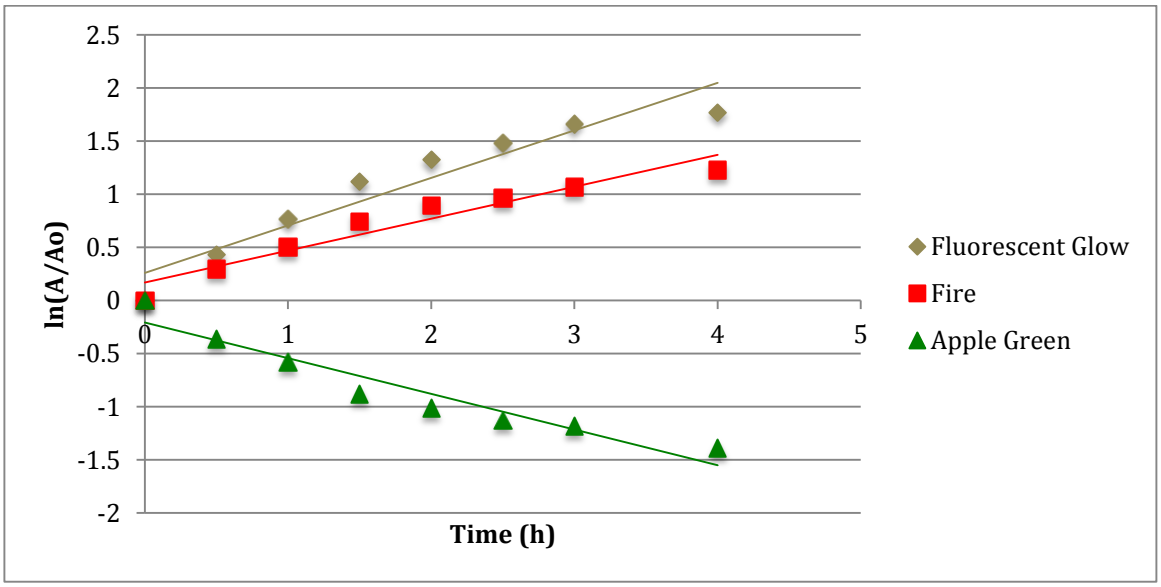

FIGURE D.4: KINETICS DATA FOR COMMERCIAL DYES IN TAP WATER WITH AN ABSORPTION PEAK AT A WAVELENGTH OF APPROXIMATELY 443 NM.

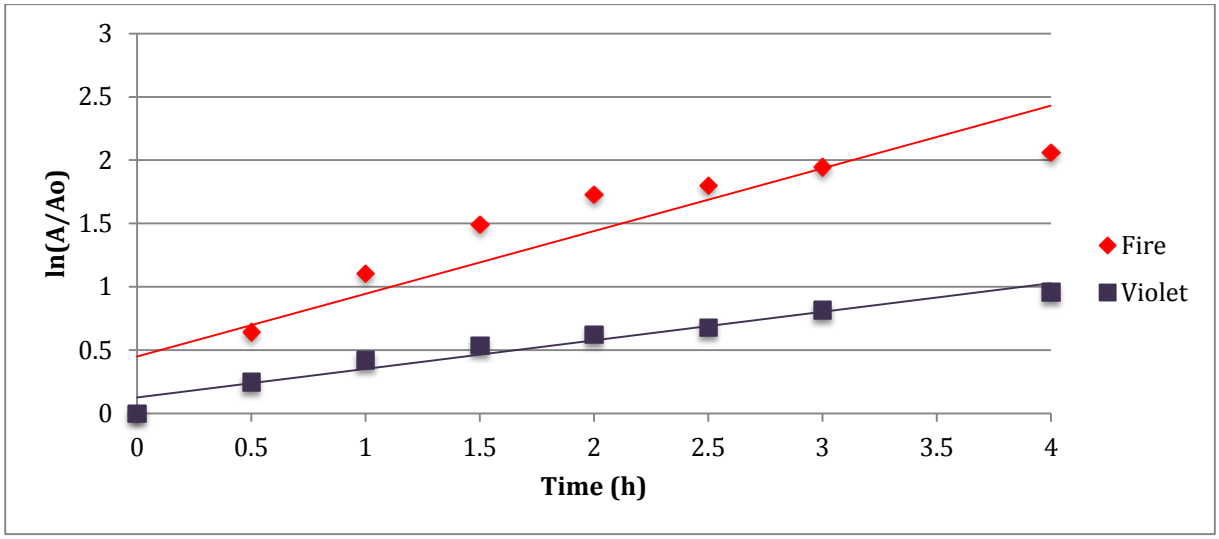

FIGURE D.5: KINETICS DATA FOR COMMERCIAL DYES IN DI WATER WITH AN ABSORPTION PEAK AT A WAVELENGTH OF APPROXIMATELY 540 NM.

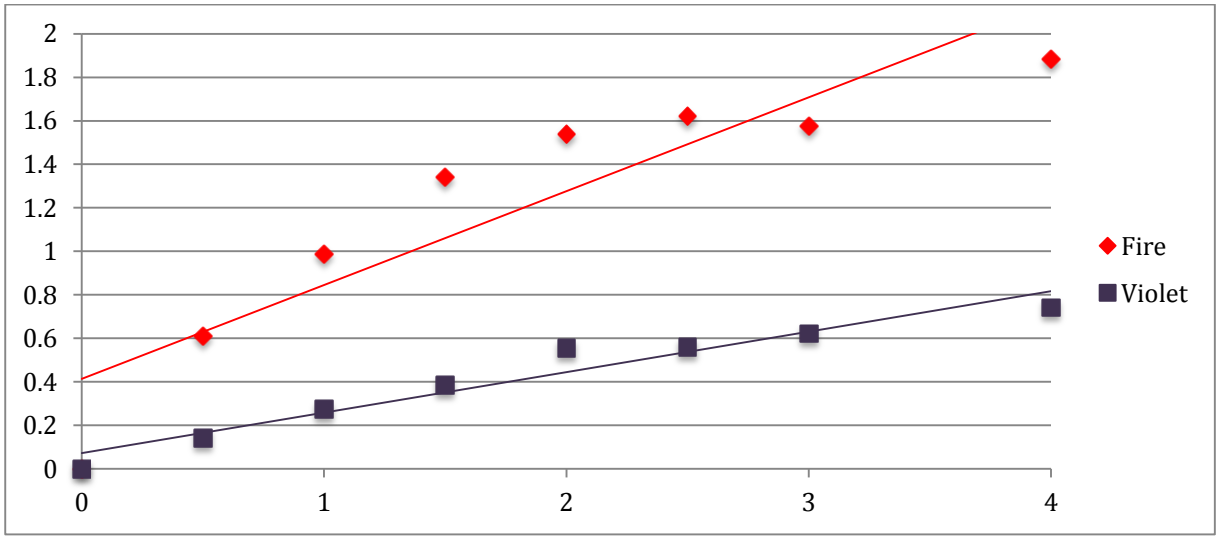

FIGURE D.6: KINETICS DATA FOR COMMERCIAL DYES IN TAP WATER WITH AN ABSORPTION PEAK AT A WAVELENGTH OF APPROXIMATELY 540 NM.

TABLE D1: AVERAGED RATE OF DEGRADATION AT EACH ABSORPTION PEAK FOR ALL DYES.

	Dye	Wavelength (nm)	Kapp (h^{-1})
Distilled Water	Fluorescent Glow	254	0.3042
		443	0.5479
	Fire	254	0.2626
		443	0.3384
		525	0.4953
	Lagoon Blue	253	0.0921
	Apple Green	253	0.2236
		445	0. 2179
	Violet	253	0.1224
		550	0.2509
	Moroccan Henna	267	0.2688
		445	0.3364
	Tunisian Henna	337	0.1655
		429	0.1278
Tap Water	Fluorescent Glow	254	0.2649
		443	0.4473
	Fire	254	0.2337
		443	0.3522
		525	0.522
	Lagoon Blue	253	0.1154
	Apple Green	253	-0.0442

		443	-0.2634
	Violet	253	0.1228
		550	0.2057

Appendix E: Non-Purgeable Organic Carbon and Total Nitrogen

TABLE E.1: NON-PURGEABLE ORGANIC CARBON AND TOTAL NITROGEN INITIAL AND FINAL VALUES AND % YIELD FOR EACH EXPERIMENT

Sample	Initial NPOC (mgC/L)	Final NPOC (mgC/L)	% Yield	Initial TN (mgN/L)	Final TN (mgN/L)	% Yield
1	107.7	14.98	13.91	1.291	1.658	128.428
2	104.3	8.404	8.06	1.379	1.622	117.621
3	104.3	5.57	5.34	1.379	0.7677	55.671
4	48.47	9.552	19.71	2.419	2.345	96.941
5	29.86	13.82	46.28	2.293	2.595	113.171
6	82.03	10.82	13.19	1.523	0.8814	57.873
7	76.25	6.977	9.15	1.387	0.6115	44.088
8	50.24	12.76	25.40	2.855	2.87	100.525
9	34.58	17.25	49.88	2.816	3.163	112.322
10	324.3	39.18	12.08	3.825	1.484	38.797
11	194.2	7.305	3.76	0.8602	0.4478	52.058
12	190.8	28.15	14.75	0.8562	0.4718	55.104
13	131.2	96.78	73.77	1.916	0.4989	26.039
14	113.6	11.93	10.50	1.967	0.676	34.367
15	234.4	9.971	4.25	1.197	0.5272	44.043
16	180.9	4.916	2.72	1.272	0.4255	33.451
17	127.7	12.54	9.82	2.135	0.8824	41.330
18	77.7	10.95	14.09	1.726	0.9112	52.793
19	196.9	8.339	4.24	1.268	0.7943	62.64
20	185.5	10.35	5.58	1.187	0.4431	37.33
21	56.99	20.68	36.29	1.914	1.195	62.43
22	46.04	37.79	82.08	1.125	2.18	193.73
23	35.8	25.24	70.50	1.026	1.265	123.29
24	300	36.72	12.24	1.577	1.201	76.16

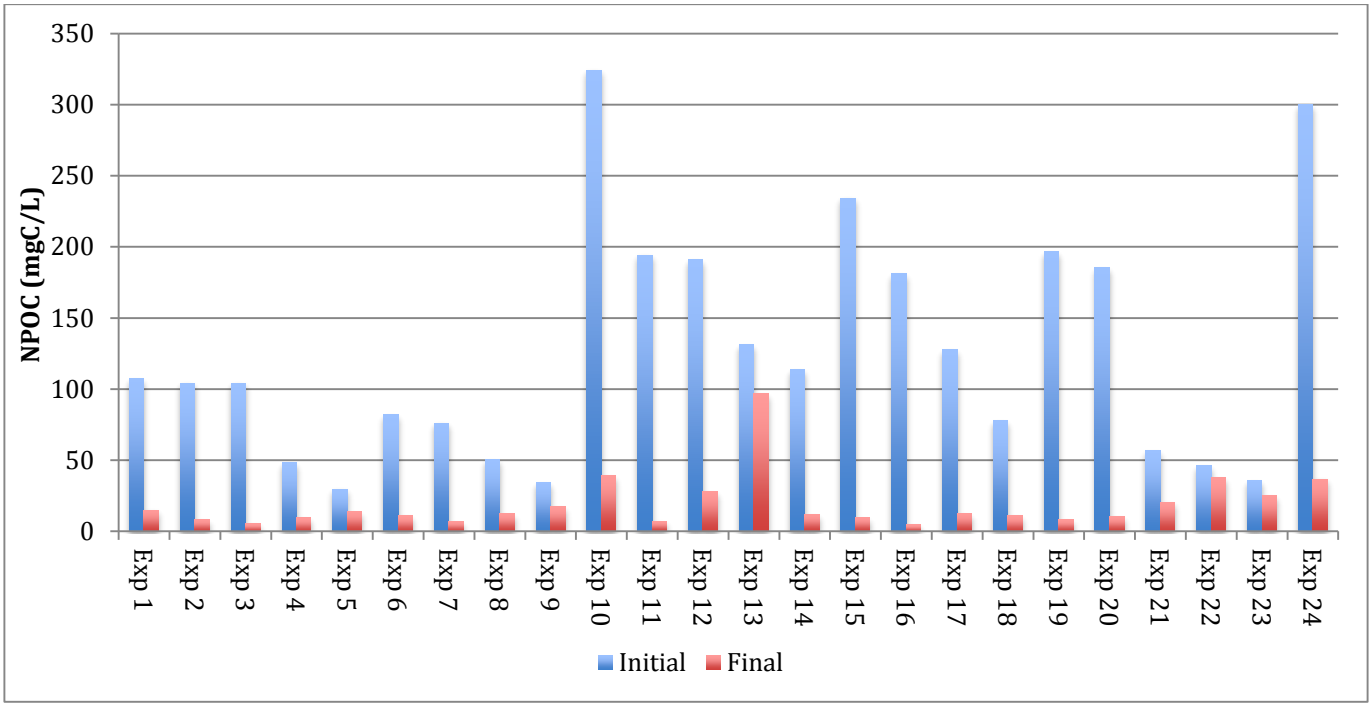

FIGURE E.1: NON-PURGEABLE ORGANIC CARBON CONTENT FOR EACH EXPERIMENT AT T = 0 H AND T= 24 H

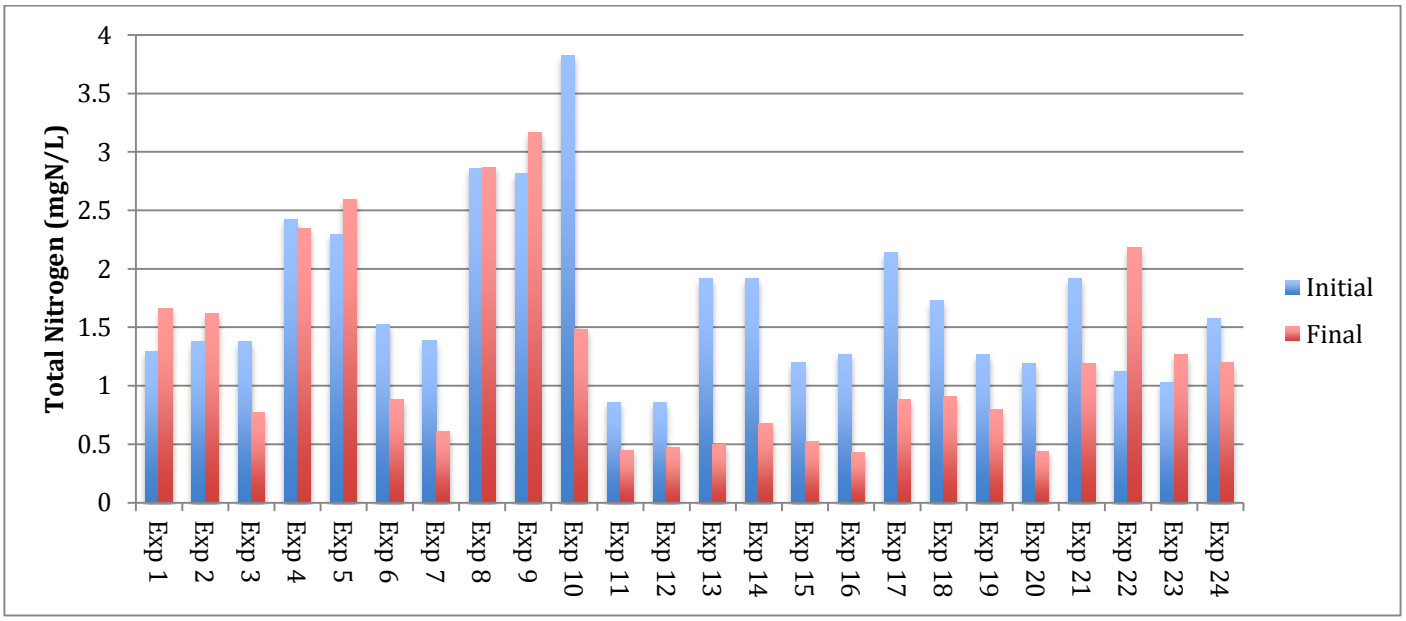

FIGURE E.2: TOTAL NITROGEN CONTENT FOR SAMPLES AT T = 0 H AND T = 24 H

Appendix F: pH Values

TABLE F.1: INITIAL AND FINAL PH VALUES FOR ALL DYES.

Exp #	Name	Initial pH		Final pH	
1	Fluorescent Glow in Distilled Water	4.70	3.96	8.59	8.26
2	Fluorescent Glow in Distilled Water (1)	4.47	4.24	8.09	8.55
3	Fluorescent Glow in Distilled Water (2)	4.07	4.13	7.94	7.87
4	Fluorescent Glow in Tap Water (1)	7.37	7.40	7.78	7.73
5	Fluorescent Glow in Tap Water (2)	7.25	7.29	6.64	7.20
6	Fire in Distilled Water (1)	4.31	4.07	6.37	6.63
7	Fire in Distilled Water (2)	4.0	3.92	6.17	6.28
8	Fire in Tap Water (1)	6.87	6.90	6.74	6.93
9	Fire in Tap Water (2)	6.97	6.93	7.07	7.10
10	Moroccan Henna in Distilled Water	5.13	4.96	7.08	7.21
11	Lagoon Blue in Distilled Water (1)	3.98	3.87	6.51	6.69
12	Lagoon Blue in Distilled Water (2)	4.27	4.06	6.10	6.36
13	Lagoon Blue in Tap Water (1)	7.20	7.30	6.94	6.97
14	Lagoon Blue in Tap Water (2)	7.34	7.53	7.15	7.24
15	Apple Green in Distilled Water (1)	3.84	3.69	6.89	7.02
16	Apple Green in Distilled Water (2)	3.84	3.90	6.36	6.36
17	Apple Green in Tap Water (1)	6.86	6.95	6.93	6.99
18	Apple Green in Tap Water (2)	7.07	7.24	7.22	7.19
19	Violet in Distilled Water (1)	3.98	3.89	7.18	7.26
20	Violet in Distilled Water (2)	3.82	3.82	7.71	7.51
21	Violet in Tap Water (1)	7.43	7.58	8.35	8.33
22	Violet in Tap Water (2)	8.06	8.13	7.29	7.38
23	Violet in Tap Water (3)	7.23	7.40	7.27	7.41
24	Tunisian Henna in Distilled Water	4.70	4.77	7.19	7.02

Appendix G: Lettuce Test

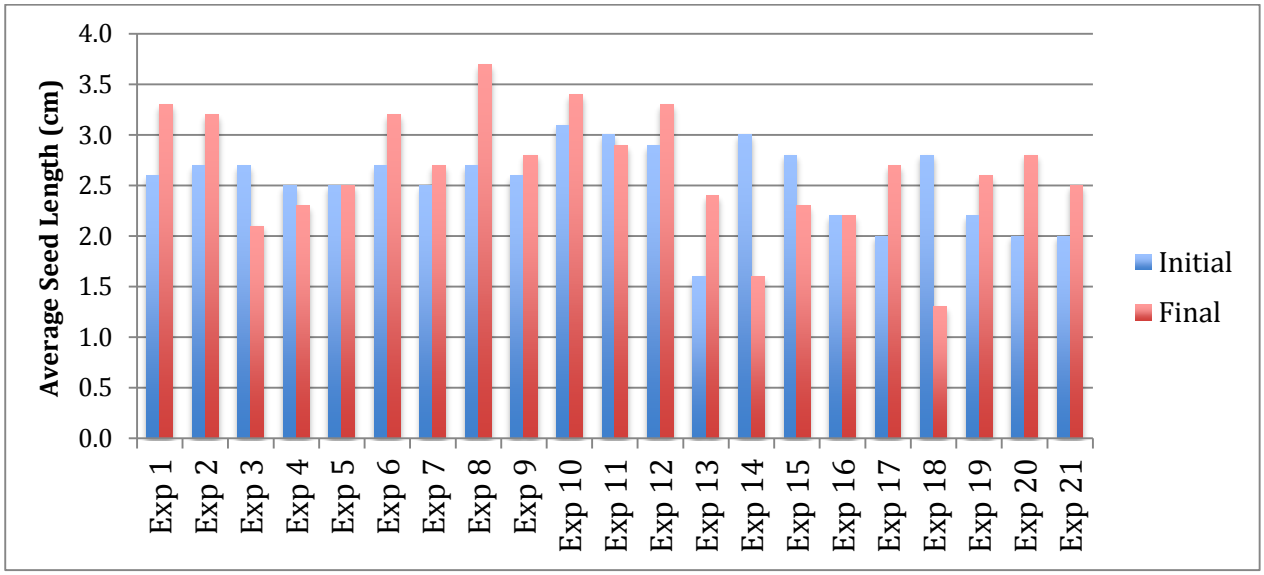

FIGURE G.1: AVERAGE SEED LENGHT RESULTS FOR EXP 1-21

TABLE G.1: SEED LENGTHS FOR POSITIVE AND NEGATIVE CONTROLS

Seed Lengths in Experimental Controls							
	Positive Controls				Negative Control		
	Vittel 1	Vittel 2	Crystalline 1	Crystalline 2	Vittel + NaCl		
1	4	3	3,1	3	1	1,6	1,7
2	3,2	2,5	3,9	2,6	2	2,1	1,3
3	3,5	2,5	3,1	2	3	2,3	1,9
4	2,9	2,5	1,9	3	4	1,5	1
5	3	0,8	3,4	2,8	5	1,6	1,4
6	3,2	2	3	3,5	6	1,8	1,7
7	3,8	1,6	2,7	3,1	7	1,6	1,5
8	3,2	2,7	3,1	3,1	8	1,7	1,5
9	3,5	2,7	2,4	2,7	9	1,6	1,3
10	3,6	2,8	2,5	3,3	10	1,4	1,5
11	4	2,9	0,4	2	11	1,2	0
12	1,5	0	0	0	12	0	0
Ave L	3,3	2,2	2,5	2,6	**Ave L**	1,5	1,2

TABLE G.2: SEED LENGTHS FOR FLUORESCENT GLOW IN DI WATER

Exp 1 Fluorescent Glow DI (1)			Exp 2 Fluorescent Glow DI (2)			Exp 3 Fluorescent Glow DI (3)		
Seed	t = 0 h	t =5 h	Seed	t = 0 h	t = 24 h	Seed	t = 0 h	t = 24 h
1	3.5	4.5	1	2.9	3	1	2.9	3.9
2	3	4	2	2.4	3.9	2	3	3.2
3	3.5	3.5	3	3.1	3.3	3	2.5	3.9
4	3.5	3.5	4	3.4	4.2	4	2.5	1.3
5	3.8	2.7	5	1.8	3.4	5	2.4	0.7
6	4	1.7	6	3.3	3.5	6	3.3	4.5
7	2.6	3.5	7	2.7	2.5	7	2	3.5
8	2.5	3.3	8	3.2	3	8	3.1	1.3
9	2.5	2.6	9	3.6	3.1	9	3.1	1.2
10	2.2	4	10	2.5	4.4	10	2.5	1.5
11	0	3.3	11	3	1.2	11	2.6	0
12	0	3.5	12	0.7	3	12	3	0
Ave L (cm)	2.6	3.3	Ave L (cm)	2.7	3.2	Ave L (cm)	2.7	2.1
RT	0.4	0.0	RT	0.3	0.0	RT	0.3	0.7
ΔRT	-0.4		ΔRT	-0.3		ΔRT	0.4	

TABLE G.3: SEED LENGTHS FOR FLUORESCENT GLOW IN TAP WATER

Exp 4 Fluorescent Glow Tap Water (1)			Exp 5 Fluorescent Glow Tap Water (2)		
Seed	t = 0	t = 24h	Seed	t = 0	t = 24h
1	3.3	3.9	1	3.6	2.7
2	3.1	2.5	2	2.6	2.4
3	3	3.6	3	2.8	3
4	2.7	3.2	4	3.3	3.2
5	3.7	4.3	5	3.5	3
6	2.5	1.5	6	2.9	3
7	3	4.1	7	3.2	3.3
8	2.8	3.3	8	3.1	3
9	2.6	0.9	9	3.3	3
10	3.1	0.3	10	1	0
11	0	0	11	0.7	0
12	0	0	12	0	3.8
Ave L (cm)	2.5	2.3	Ave L (cm)	2.5	2.5
RT	0.5	0.6	RT	0.4	0.4
ΔRT	0.1		ΔRT	0.0	

Table G.4: Seed Lengths for Fire in DI Water

Exp 6 Fire DI Water (1)			Exp 7 Fire DI Water (2)		
Seed	t = 0 h	t = 24 h	Seed	t = 0 h	t = 24 h
1	3.2	3.3	1	3	3.5
2	3.3	2.8	2	2	3.5
3	2.8	3.5	3	2.5	3.8
4	3.3	2.7	4	2.7	3.5
5	2.7	4.5	5	2.9	3.8
6	3.1	3.2	6	1.7	3.1
7	3	3.5	7	2.9	3.1
8	2.6	4.2	8	3.2	3.3
9	2.6	3.6	9	2.3	3.6
10	3.1	3	10	1.1	1
11	2.4	0.5	11	2.7	0
12	0	3.5	12	3.3	0
Ave L (cm)	2.7	3.2	Ave L (cm)	2.5	2.7
RT	0.3	0.1	RT	0.4	0.3
ΔRT	-0.3		ΔRT	-0.1	

Table G.5: Seed Lengths for Fire in Tap Water

Exp 8 Fire Tap Water (1)			Exp 9 Fire Tap Water (2)		
Seed	t = 0 h	t = 24 h	Seed	t = 0 h	t = 24 h
1	3.2	4.1	1	3.4	3.6
2	3.1	4.4	2	2.9	3.1
3	3.2	4.1	3	2.9	3
4	3.5	3	4	3.5	4.3
5	3.2	4.2	5	3.1	3.5
6	4	3.8	6	2.8	3.1
7	3	2.5	7	3.5	3.4
8	3.1	2.6	8	2.8	3.7
9	3.2	3.9	9	2.1	3.6
10	3.1	3.4	10	1	2.4
11	0	4	11	1.9	0
12	0	3.8	12	1.4	0
Ave L (cm)	2.7	3.7	Ave L (cm)	2.6	2.8
RT	0.3	-0.2	RT	0.4	0.3
ΔRT	-0.5		ΔRT	-0.1	

Table G.6: Seed Lengths for Moroccan Henna in DI Water

Exp 10 Moroccan Henna DI Water		
Seed	t = 0	t = 24h
1	2.7	4
2	2	4
3	4	3.4
4	3.8	4.1
5	3.6	3.4
6	2.5	3.7
7	3.6	3.7
8	3.6	3.4
9	3.2	4.1
10	3.3	3.1
11	1.2	2.8
12	3.2	1.2
Ave L (cm)	3.1	3.4
RT	0.1	-0.1
ΔRT	-0.2	

Table G.7: Seed Lengths for Lagoon Blue in DI Water

Exp 11 Lagoon Blue DI Water (1)			Exp 12 Lagoon Blue DI Water (1)		
Seed	t = 0 h	t = 24 h	Seed	t = 0 h	t = 24 h
1	3.1	3.7	1	0	3.5
2	3.7	3.5	2	2.8	4.7
3	2.6	3.7	3	3.1	3.9
4	2.6	2.7	4	3.2	3.1
5	2.9	3.3	5	2.3	3.6
6	3.4	3.1	6	3.3	4.3
7	3.1	2	7	4	0.5
8	3.4	4.2	8	3.4	3.5
9	3	3.4	9	3.1	3.4
10	3.4	1.2	10	2.9	3
11	1.3	3.2	11	2.8	4.1
12	2.9	0.7	12	3.5	2
Ave L (cm)	3.0	2.9	Ave L (cm)	2.9	3.3
RT	0.2	0.2	RT	0.2	0.0
ΔRT	0.0		ΔRT	-0.2	

Table G.8: Seed Lengths for Lagoon Blue in Tap Water

Exp 13 Lagoon Blue Tap Water (1)			Exp 14 Lagoon Blue Tap Water (2)		
Seed	t = 0 h	t = 24 h	Seed	t = 0 h	t = 24 h
1	3.2	3.4	1	3.6	1.5
2	2.8	2.3	2	3	2.4
3	2.9	2.1	3	2.7	2.1
4	2.9	2.9	4	2.9	2.1
5	2.3	3.5	5	3.2	2.1
6	2.2	3.1	6	3.2	2.1
7	2.3	3.8	7	3.4	2
8	0	3.3	8	3	1.9
9	0	1	9	3	2.6
10	0	3.6	10	3.4	0
11	0	0	11	1.2	0
12	0	0	12	3	0
Ave L (cm)	1.6	2.4	Ave L (cm)	3.0	1.6
RT	1.0	0.5	RT	0.2	1.0
ΔRT	-0.5		ΔRT	0.8	

Table G.9: Seed Lengths for Apple Green in DI Water

Exp 15 Apple Green Dist			Exp 16 Apple Green Dist		
Seed	t = 0	t = 24h	Seed	t = 0	t = 24h
1	3.2	2.6	1	3.6	3.8
2	3.6	3	2	2	3
3	3.5	1.4	3	3.8	1.5
4	3.4	2.7	4	3	3.5
5	3.4	3.3	5	1.3	2.6
6	2.9	2.6	6	3.3	2.5
7	3	2	7	2.3	3.1
8	0.5	2.7	8	2.8	2.8
9	3	2.1	9	1.4	2.9
10	2	3	10	0.5	0.5
11	3	2.7	11	2.5	0.4
12	2.5	0	12	0	0
Ave L (cm)	2.8	2.3	Ave L (cm)	2.2	2.2
RT	0.3	0.5	RT	0.6	0.6
ΔRT	0.3		ΔRT	0.0	

Table G.10: Seed Lengths for Apple Green in Tap Water

Exp 17 Apple Green Tap			Exp 18 Apple Green Tap		
Seed	t = 0	t = 24h	Seed	t = 0	t = 24h
1	2.8	2.8	1	3.3	2.4
2	2	3.1	2	3	2.1
3	1.7	3	3	3.1	1.4
4	3.1	2.7	4	3	2.1
5	3	2.7	5	2.5	3.2
6	3	3.5	6	3.4	1.8
7	3	2.6	7	3	2.5
8	2.5	2.9	8	2.9	0.6
9	2.5	2.7	9	2.8	0
10	0.5	1.1	10	2.4	0
11	0	3	11	2.4	0
12	0	0	12	1.5	0
Ave L (cm)	2.0	2.5	Ave L (cm)	2.8	1.3
RT	0.7	0.4	RT	0.3	1.1
ΔRT	-0.3		ΔRT	0.8	

Table G.11: Seed Lengths for Violet in DI Water

Exp 19 Violet Dist			Exp 20 Violet Dist		
	t = 0	t = 24h		t = 0	t = 24h
1	2.9	3.5	1	3.1	3.7
2	2.5	3	2	3.2	2.8
3	2.6	2.3	3	3.6	3.2
4	2.8	3.1	4	2.9	2.5
5	2.5	2.2	5	3.2	2.1
6	1.5	2.8	6	2.7	2.8
7	2.7	3.2	7	3.1	3.1
8	2.6	2.9	8	2.6	2.8
9	2.4	3.3	9	0	3.2
10	2.8	3	10	0	2.3
11	0.7	1.7	11	0	3
12	0.3	0.7	12	0	2.6
Ave L (cm)	2.2	2.6	Ave L (cm)	2.0	2.8
RT	0.6	0.4	RT	0.7	0.3
ΔRT	-0.3		ΔRT	-0.5	

TABLE G.12: RELATIVE TOXICITY DATA FOR ALL DYES EXCEPT TUNISIAN HENNA

		N germ			L sample			Relative Toxicities		
				Average			Average			Average
Fluorescent Glow Distilled Water	Initial	12	12	12	2.7	2.7	2.7	0.0	0.0	0.0
	Final	12	12	12	2.1	3.2	2.7	0.5	-0.3	0.1
Fluorescent Glow Tap Water	Initial	10	11	10.5	2.5	2.5	2.5	0.2	0.2	0.2
	Final	10	10	10	2.3	2.5	2.4	0.3	0.2	0.3
Fire Distilled Water	Initial	11	12	11.5	2.7	2.5	2.6	0.0	0.2	0.1
	Final	12	10	11	3.2	2.7	3.0	-0.3	0.0	-0.1
Fire Tap Water	Initial	10	12	11	2.7	2.6	2.7	0.0	0.1	0.1
	Final	12	10	11	3.7	2.8	3.3	-0.7	0.0	-0.4
Lagoon Blue Distilled	Initial	12	12	12	3	2.9	3.0	-0.2	-0.1	-0.1
	Final	11	12	11.5	2.9	3.3	3.1	-0.1	-0.4	-0.3
Lagoon Blue Tap	Initial	7	10	8.5	1.6	3	2.3	0.8	-0.2	0.3
	Final	12	9	10.5	2.4	1.6	2.0	0.3	0.8	0.5
Apple Green Distilled	Initial	12	11	11.5	2.8	2.2	2.5	0.0	0.4	0.2
	Final	11	11	11	2.3	2.2	2.3	0.3	0.4	0.4
Apple Green Tap	Initial	10	12	11	2	2.8	2.4	0.5	0.0	0.3
	Final	11	8	9.5	2.7	1.3	2.0	0.0	1.0	0.5
Violet Distilled	Initial	11	8	9.5	2.2	2	2.1	0.4	0.5	0.5
	Final	12	12	12	2.6	2.8	2.7	0.1	0.0	0.0
Violet Tap	Initial	10		10	2		2.0	0.5	2.0	1.3
	Final	11		11	2.5		2.5	0.2	2.0	1.1
Moroccan Henna Distilled	Initial	12		12	3.1		3.1	-0.3		-0.3
	Final	12		12	3.4		3.4	-0.5		-0.5
Controls	Positive Vittel	12	11	11.5	3.3	2.2	2.8			0.0
	Crystalline	11	11	11	2.5	2.6	2.6			0.0
	Negative Vittel + NaCl	11	10	10.5	1.5	1.2	1.4			1.0